Copyright Warning & Restrictions

The copyright law of the United States (Title 17, United States Code) governs the making of photocopies or other reproductions of copyrighted material.

Under certain conditions specified in the law, libraries and archives are authorized to furnish a photocopy or other reproduction. One of these specified conditions is that the photocopy or reproduction is not to be "used for any purpose other than private study, scholarship, or research." If a, user makes a request for, or later uses, a photocopy or reproduction for purposes in excess of "fair use" that user may be liable for copyright infringement,

This institution reserves the right to refuse to accept a copying order if, in its judgment, fulfillment of the order would involve violation of copyright law.

Please Note: The author retains the copyright while the New Jersey Institute of Technology reserves the right to distribute this thesis or dissertation

Printing note: If you do not wish to print this page, then select "Pages from: first page # to: last page #" on the print dialog screen

ABSTRACT

PROTEIN ENGINEERING OF COTA LACCASE BY USING *BACILLUS SUBTILIS* SPORE DISPLAY

by
Silu Sheng

Spore display offers advantages over more commonly utilized microbe cell-surface display systems. For instance, protein-folding problems associated with the expressed recombinant polypeptide crossing membranes are avoided. Hence, a different region of protein space can be explored that previously was not accessible. In addition, spores tolerate many physical/chemical extremes. The aim is to improve pH stability using spore display. The maximum activity of CotA is between pH 4 and 5 for the substrate ABTS (ABTS = diammonium 2, 2'–azino-bis(3-ethylbenzothiazoline-6-sulfonate)). However, the activity dramatically decreases at pH 4. The activity is not significantly altered at pH 5. CotA is used as a model to prove that enzymes could be improved for pH resistance by using *Bacillus subtilis* spore display. First, CotA is evolved for increased half-life ($t_{1/2}$) at pH 4. Next, a double mutant is constructed. This variant combines the amino acid substitutions from the improved $t_{1/2}$ variant (E498G) and organic solvent tolerant mutant (T480A). The $t_{1/2}$ and kinetic parameters are evaluated for the double mutant. Consequently, T480A/E498G-CotA is constructed and the $t_{1/2}$ is 62.1 times greater than wt-CotA. Finally, T480A/E498G-CotA yields 5.3-fold more product than does wt-CotA after recycling the biocatalyst seven times over 42 h. Also, the mutant and wild-type are overexpressed in *E. coli* and purified. The enzymes immobilized in the spore coat are compared with the purified free protein. The $t_{1/2}$ and catalytic efficiency follow the same

trends for spore or *E. coli* expressed wt-CotA and E498G-CotA, although the kinetic parameters are different.

In a previous investigation, a laccase (CotA), which is found on the spore coat of *Bacillus subtilis*, was engineered by directed evolution for improved activity in organic solvents. A CotA variant was identified with a Thr480Ala (T480A-CotA) amino acid substitution after only one round of evolution. The screen was performed at 60 % DMSO and it was 2.38-fold more active than the wild-type CotA (wt-CotA) with substrate ABTS. T480A-CotA was more active from a range of 0 – 70 % DMSO. In addition, the variant was more active in ethanol, methanol and acetonitrile. In this study, the catalysis of T480A-CotA and wt-CotA in the spore coat is determined with natural phenolic compounds, such as (+)-catechin, (-)-epicatechin and sinapic acid in aqueous-organic media. In general, the catalytic efficiency (V_{max}/K_m ($\delta A/OD_{580}$)/mM) of T480A-CotA is higher than wt-CotA for all the substrates. Then, the V_{max} for T480A-CotA is greater than the wt-CotA in all organic solvents used in this study. The V_{max} for T480A-CotA is up to 3.4-fold, 7.9-fold and 6.4-fold greater than wt-CotA for substrate (+)-catechin, (-)-epicatechin and sinapic acid, respectively. In addition, the catalyst can be easily removed from the reaction solution and reused. This allows for simpler recovery of the product from the enzyme. This investigation indicates that enzymes expressed on the spore coat can be utilized for industrial applications.

PROTEIN ENGINEERING OF COTA LACCASE BY USING *BACILLUS SUBTILIS* SPORE DISPLAY

by
Silu Sheng

A Dissertation
Submitted to the Faculty of
New Jersey Institute of Technology
in Partial Fulfillment of the Requirements for the Degree of
Doctor of Philosophy in Chemistry

Department of Chemistry and Environmental Science

May 2017

.

APPROVAL PAGE

PROTEIN ENGINEERING OF COTA LACCASE BY USING *BACILLUS SUBTILIS* SPORE DISPLAY

Silu Sheng

Dr. Edgardo T. Farinas, Dissertation Advisor — Date
Associate Professor of Chemistry and Environmental Science, NJIT

Dr. Somenath Mitra, Committee Member — Date
Distinguished Professor of Chemistry and Environmental Science, NJIT

Dr. Tamara Gund, Committee Member — Date
Professor of Chemistry and Environmental Science, NJIT

Dr. Mengyan Li, Committee Member — Date
Assistant Professor of Chemistry and Environmental Science, NJIT

Dr. Cristiano L. Dias, Committee Member — Date
Assistant Professor of Physics, NJIT

BIOGRAPHICAL SKETCH

Author: Silu Sheng

Degree: Doctor of Philosophy

Date: May 2017

Undergraduate and Graduate Education:

- Doctor of Philosophy in Chemistry,
  New Jersey Institute of Technology, Newark, NJ, 2017

- Master of Science in Chemistry,
  New Jersey Institute of Technology, Newark, NJ, 2009

- Bachelor of Science in Chemistry,
  Wuhan University, Wuhan, P. R. China, 2008

Major: Chemistry

Presentations and Publications:

Silu Sheng, Han Jia, Sidney Topiol and Edgardo T Farinas, "Engineering CotA laccase for acidic pH stability using *Bacillus subtilis* spore display," *Journal of Microbiology and Biotechnology*, Vol. 27(3), March 2017.

Silu Sheng, Nirupama Gupta and Edgardo T Farinas, "Directed Evolution of CotA Laccase for Increased Substrate Specificity Using *Bacillus subtilis* Spores," 241st ACS National Meeting & Exposition, Anaheim, CA, United States, March 2011.

Silu Sheng, Nirupama Gupta and Edgardo T Farinas, "Directed Evolution of CotA Laccase for Increased Substrate Specificity Using *Bacillus subtilis* Spores," New York Structural Biology Discussion Group - 6th Winter Meeting, New York, United States, January 2011.

ACKNOWLEDGMENT

I want to thank my advisor Dr. Edgardo T. Farinas. He is the person who started my career. When I first came into his group, I barely knew anything about biochemistry. Now I am professional in protein engineering. Without his support and guidance, I cannot complete this thesis. Also I want to thank my committee members Dr. Somenath Mitra, Dr. Tamara Gund, Dr. Mengyan Li and Dr. Cristiano L. Dias for their precious advice about my program.

I want to thank Ms. Genti M. Price and Ms. Sylvana Brito a lot in the office of Department of Chemistry and Environmental Science. They are extremely helpful with all administrative procedures and care every graduate student in our department for real. They are also kind enough for decorating our department during holidays such as Christmas. They are like my family in this department. The department cannot run smoothly without them. I am also grateful to Mr. Yogesh Gandhi and Dr. Ping Gu. They are nice and assisted me a lot for my teaching assistance assignments. I won't forget to thank National Science Foundation (NSF) for providing funds for my research.

Additionally, I would like to thank everyone in my group, Dr. Nirupama Gupta, Dr. Da Jeong Shim, Dr. Han Jia, Mr. Yuchen peng and Mr. Joydeep Chakraborty for friendship, assistance, and exchange ideas and experience. They all contributed to the completion of my thesis.

Finally, I thank my wonderful family, especially my mother, for their love and support throughout my life. I thank my love, Yan Zhang, for her support and understanding during my PhD program.

Finally...

Special Thanks to My Love 张丽

TABLE OF CONTENTS

Chapter		Page
1	INTRODUCTION……..…….	1
	1.1 Evolution in Nature ……..……...	1
	1.2 Directed Evolution …….…….…….…...	4
	1.3 Protein Display ……	10
	1.3.1 *In vitro* Protein Display …….	11
	1.3.2 *In vivo* Protein Display ……..	12
	1.3.3 *E. coli* Cell Surface Display ……..	19
	1.3.4 Yeast Cell Surface Display ……...	21
	1.4 Spore Display ……..	22
	1.4.1 Composition of the *B. subtilis* Endospore …….	24
	1.4.2 Protein Displayed by *B. subtilis* Spores ……	26
	1.5 Laccase ……	29
2	DIRECTED EVOLUTION OF COTA LACCASE FOR ACIDIC PH STABILITY BY USING BACILLUS SUBTILIS SPORE DISPLAY ……...	33
	2.1 Materials ……..	35
	2.1.1 Library Creation …….....	36
	2.2 Methods ……..	39
	2.2.1 Spore Screening for Acidic pH Stability …….....	39
	2.2.2 Acid Inactivation …….....	40
	2.2.3 Kinetics Measurement of CotA and Its Variants ……..	40

TABLE OF CONTENTS
(Continued)

Chapter **Page**

2.2.4 Product Yield of CotA and Its Variants …… 41

2.2.5 Cell Viability ……..... 41

2.2.6 Overproduction and Purificaiton of CotA and Its Variants …….. 41

2.2.7 Acid Inactivation and Kinetics Measurement of Purified CotA ……... 43

2.3 Results and Discussion …… 43

2.4 Conclusion ……. 64

3 OXIDATION OF PHENOLIC COMPOUNDS WITH COTA LACCASE AND ITS MUTANT ON BACILLUS SUBTILIS SPORE COAT IN ORGANIC MEDIA ……... 65

3.1 Materials ……..….. 69

3.2 Methods ……..….. 69

3.2.1 Wt-CotA and T480A-CotA Activity Versus pH ……... 69

3.2.2 Determination of Kinetic Parameters of Wt-CotA and T480A-CotA ….. 70

3.2.3 Wt-CotA and T480A-CotA Activity in Organic Solvents …… 71

3.2.4 Wt-CotA and T480A-CotA Recylcing in Organic Solvents ……. 71

3.3 Results and Discussion …… 72

3.3.1 Wt-CotA and T480A-CotA Activity Versus pH ……... 72

3.3.2 Determination of Kinetic Parameters of Wt-CotA and T480A-CotA ….. 75

3.3.3 Activity of Wt-CotA and T480A-CotA in Organic Solvent ……. 78

3.3.4 Wt-CotA and T480A-CotA Recylcing in Organic Solvents ……. 81

3.4 Conclusion ……... 84

TABLE OF CONTENTS
(Continued)

Chapter	Page
APPENDIX ENZYME DISPLAY FOR ALKANE OXIDATION ……...	85
REFERENCES ……...	119

LIST OF TABLES

Table		Page
1.1	Number of Amino Acid Changes versus Number of Variants…...……...	7
2.1	Kinetic Parameters and Half-life of Wild-type CotA and CotA Variants …….	46
2.2	Product Yields of Wild-type CotA and CotA Variants ……..…...……..	56
2.3	Kinetics Parameters of Purified Wild-type CotA and E498G-CotA...……..…….	61
3.1	Kinetics Parameters of Wt-CotA and T480A-CotA with Different substrates...…	77
3.2	V_{max} ($\delta A/OD_{580}$) of Wt-CotA and T480A-CotA in 0 – 70 % Organic Solvents for Substrate (+)-Catechin (A), (-)-Epicatechin (B) and Sinapic Acid (C)…….	80
3.3	The (+)-Catechin Products Yields for Wt-CotA and T480A-CotA Were Determined for 7 Cycles Over A 23 h Period…….	83

LIST OF FIGURES

Figure		Page
1.1	The evolutionary tree of life……..…….	1
1.2	Evolution of red beetles……..……	3
1.3	Myoglobin Evolution ..…..……...…...……..……	4
1.4	An illustration of directed evolution...……..……..	6
1.5	Scheme of random mutagenesis…..……	9
1.6	Scheme of DNA shuffling……..	10
1.7	Scheme of available display technologies……..	11
1.8	“Traditional” methods of protein display…...……	13
1.9	Two strategies of screening……...…….	14
1.10	Screening protein libraries in the cell……...……..	15
1.11	Genotype/phenotype connection for proteins expressed inside the cell….……	16
1.12	An example of directed evolution by cell surface display….…….	17
1.13	Problems in traditional cell surface protein display…..……...	18
1.14	Cell membrane structure of *E. coli*…..……	19
1.15	Different strategies to display passenger proteins on the surface of *E. coli*……...	20
1.16	Schematic illustration of a yeast cell surface display…..……	22
1.17	*B. subtilis* sporulation process…..……	23
1.18	Illustration of traditional display and spore display…..……...	24
1.19	Structure of *B. subtilis* spore under transmission electron microscopy (TEM)…..	25
1.20	Model of spore coat assembly…..……	28

Figure **Page**

1.21 Reaction of catalysis of laccase…. 29

1.22 Ribbon diagram of the ABTS-CotA complex…... 30

1.23 Ribbon diagram of Thr260Leu-CotA…. 31

1.24 Ribbon diagram of Thr480Ala-CotA…. 32

2.1 pH effect on enzyme activity…. 34

2.2 CotA was amplified with error prone PCR and transformed into *E. coli*…….. 37

2.3 CotA library was transformed into *Bacillus subtilis* and displayed on cell surface……... 38

2.4 CotA was integrated into the genome of *Bacillus subtilis* by double-cross recombination.…….. ……. 38

2.5 Optimal enzymatic activity was found at pH 4.0 – 5.0 for ABTS …..…… 44

2.6 An example of one microtiter plate of coefficient of variance (CV)…. 45

2.7 Molecular model of ABTS-Y19…. 47

2.8 The $t_{1/2}$ at pH 4 of wt-CotA and CotA variants …. 48

2.9 Kinetic parameters of wt-CotA and CotA variants on *Bacillus subtilis* spore coat.……... 49

2.10 V_{max} (μM/min/OD_{580nm}) of wt-CotA (light shaded bars), T480A/E498G-CotA (dark shaded bars) and E498G-CotA (white bars) in 0 – 70 % organic solvents.…….. 54

2.11 Product yields of $ABTS^{+}$ of wt-CotA and its variants over 42 h …..…….. 57

2.12 Extraction of spore coat proteins…... 58

2.13 Viability assay of spores in citrate phosphate buffer (100 mM, pH 4)…. 59

2.14 SDS-PAGE analysis of CotA overproduction in *E. coli* …... 60

2.15 The $t_{1/2}$ at pH 4 of wt-CotA and E498G-CotA…... 62

Figure **Page**

2.16 Kinetics parameters of purified wt-CotA and E498G-CotA from *E.coli*…….. 63

3.1 Structure of phenolic substrates ….…… 67

3.2 Oxidation of phenols by laccase ….……... 68

3.3 Effect of pH on laccase-catalyzed oxidation of (+)-catechin (A), (-)-epicatechin (B), and sinapic acid (C).……..…….. 74

3.4 Kinetic parameters of wt-CotA and T480A-CotA on Bacillus subtilis spore coat for substrates (+)-catechin, (-)-epicatechin and sinapic acid.……..……... 76

3.5 V_{max} (δA/OD580) of wt-CotA (black bars) and T480A-CotA (grey bars) in 0 – 70 % organic solvents for substrate (+)-catechin (A), (-)-epicatechin (B), and sinapic acid (C).……..……. 79

3.6 The (+)-catechin products yields for wt-CotA (black bars), and T480A-CotA (white bars) were determined for 7 cycles over a 23 h period……... 83

CHAPTER 1

INTRODUCTION

1.1 Evolution in Nature

Evolution is the process by which organisms have descended from ancient ancestors. Time is not the main factor in evolution, but it is genetic inheritance [1]. In Darwin's theory, all organisms share common ancestors [2]. Species change over time and space. Species living today are different from those in the past. This evolutionary change can be gradual and slow (Figure 1.1) [3].

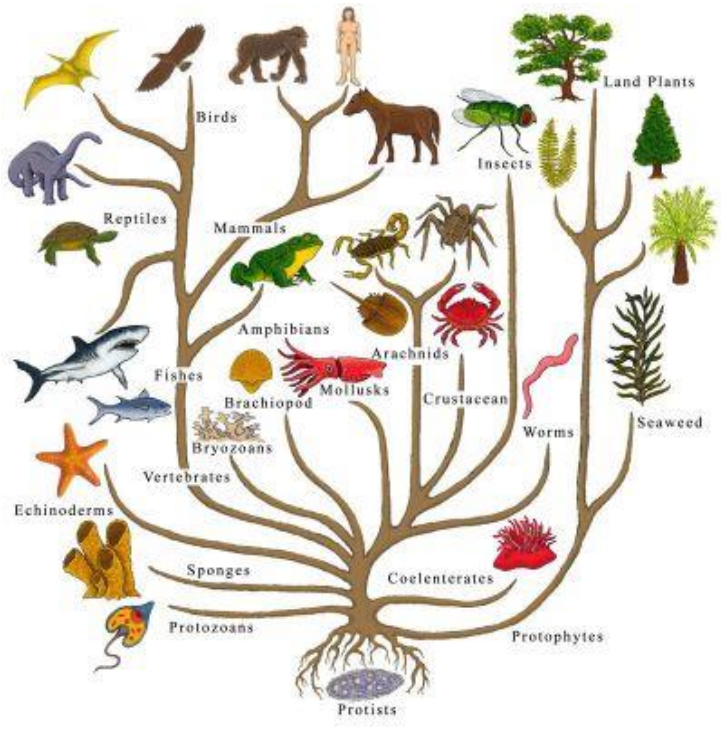

Figure 1.1 The evolutionary tree of life. Natural biological evolution is modification through genetic inheritance that passing on from parents to offspring.
Source: https://bethbuddenteacher.wordpress.com/2015/01/02/teaching-evolution/ (accessed on April 18, 2017)

The primary mechanism of evolutionary change is natural selection. Charles Darwin introduced this concept in 1859 [4]. Variation exists within all populations of organisms and occurs partly because random mutations that take place in the genome of an individual organism. These mutations can be passed on from parent to offspring, therefore, such changes are heritable [5]. The struggle for resources will favor individuals with some variations over others from one generation to the next, and thereby change the frequency of traits within the population (Figure 1.2) [6]. For example, there may have a population of red beetles in ancient times. A mutation occurred in the DNA which caused the parents with genes for red coloration to have offspring with a gene for green coloration. This species lives on the tree; therefore, red beetles are easier for birds to identify and eat. Green beetles are a little more likely to survive to produce offspring. They pass their genes for green coloration on to their offspring because they blend into the background. As time goes, this species will evolve from red to green under natural selection.

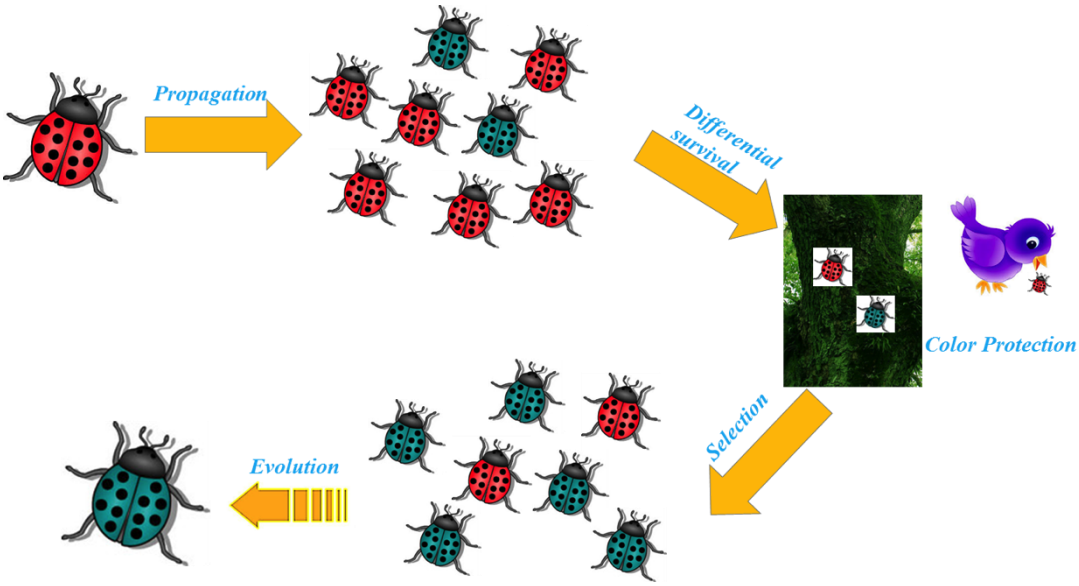

Figure 1.2 Evolution of red beetles. Evolution in nature happens over time based on differential survival of offspring.

Evolution can also occur on the single molecule level, such as proteins. For example, myoglobin is an oxygen-binding protein found in the muscle tissue in almost all mammals. Myoglobin from human and whale contain 153 and 154 amino acids, respectively. There are 25 amino acid differences by comparing the sequences of both myoglobins (Figure 1.3) [7]. Thus, the proteins had a common ancestor and the number of amino acid substitutions in two related proteins is roughly proportional to the evolutionary time. These proteins have evolved in the context of the organism in order to survive. In essence, a whale myoglobin may not function properly in a human.

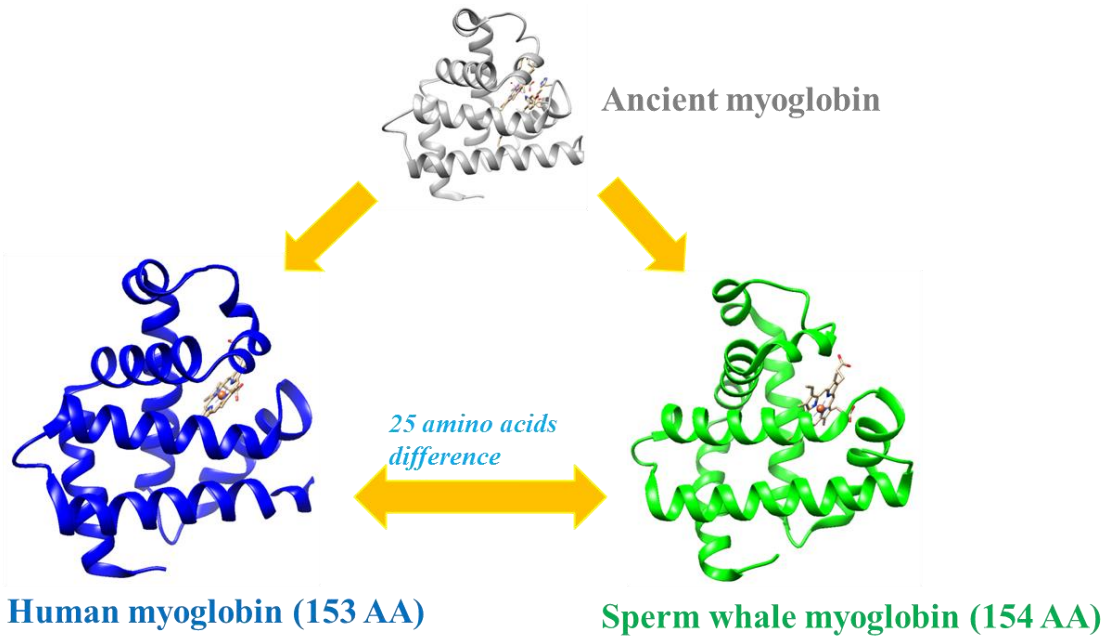

Figure 1.3 Myoglobin evolution. Evolution can also occur on the single molecule level such as proteins.

1.2 Directed Evolution

Enzymes are potentially catalysts and can be used in industrial processes. They can be used as "green" catalyst because they operate at room temperature and aqueous solutions. Furthermore, they have high substrate specificity and can produce chiral products with high enantiomeric excess [8]. However, these advantages can also be shortcomings when used in industrial conditions, because they have evolved for millions of years and adopted specific properties. In industry, extreme conditions are used such as high salt concentration, temperature, and organic solvents. These conditions often inactive enzymes [9]. As a result, an efficient method must be used to engineer and optimize the enzymes.

The two extremes of protein engineering are rational design and evolutionary

(irrational) methods. Rational design requires in-depth knowledge of the protein structure, and its catalytic mechanism [10]. Amino acid substitutions are guided by the structure of the protein. However, it is still extremely difficult to predict the effect of an individual amino acid mutation even with a known structure. Therefore, this method is not always reliable for protein engineering and optimization. On the other hand, evolutionary methods do not require a structure or details of the mechanism of the desired activity [11]. The only requirement is the gene of interest. This method uncovers amino acid substitutions than one can never predict. For example, amino acid substitutions that improved catalytic activity can be far from the active site [12]. As a result, evolutionary strategies, also known as directed or laboratory evolution, have become the methods of choice. It opens a way to overcome some of the barriers to implement proteins for application in industry, biotechnology, and pharmaceuticals [13].

Directed evolution is a protein engineering method that mimics natural evolution. The main goal of this engineering strategy is to obtain proteins with improved or optimized properties, for example resistance to unusual pH, temperature, organic solvent, etc. Furthermore, amino acid substitutions uncovered that optimize a protein can be used to study structure/function relationships [14].

Directed evolution is an iterative process and there are four general steps: (1) diversification: generate gene library of the target protein (2) expression of protein library (3) screen the library under a specific condition for desired functions and (4) amplify the selected “winner” (a member in the library) (Figure 1.4).

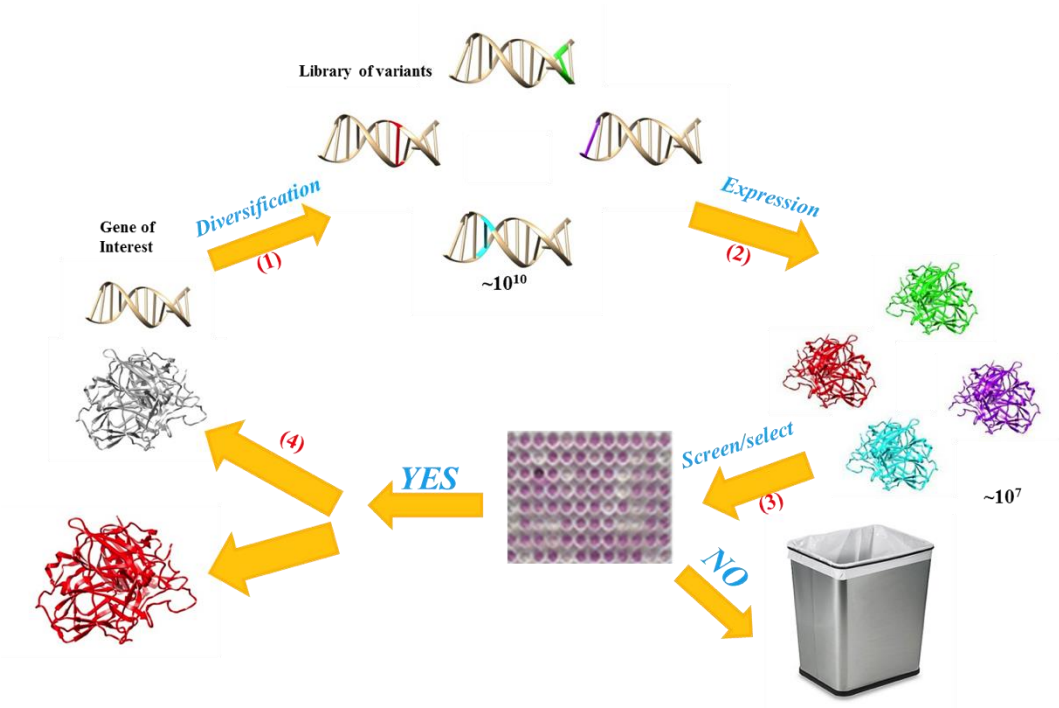

Figure 1.4 An illustration of directed evolution. Directed evolution is a protein engineering method that mimics natural evolutions.

The size of DNA library needs to be addressed. The mutation rate needs to be controlled to make the library size manageable because libraries may have to be exhaustedly screened to discover a winner. It is physically impossible to screen extremely large libraries. The number of variants V of a protein of amino acid length L that differ by a mutation number of H is given by the Equation 1.1 [15]:

$$V = 19^{H}\left[\frac{L!}{H!(L-H)!}\right] \tag{1.1}$$

For example, a protein of L = 300, the number of variants with a mutation number H = 1 there are 5700 variants. If there are two amino acid substitutions (H = 2) then the number

of variants V is 1.6×10^7. Finally, the number of variants (V) with a mutation number H = 3 is 3×10^{10} (Table 1.1). It becomes physically impossible to effectively screen library sizes with a mutation rate greater than 2. As a result, the mutation rate should be approximately 2 per gene.

Table 1.1 Number of Amino Acid Changes versus Number of Variants.

Number of Amino Acid Changes	Number of Variants
0	1
1	5700
2	$1.6*10^7$
3	$3.0*10^{10}$
4	$4.3*10^{13}$
5	$4.8*10^{16}$

Note: The number of variants of a 300 amino acid long protein.

Many powerful technologies were developed to create a sizable library and generally can be divided into three categories: 1) saturation mutagenesis, which is a method to simultaneously introduce the other 19 amino acid at a specific site [16];
2) random mutagenesis, which mimics asexual reproduction [17]; 3) DNA recombination, also known as DNA shuffling, which mimics sexual reproduction [18].

Saturation mutagenesis is a technique that generate all possible (or as close to as possible) mutations at a specific site or a narrow region of a gene. It involves the

randomization of one codon of a gene using synthetic oligonucleotides possessing a randomized codon flanked by wild-type sequences. Several codons may also be randomized, simultaneously, though this results in large libraries. This technology is limited because it requires knowledge of functional important regions of the enzyme, and relies heavily on structural insights for site specific targeting in proteins.

Random mutagenesis and DNA recombination are more commonly evolutionary strategies used in the laboratory [19]. Random mutagenesis mimics asexual reproduction and introduces random mutations in the gene of interest by a thermal stable DNA polymerase [20]. The reaction condition of the polymerase chain reaction (PCR), which amplifies DNA, is altered in order to introduce random mutations in the gene [21]. This is called error prone PCR (ep-PCR). Ep-PCR has several steps (Figure 1.5): (1) The gene is selected; (2) the target gene is amplified; (3) the PCR products are inserted into a carrier plasmid; (4) the plasmids containing the target gene are translated to proteins.

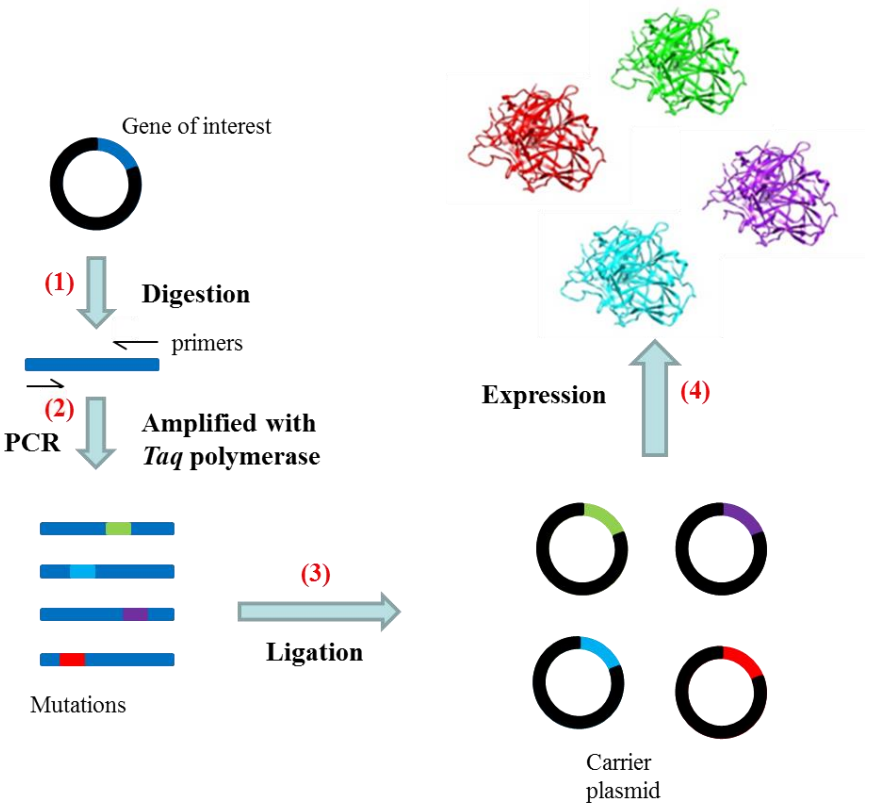

Figure 1.5 Scheme of random mutagenesis. Random mutagenesis mimics asexual reproduction and is commonly done by epPCR.

The second type is recombination of genes that mimics sexual reproduction: DNA shuffling [22,23]. Generally, DNA shuffling can be divided into several steps (Figure 1.6). (1) The gene fragments are first created by DNAse digestion. Each fragment may contain mutations. The different colors along the genes in Figure 1.6 represent different mutations. For example, yellow may denote blond hair, and blue may represent blue eyes. (2) The full-length of DNA is generated PCR. (3) After amplification, the target DNA is inserted in a carrier plasmid. (4) Proteins are expressed like in random mutagenesis.

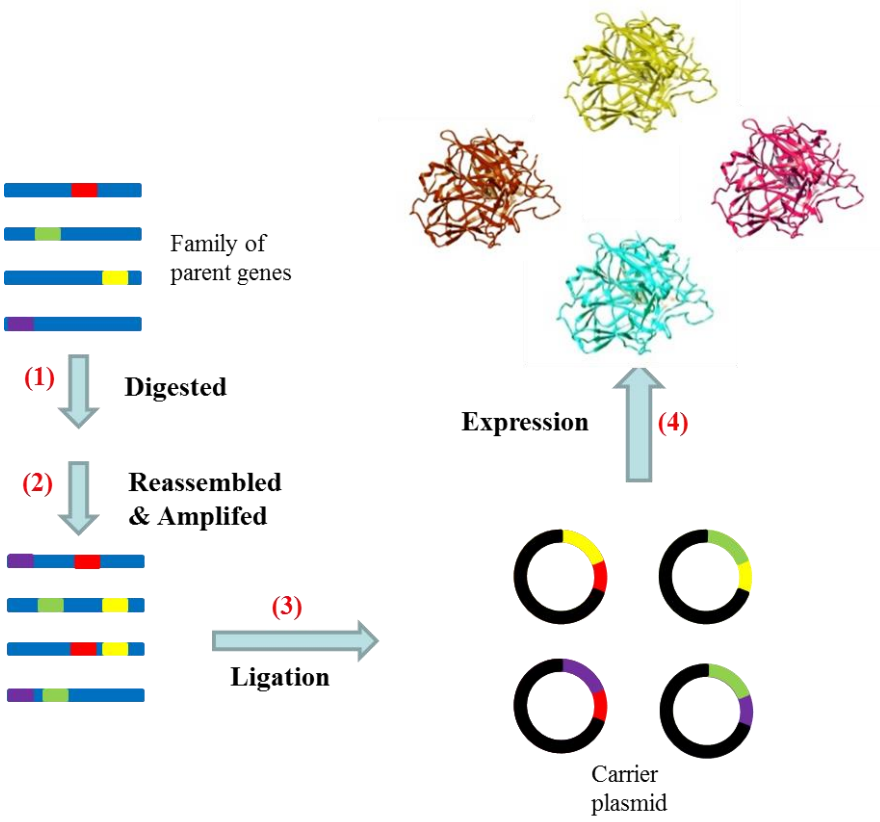

Figure 1.6 Scheme for DNA shuffling. DNA shuffling was developed to mimic sexual reproduction.

1.3 Protein Display

The principle of protein display technologies is the ability to physically link phenotypes of polypeptides displayed in a certain system to their corresponding genotype, which was first shown for phage display [24]. This connection must remain intact for a successful evolution experiment. These technologies could be divided into two major categories, *in vivo* and *in vitro*. *In vitro* includes phage and cell surface display, while *in vivo* consists of ribosome, RNA and DNA display (Figure 1.7) [25].

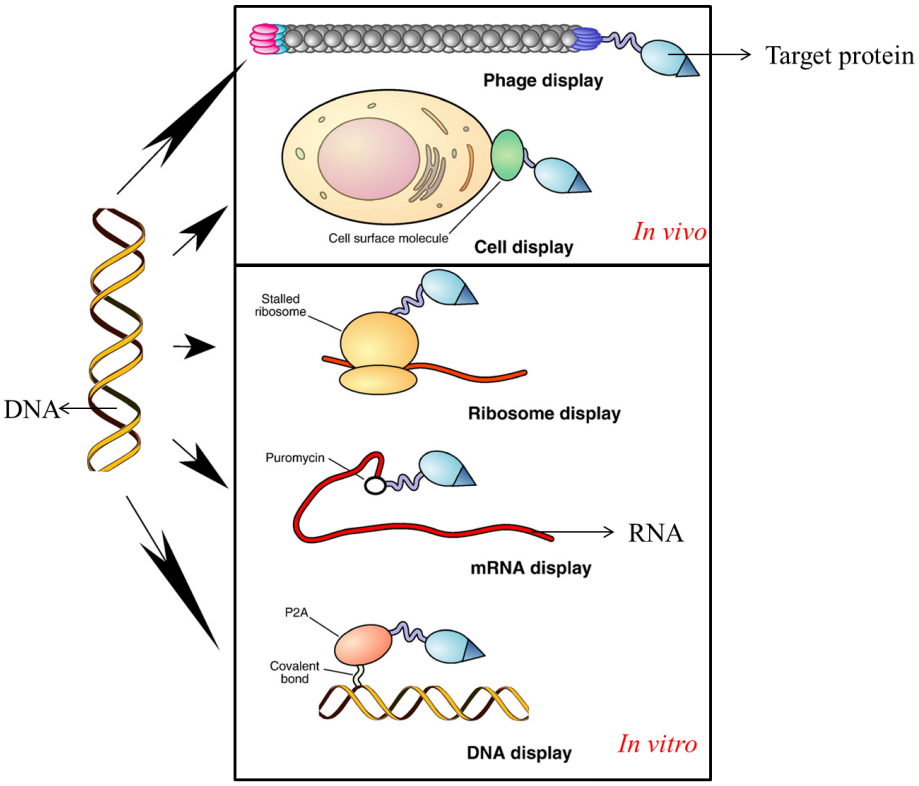

Figure 1.7 Scheme of available display technologies. All display platforms are based on the ability to physically link the polypeptide produced by a library clone to its corresponding genotype. This allows one to recover the DNA encoding the clone selected based on the desired polypeptide phenotype, such as binding to the target [25].

1.3.1 *In vitro* Protein Display

The major potential advantage of *in vitro* protein display over *in vivo* methods is the size of the libraries that can be displayed and therefore the diversity subject to selection, because in cell-free assays there is no transformation step and no limit for library diversity [26]. However, *in vitro* methods have limitations. For example, mRNA display is not suitable for displaying membrane-bound proteins due to the difficulty in expressing such proteins using *in vitro* translation systems [27]. Also, screening conditions that may break the genotype/phenotype connection should not be applied. These technologies were

usually used to screen for specific high-affinity target-binding molecules including peptides, antibody fragments, and whole functional proteins presented by various scaffolds [28,29].

The connection between the genotype and phenotype is achieved by different strategies in these *in vitro* technologies (Figure 1.7). In ribosome display, linkage between the gene and the encoded polypeptide is achieved by stabilization of complexes between the ribosome, mRNA and the encoded polypeptide upon termination of elongation with a permissive marker, such as chloramphenicol or low temperature [30]. In mRNA display, linkage between the gene and the encoded polypeptide is achieved by a puromycin molecule covalently bonding the mRNA 3'-end and the translated polypeptide upon the ribosome stalling at the junction of mRNA and an engineered single-stranded DNA linker [28]. In covalent DNA display, linkage between the gene and the encoded polypeptide is achieved by covalent bond that forms between the DNA-binding protein P2A (produced as a fusion with polypeptide) with the DNA encoding the fusion [28].

1.3.2 *In vivo* Protein Display

Generally the screening can be performed under *in vivo* conditions [31]. This means proteins translated from DNA libraries can be transported to the microorganism. "Traditional" methods such as phage display [32], bacterial display [33,34] and yeast display [35,36] are suitable when the evolved protein is to be used in living organisms (Figure 1.8).

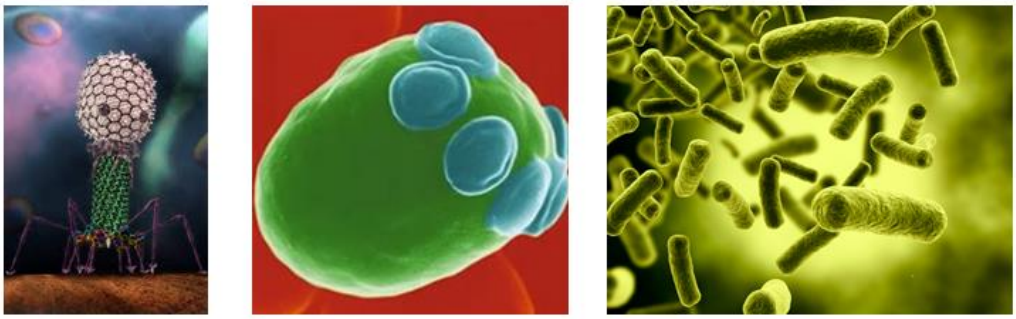

Figure 1.8 "Traditional" methods of protein display. Protein can be displayed with (A) phage, (B) yeast or (C) *Escherichia coli* (*E. coli*).

In general, there are two screening strategies. The first one is expressing protein libraries inside the host, for example, in the cytoplasm of *E. coli* (Figure 1.9A). The other way is first expressing protein libraries inside the host, and then transporting the protein to the surface to be displayed outside the host cells (Figure 1.9B). This strategy is called cell surface display. The protein displayed on the cell surface is often fused to a carrier protein. The carrier protein is usually a natural occurring protein found on the surface or outer membrane, which is represented as a green circle in Figure 1.9B.

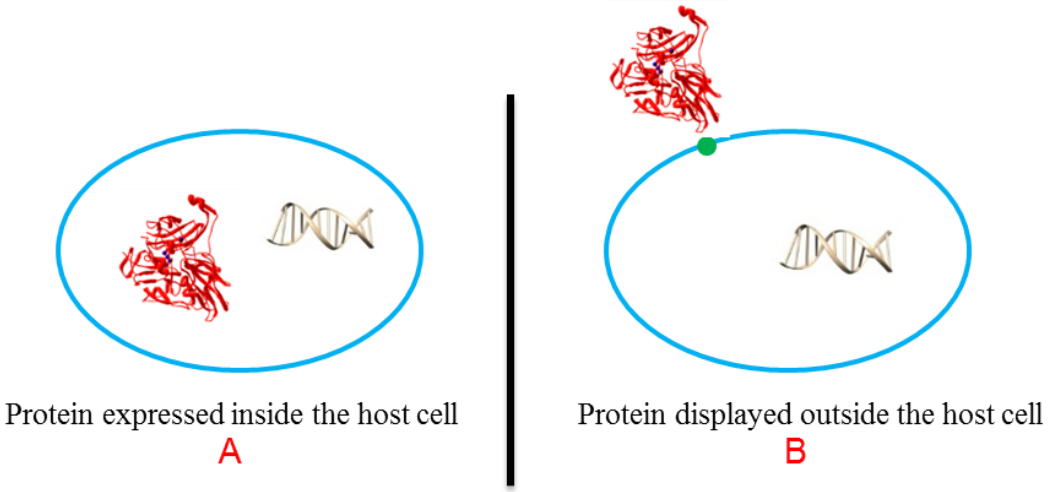

Figure 1.9 Two strategies of screening. (A) Proteins are expressed inside the host. Red structure represents proteins, grey structure represents DNA, and in blue is the cell surface; (B) Protein displayed outside the host cell. Green circle represents carrier proteins.

Displaying proteins libraries on the cell surface has advantages over expressing libraries inside the cells. If the protein is displayed inside, then the cells must be lysed to gain access to the protein for the assay (Figure 1.10). Therefore, the connection between genotype and phenotype will be lost (Figure 1.11). In other words, the improved protein and the gene that codes for it is separated and must be retrieved from another plate (Figure 1.10). In addition, the assay is hindered because of multiply liquid handling steps. For example, the cell lysates require centrifugation in order to pellet the cell debris and the supernatant may be pipetted into another reaction vessel for the assay (Figure 1.10). Finally, the assay solution is complicated furthermore by the soluble contents of the cell, which may include DNA, RNA, proteins, etc…

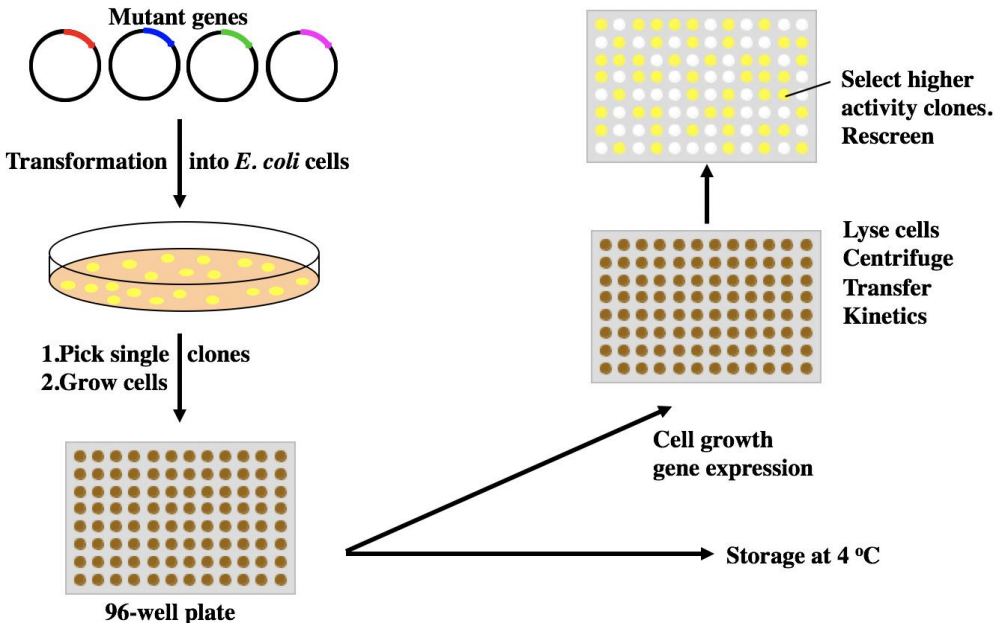

Figure 1.10 Screening protein libraries in the cell. 1) Library is transformed into cells. 2) Single colonies are picked into microtiter plate and grown. 3) A duplicate plate is made and the original plate is stored to retrieve the gene of the improved protein variant. This gene is used a parent for the next rounds of evolution.

Cell surface display may overcome issues discussed above. First, the genotype/phenotype connection remains intact. Next, substrates or protein targets are freely accessible. Furthermore, liquid handling is minimal. In addition, there is more control of the assay conditions because it is not complicated by addition of the soluble contents of the cell. Finally, the reaction solution can be easily exchanged by centrifugation.

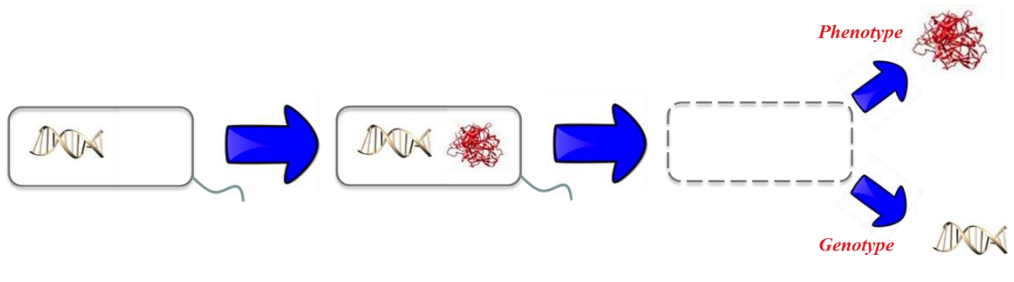

Figure 1.11 Genotype/phenotype connection for proteins expressed inside the cell. Cell lysis is necessary to gain access to the protein. As a result, the genotype-phenotype connection will be lost.

Many strategies are developed for directed evolution by using cell surface display. Figure 1.12 shows steps of an example of evolving a protein to bind a specific target: (1) Gene libraries are transformed into cells. (2) The library is expressed on the cell surface and each cell contains a unique member of the gene library. (3) The library is screened for binding a target. (4) The proteins that bind nonspecifically are eliminated by a wash step. (5) The improved protein is released from the target. (6) The cells are cultured and the gene is isolated for another round of evolution.

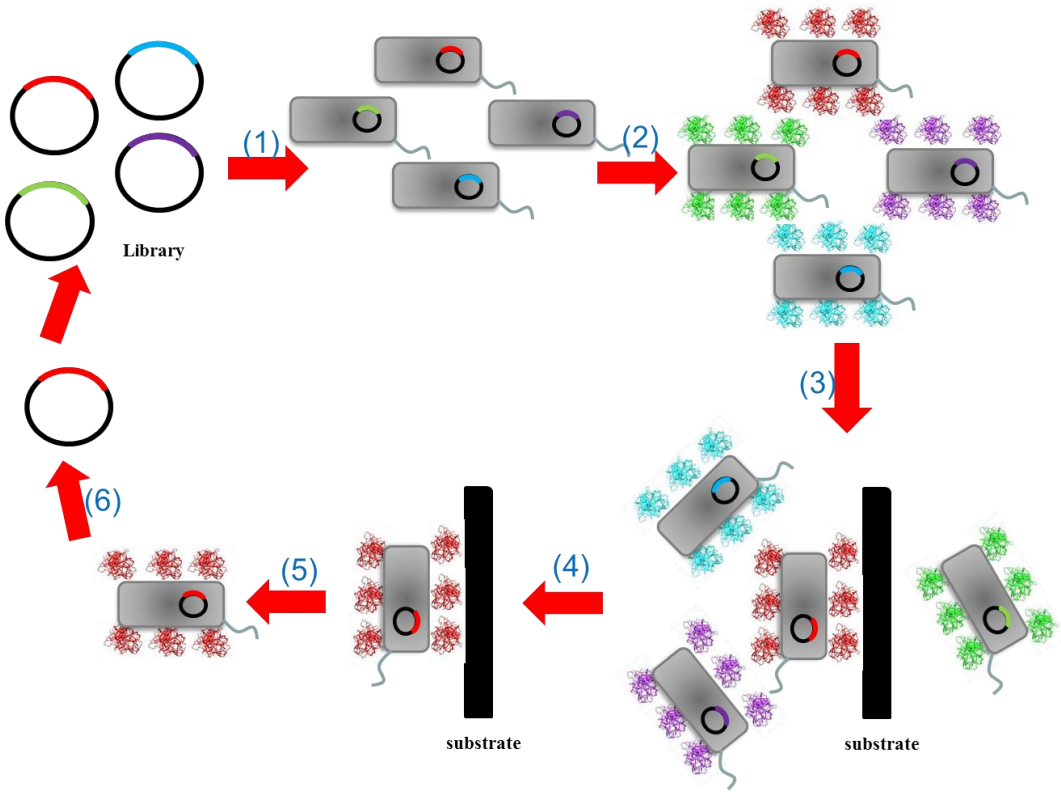

Figure 1.12 An example of directed evolution by cell surface display. A library is screened by using affinity binding assay.

Traditional cell surface display methods are powerful and many proteins were evolved for improved properties or functions [37]. This technology has transformed protein discovery in industry and academia. For example, *E. coli* is considered an attractive host because of the availability of various genetic tools and mutant strains and the high transformation efficiency for screening of a large peptide or protein library after surface display [38]. Screening displayed proteins with extreme properties has many advantages in designing pharmaceuticals and industrial catalyst. Although protein display seems ideal, there are some severe limitations, which are cell viability and protein folding.

Cell viability is a major issue. For example, industrial reaction conditions may require elevated temperatures or organic solvents to dissolve hydrophobic substrates. However, screening with harsh assay conditions will lyse the cells and the genotype/phenotype connection will be lost (Figure 1.12, step 3; Figure 1.13). Furthermore, screening under extreme conditions or toxic substrates, the cell will not remain viable. As a result, the cells cannot be cultured and the gene cannot be isolated (Figure 1.12, step 5 & 6).

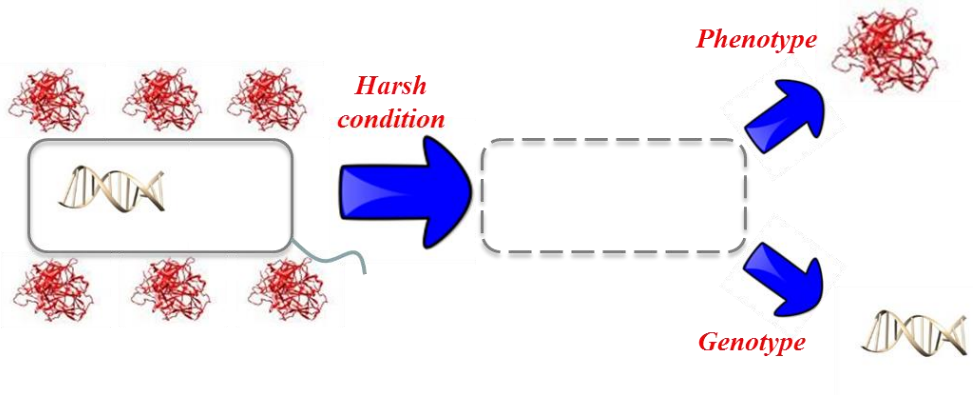

Figure 1.13 Problems in traditional cell surface protein display. The connection of genotype and phenotype will be gone if the cell is lysed under harsh condition.

Also, there are protein folding issues. In *E. coli* for instance, disulfide bonds cannot properly form because the proteins are expressed in the cytoplasm, which is a reducing environment [39]. Also, the target proteins must travel through several membranes to reach cell surface. First, the protein travels through the inner membrane, and then passes across the peptidoglycan layer, and finally the protein travels to the outer

membrane (Figure 1.14). This causes misfolded and nonfunctional proteins. Taken together, these technologies limit the numbers of proteins that can be displayed [40,41].

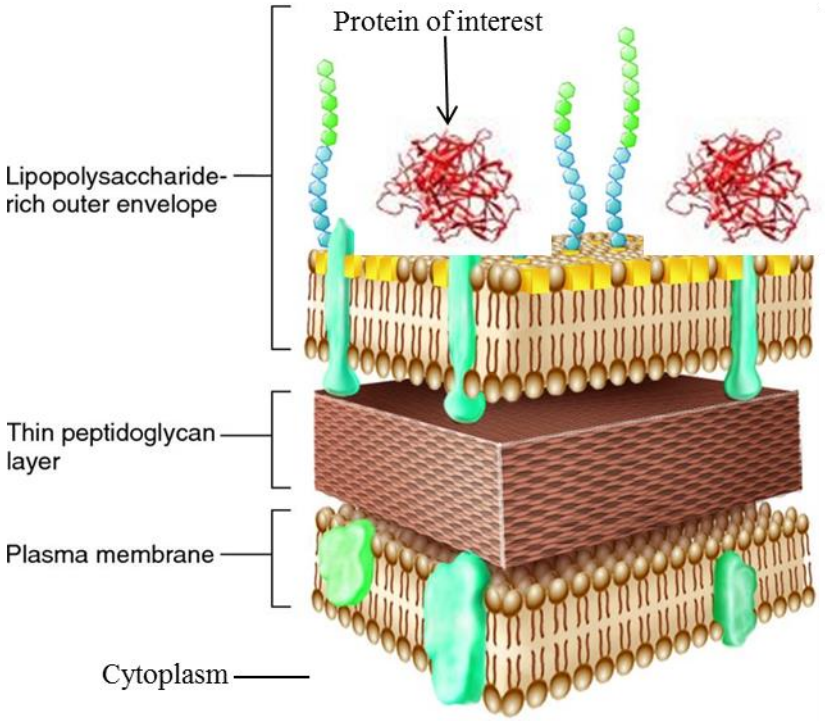

Figure 1.14 Cell membrane structure of *E. coli*. Proteines are first expressed in cytoplasm. They may misfold when travelling across membranes to the surface.

1.3.3 *E. coli* Cell Surface Display

Among Gram negative bacteria, *E. coli* has been extensively investigated in cell surface engineering. It is an attractive host for cell surface display because of the availability of various genetic tools and mutant strains and the high transformation efficiency for screening of a large peptide or protein library. To display heterologous proteins onto the surface of *E. coli*, different strategies were used. These include the insertion of the target sequences into the surface exposed outer membrane proteins; insertion of target sequences into a protein forming part of a cell surface structure such as a flagellum; or

the fusion of target sequences to the N-terminus of lipoproteins (Figure 1.15).

The major problem is the target proteins need to cross two bacterial membranes to reach the extracellular surface. This may cause protein misfolding and disfunction. Also, the fragility of outer membrane caused by the display of proteins can be a problem. In addition, this method cannot be used to evolve proteins with extreme properties, which is due to viability issues as mentioned above.

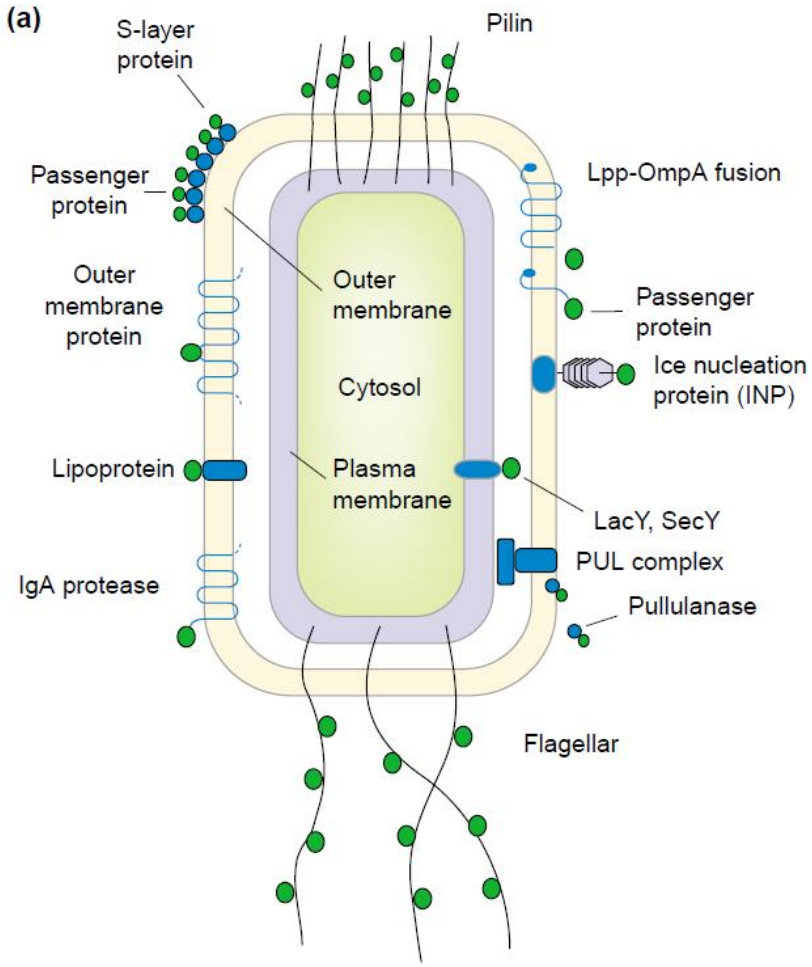

Figure 1.15 Different strategies to display passenger proteins (green circles) on the surface of *E. coli*.
Source: [38]

1.3.4 Yeast Cell Surface Display

Yeast surface display involves the expression of protein of interest on the yeast cell wall by using N-terminal fusion or C-terminal fusion and it can be used for post-translational modification found in eukaryotic organisms (Figure 1.16) [35]. Using α-galactosidase as a target protein, it was demonstrated that a number of cell wall proteins (Cwp1p, Cwp2p, Agα1p, Tip1p, Flo1p, Sed1p, YCR89w, and Tir1) could be used as N-terminal fusion [42]. For C-terminal fusion, the most widely used anchor is Aga2. The cell wall protein a-agglutinin consists of two subunits, Aga1p and Aga2p. Aga1p is incorporated into the cell wall, whereas Aga2p fused with a target protein is conjugated to Aga1p via a disulfide bond.

Glycosylated proteins have been successfully displayed on yeast. However, differential glycosylation may interfere with the function of the displayed protein [43]. A potential disadvantage of yeast display is that the library size is limited to 10^6-10^7 because of low transformation efficiency. In addition, this method also suffers from viability concerns when screen under extreme conditions.

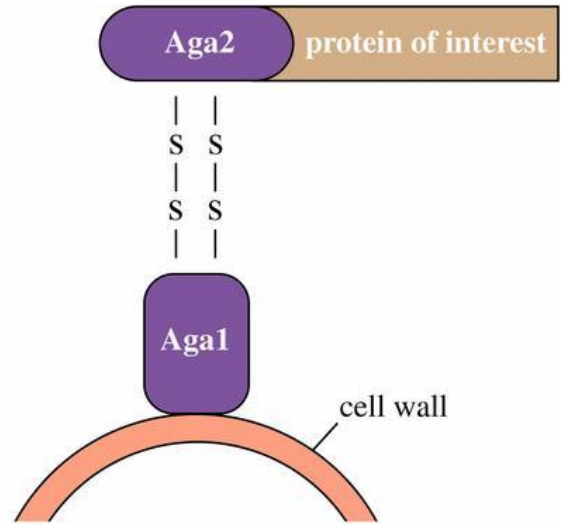

Figure 1.16 Schematic illustration of a yeast cell surface display.

1.4 Spore Display

Spores may overcome the problems associated with traditional protein display. A brief overview of sporulation needs to be discussed for the gram-positive organism *Bacillus subtilis*. Bacterial spores are formed in response to starvation. The best studied spore-forming bacteria is *B. subtilis*, which is found to have no safety concerns for labotory use. Sporulation of *B. subtilis* (Figure 1.17) proceeds through a well-defined series of morphological and biosynthetic steps: (1) an asymmetric division of the sporulating cell creates a sporangium composed of two compartments: the mother cell and the forespore. The mother cell nurtures the forespore and the proteins that make up the coat are synthesized. (2) The mother cell engulfs the forespore as the spore coat is formed. Coat assembly begins just after the initiation of engulfment and continues

throughout sporulation. (3) The spore is formed. (4) The cells are lysed. (5) The spores are released.

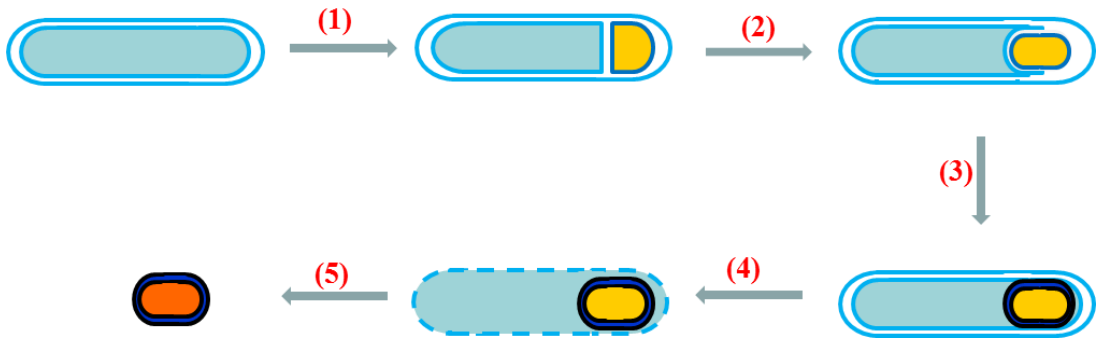

Figure 1.17 *B. subtilis* sporulation process.

Spores are the most resistant form of life on earth and remain viable under extreme chemical and physical conditions and they do not lyse. As a result, proteins can be evolved to possess extreme properties. For example, displayed proteins can be evolved to remain active in organic solvents [44]. Screening under these conditions would lyse the cell in traditional protein display, which would separate the gene from the improved protein (Figure 1.18A). In short, spore display maintains the genotype/phenotype connection intact (Figure 1.18B). In addition, protein folding problems associated with the target protein traveling through cell membranes is eliminated, which is due to the natural sporulation process [45]. Furthermore, the mother cell contains ATP-dependent chaperone proteins, which assist in folding proteins.

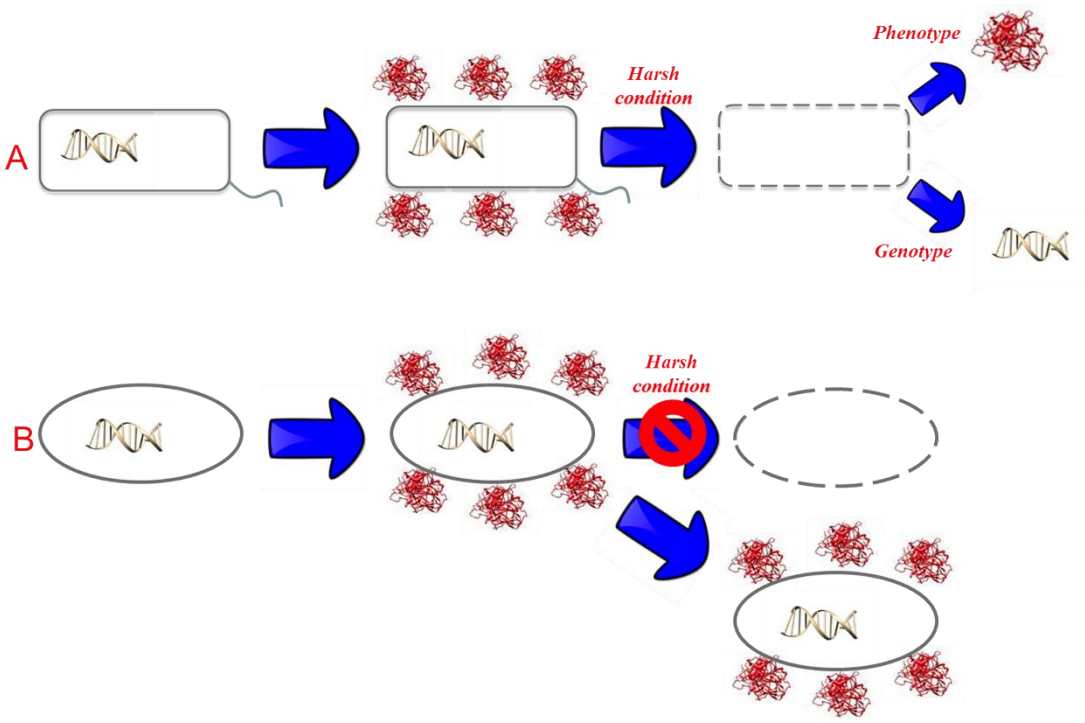

Figure 1.18 Illustration of traditional display and spore display. (A) The connection of genotype and phenotype is lost under harsh conditions in traditional display methods. (B) The connection of genotype and phenotype remain intact under harsh conditions in spore display.

Spore displayed proteins is convenient and has economic advantages in industrial application. For example, enzymes are immobilized on the inert surface of spore coat and become more stable. Next, spores can be easily removed from the reaction mixture to ease in product purification.

1.4.1 Composition of the *B. subtilis* Endospore

The *B. subtilis* spores are encased in a well protecitve coat consisting of an inner coat and outer coat that make the spores can withstand extremes of heat, desiccation, and

chemicals (Figure 1.19). The coat outside the spores are composed of >70 different proteins (Figure 1.20). The layer beneath the inner coat is called cortex, separated from the coat by a outer membrane. The cortex is composed predominantly of peptidoglycan with a structure similar to that of peptidoglycan in growing cells. The cortex is essential for the attainment and maintenance of the dehydrated state of the spore core, for spore mineralization and for dormancy [45]. The central part of the spore is the core, separated from the cortex by a inner membrane. It contains one copy of the bacterial chromosome and plasmid copies if present in the vegetative cell. The DNA molecules in the core are complexed with small acid-soluble proteins (SASPs), making up as much as 20 % of the total spore protein [46].

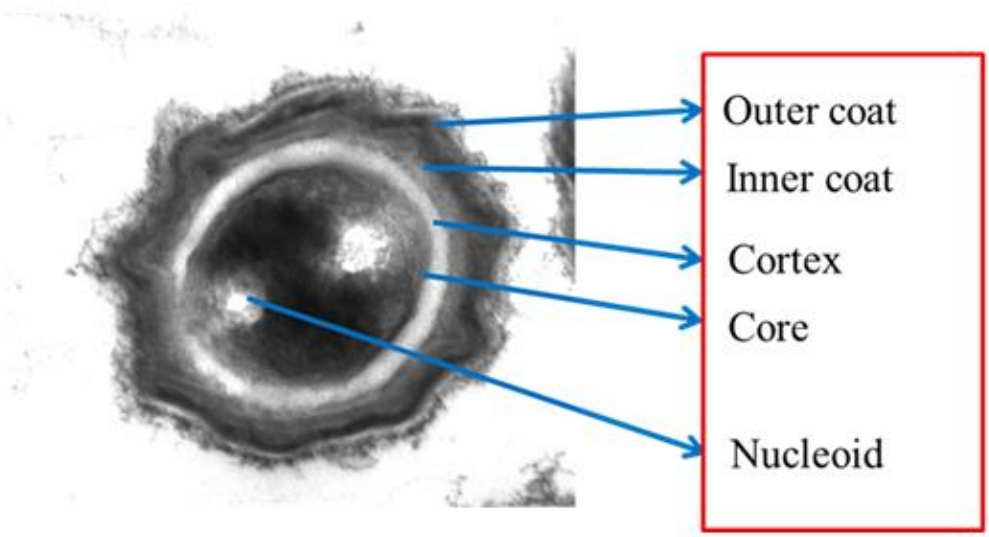

Figure 1.19 Structure of *B. subtilis* spore under transmission electron microscopy (TEM).

1.4.2 Protein Displayed by *B. subtilis* Spores

As descirbed above, the proteins on the spore coat are synthesized inside the sporulating mother cells and deposited on the spore surface as prespores emerge (Figure 1.17). Thus, proteins can be displayed on the spore surface by fusing with coat proteins (Figure 1.20). Up to now, *B. subtilis* spore display has been used for a range of biotechnological applications, such as vaccine development [38,47-49] and whole-cell biocatalysts [50]. Our group first demonstrated that the spore display system could be used for directed evolution [51].

The spore-display system is based on the construction of gene fusions between heterologous DNA and a *B. subtilis* gene coding for a spore coat protein that located on the spore surface. The outer surface proteins CotG, CotB, and CotC were demonstrated to be able to display enzymes and heterologous antigens. All three proteins are tyrosine-rich and present as multimers within the spore coat [52]. CotG has a central region formed by nine tandem repeats of a lysine-, serine-, and arginine-rich motif [53]. CotB is a 46-kDa polypeptide which is posttranslationally converted into a form of about 66 kDa [54]. CotC forms multimeric species with itself [55].

Until now, CotG has been used to display β-galactosidase (β-Gal) [50]. β-Galactosidase is a very large protein (116 kDa per monomer), and active only as a tetramer and known to be toxic to the host cell. The successful display of this protein functionally on spore coat demonstrated the advantage of spore display. Also, solvent

stability of surface expressed β-galactosidase in organic solvents was significantly increased as compared to the free form of soluble β-galactosidase. CotB and CotC was used to display the amyQ-encoded α-amylase and GFPuv [56]. Enzymes displayed on spores behave like immobilized enzymes, showing correct function, and enhanced stability toward heat and solvents. They can be used as spore-immobilized biocatalysts. Two heterologous antigens, tetanus toxin fragment C (TTFC) from *Clostridium tetani,* and a heat-labile toxin of *E. coli* (LTB), are displayed on the spore surface with CotC, and could be used to create a combination vaccine.

Highly expressed proteins may also be adsorbed to the spore surface via hydrophobic or electrostatic protein–protein interactions, other than fusing to a carrier protein on spore coat [57]. This method broadened the application of spore display for protein engineering, because the fusion protein hinders the correct conformation, and some proteins are not amenable to N-terminal or C-terminal fusion. However, the absorbed enzyme may diffuse from the surface. This would complicate product isolation in a reaction solution because the enzyme is in mixture.

There are several ways to improve spore display. First, the majority of spore display examples often rely on stable integration of an expression construct into the chromosome of *B. subtilis*. However, this approach presents several limitations, such as low expression level and complex operation. Utilizing a high copy number *E. coli–B. subtilis* shuttle vector can help to overcome these problems [56,58]. Also, *B. subtilis* cells

produce a variety of intra- and extracellular proteases. Target proteins anchored on the spore surface are first exposed to intracellular proteases and, after lysis of the mother cells, to extracellular proteases. To prevent the degradation of target proteins, the eight-fold protease-deficient strain *B. subtilis* was used [59]. Finally, the spore surface could be re-engineered to enhance molecular display. The spores are covered with coat and spore crust proteins, therefore, evolved coat proteins may further improve the efficiency of display.

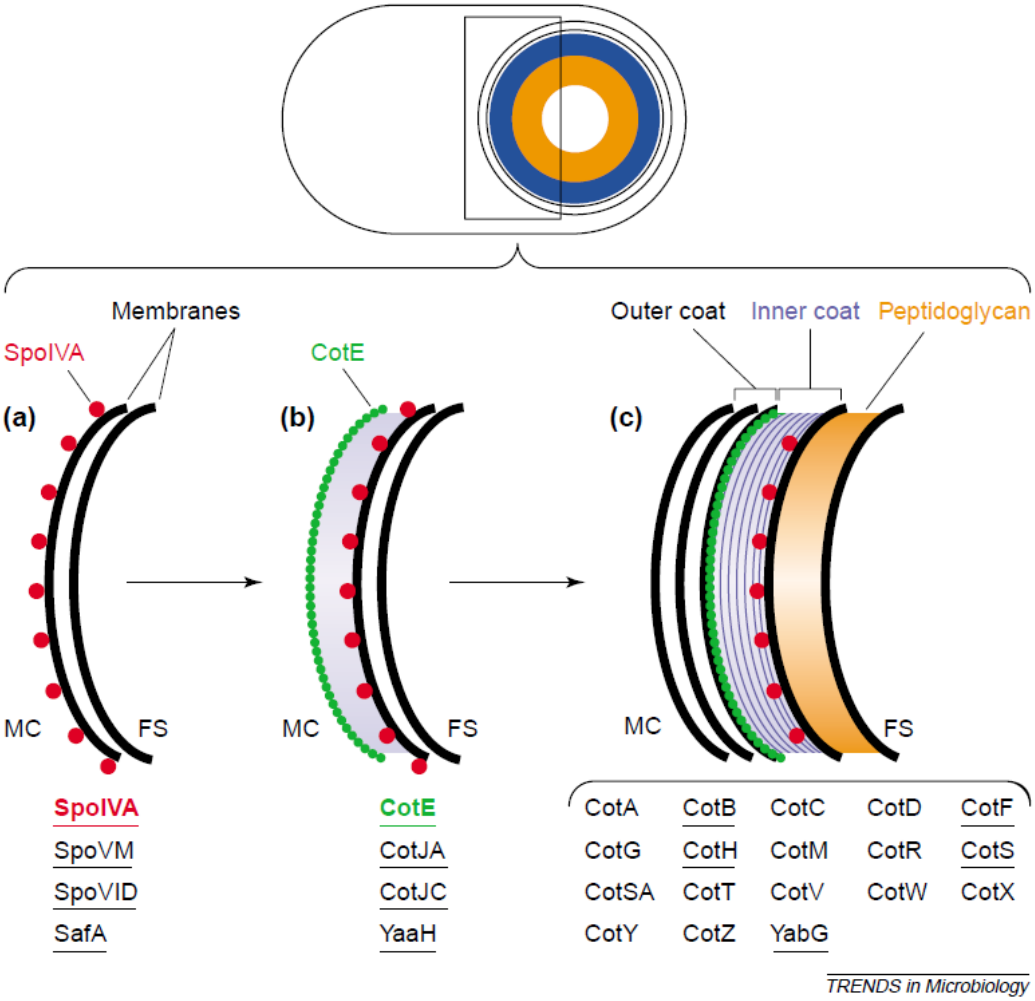

Figure 1.20 Model for spore coat assembly.
Source: [60]

1.5 Laccase

Laccases are members of multicopper oxidase family enzymes. It was first found in the sap of the Japanese lacquer tree *Rhus vernicifera* [61]. Hence, the name of the enzyme is laccase. They have diverse physiological roles such as lignin synthesis [62], lignin degradation [63], pathogenesis [64] and morphogenesis [65]. They catalyze many substrates. In laccase-catalyzed one-electron oxidation processes, four molecules of substrate are oxidised in order to reduce a dioxygen molecule to two waters molecules. Substrate oxidation occurs at the mononuclear T1 centre and then the electrons are shuttled, along a T1 coordinating cysteine, to the two histidines that are coordinating the T3 coppers of the trinuclear centre, where reduction of dioxygen occurs (Figure 1.21). Laccases have applications in the textile industry, paper bleaching, chemical synthesis, biofuel cells, and bioremediation [66].

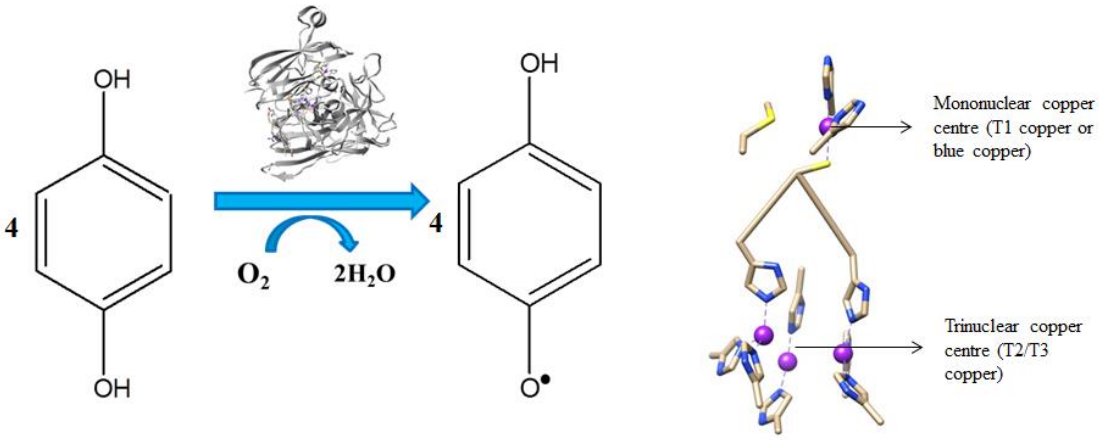

Figure 1.21 Reaction of catalysis of laccase.

CotA, a laccase, is an endospore coat protein in *B. subtilis* (Figure 1.22). The physiological role of CotA in *B. subtilis* has not been determined. Spores have a characteristic brown color. If CotA is knocked out of the genome, the spores lose this color. The color protects the spores from UV light and peroxide [67]. In addition, it assists with melanin biosynthesis and cross-link coat protein structure components.

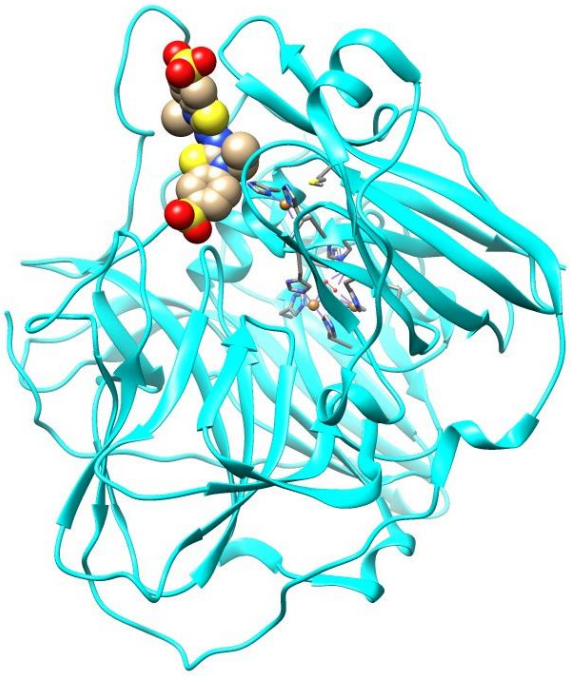

Figure 1.22 Ribbon diagram of the ABTS–CotA complex. ABTS is shown as colored spheres. The model of ABTS-CotA complex was generated by UCSF Chimera (Resource for Biocomputing, Visualization, and Informatics (RBVI), UCSF).
Source: http://www.rcsb.org/pdb/explore/explore.do?structureId=3ZDW (accessed on April 18, 2017)

Spore display was first applied to directed evolution in our laboratory and increasing substrate specificity was the goal. A library of *cotA* were expressed on spore coat and screened for activity toward ABTS [diammonium

2,2'-azino-bis(3-ethylbenzothiazoline-6-sulfonate)] over SGZ (4-hydroxy-3,5-dimethoxy-benzaldehyde azine) [51]. A library of approximately 3000 clones was screened in one round of evolution. A threonine to leucine substitution at position 260 was uncovered and it was 120-fold more specific for ABTS (Figure 1.23).

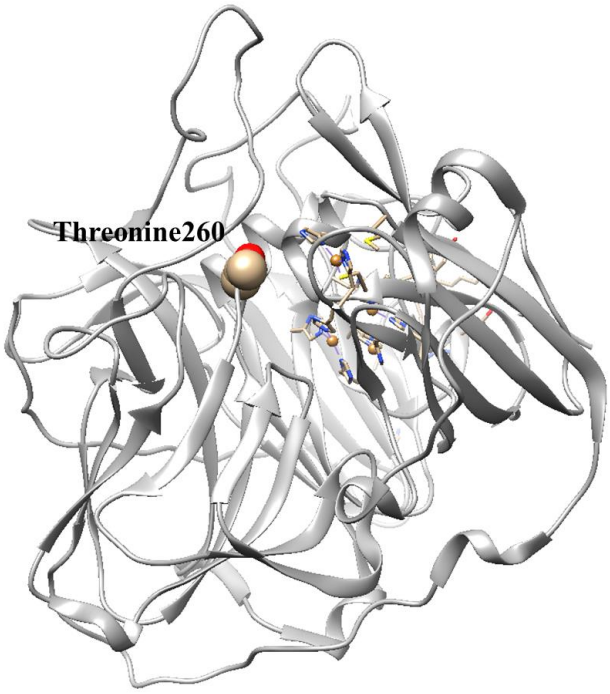

Figure 1.23 Ribbon diagram of Thr260Leu-CotA. The model of Thr260Leu-CotA was generated by UCSF Chimera (Resource for Biocomputing, Visualization, and Informatics (RBVI), UCSF).

We wanted to take advantage of the inert properties of the spore coat and evolve a protein with extreme properties. CotA was evolved for improved activity under conditions of high organic solvent concentrations [44]. A *cotA* library was expressed on spore coat and approximately 3000 clones were screened at 60 % dimethyl sulfoxide (DMSO) in one round of evolution. A threonine to alanine amino acid substitution at

position 480 variant (Figure 1.24) was identified that was 2.38 fold more active than the wild-type CotA. In addition, Thr480Ala-CotA was more active with varying concentrations of DMSO ranging from 0 – 70 %. The mutant was also found to be more active compared to wild-type CotA in different concentrations of methanol, ethanol and acetonitrile.

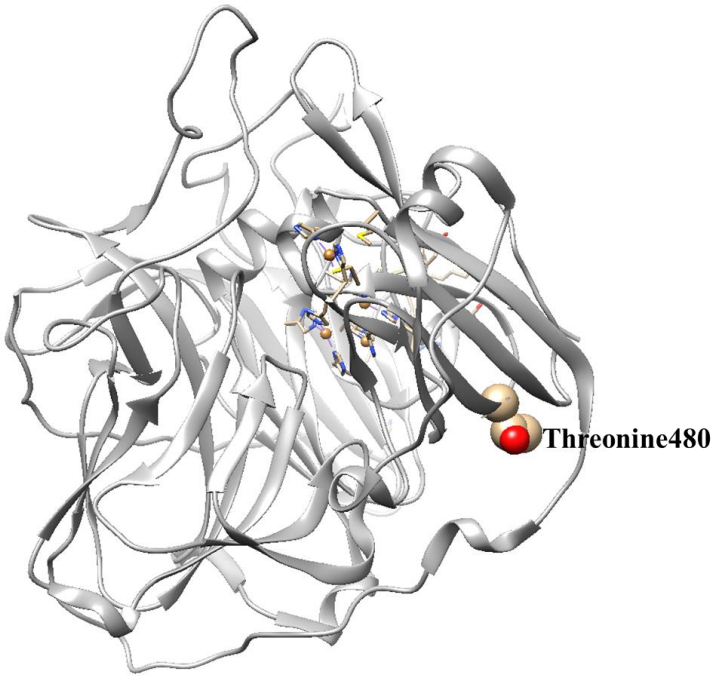

Figure 1.24 Ribbon diagram of Thr480Ala-CotA. The model of Thr480Ala-CotA was generated by UCSF Chimera (Resource for Biocomputing, Visualization, and Informatics (RBVI), UCSF).

CHAPTER 2

DIRECTED EVOLUTION OF COTA LACCASE FOR ACIDIC PH STABILITY BY USING BACILLUS SUBTILIS SPORE DISPLAY

Bacillus subtilis spores can be used for protein display to engineer and optimize protein properties. This method overcomes viability and protein folding concerns associated with traditional protein display methods. Spores remain viable under extreme conditions and the genotype/phenotype connection remains intact. In addition, the natural sporulation process eliminates protein-folding concerns that are coupled to the target protein travelling through cell membranes. Furthermore, ATP-dependent chaparones are present to assist in protein-folding. In general, proteins that are immobilized have advantages in biocatalysis. For example, the protein can be easily removed from the reaction and it is more stable.

We recently showed that spores could be utilized for directed evolution. The laccase CotA, which is a *B. subtilis* spore coat protein, was the target. A library of *cotA* genes was expressed on the spore coat, and it was evolved for improved substrate specificity [51]. Next, spores are able to remain viable under extreme conditions, and CotA was evolved for improved activity in high concentrations of organic solvents [44]. *E. coli* or yeast protein display methods are not compatible with screening with high concentrations of organic solvent because the cell would lyse and the connection between the gene and the improved protein is lost. The next goal was to optimize CotA as a whole cell biocatalyst immobilized in an inert matrix of the spore coat for improved pH stability

using spore display.

In general, pH has an effect on enzyme activity. Each enzyme has its own optimum pH to undergo catalysis. It is because pH can change the state of ionization of acidic or basic amino acid, therefore change the structure of the enzyme. Enzymes will be inactive because the 3-dimensional structure will be altered (Figure 2.1) [68]. Also, pH may change ionization state of substrates. As a result, the substrate may not bind to the enzyme. In industry, extreme low or high pH may be applied. Most enzymes will be inactive under these conditions. In this case, enzymes that can resist extreme pH are desired. For example, α-amylase was engineered to improve the stability at low pH to meet the starch industry environment [69]. Corn starch is converted to fructose/glucose syrup by α-amylase, and this process also includes steam injection to reduce the viscosity. The reaction occurs at pH 6, but a low pH is desired to prevent unwanted byproducts. Acid resistant enzymes have applications in degradation of polymeric or oligomeric carbon sources, biofuel production, textile industry, and fruit juice production [70].

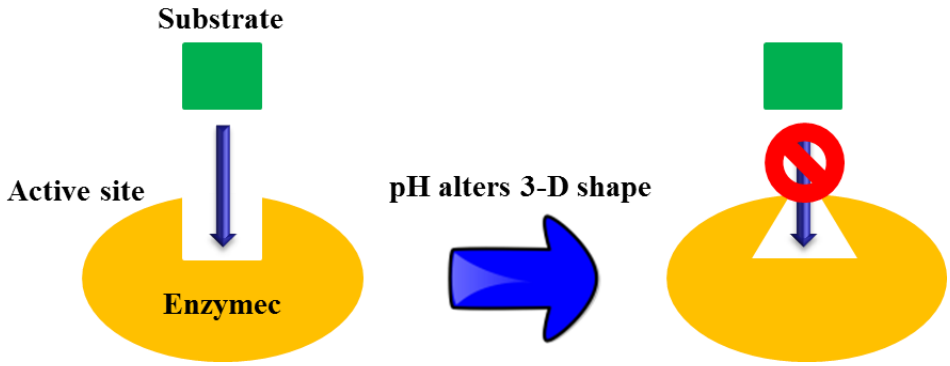

Figure 2.1 pH effect on enzyme activity.

The maximum activity of the laccase CotA with the substrate ABTS is between pH 4 and 5. However, it was found that the activity dramatically decreases at pH 4. The activity is not significantly altered at pH 5. We used CotA as a model to prove that enzymes could be improved for pH resistance by using *Bacillus subtilis* spore display. First, CotA was evolved for increased half-life ($t_{1/2}$) at pH 4. Next, a double mutant was constructed. This variant combined the amino acid substitutions from the improved $t_{1/2}$ variant and organic solvent tolerant mutant. The $t_{1/2}$ and kinetic parameters were evaluated for the double mutant.

2.1 Materials

Chemicals used were analytical grade or higher. 2,2'-azino-bis(3-ethylbenzothiazoline-6-sulphonic acid) (ABTS), citric acid, disodium phosphate, copper(II) chloride were purchased from Sigma Aldrich (St.Louis, MO). Ampicillin, spectinomycin, chloramphenicol was purchased from Fisher Scientific (Pittsburgh, PA). DNA purifications kits were purchased from Qiagen (Valencia, CA). Primers were purchased from Fisher Scientific (Pittsburgh, PA). Enzymes were purchased from Invitrogen (Carlsbad, CA) and Agilent Technologies (La Jolla, CA).

2.1.1 Library Construction

The plasmid, pDG1730CotA, was previously constructed, which contains the CotA gene under control of its natural promoter. Libraries were constructed with help from Dr. Han Jia (Figure 2.2). Random mutagenesis libraries were created by error prone PCR (ep-PCR) using GeneMorph II Random Mutagenesis (Agilent Technologies, La Jolla, CA.). A typical 50 μL GeneMorph reaction contained pDG1730CotA (3000 μg,), primers BacsubF (125 ng; 5'-GCGCGCAAGCTTGTGTCCATGGCGTT-3') and Psg1729 (125 ng; 5'GCGCGGATCCTTATTTATGGGGATCA-3'), dNTP mix (40 nmol, 10 nm each), and Mutazyme II DNA polymerase (2.5 U) and 5 μL buffer. The PCR program consisted of 30 cycles at 95 ℃ for 30 s, 56.3 ℃ for 30 s and 72 ℃ for 4 m.

Libraries were also made using *taq* polymerase. A typical 100 μL ep-PCR reaction contained pDG1730CotA (100 ng), dGTP (20 nmol), dATP (20 nmol), dCTP (100 nmol), dTTP (100 nmol), primers BacsubF and Psg1729 (500 ng each), MgCl2 (0.7 mM), Platinum *Taq* DNA Polymerase (5 U, Invitrogen, Grand Island, NY) and reaction buffer (10 μL). The PCR program consisted of 30 cycles at 95 °C for 30 s, 56.3 ℃ for 30 s and 72 ℃ for 4 m.

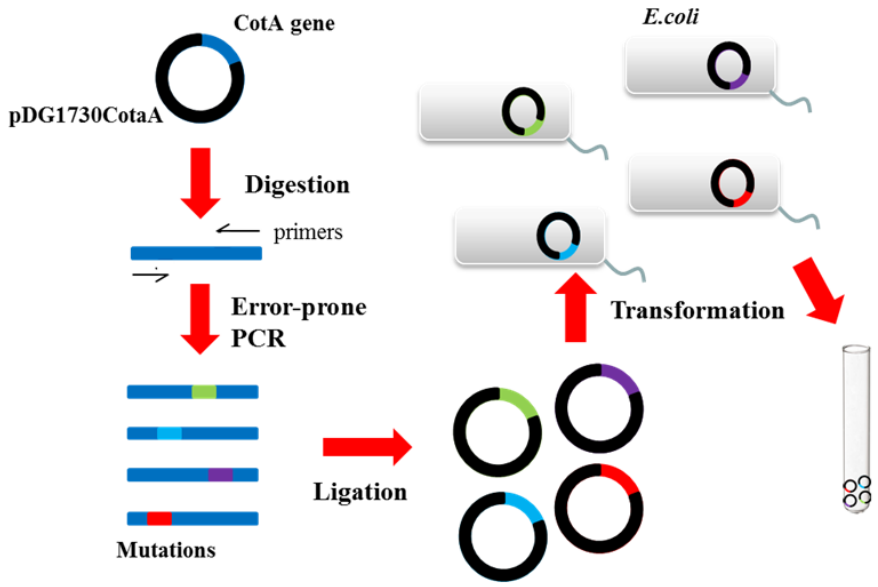

Figure 2.2 CotA was amplified with error prone PCR and transformed into *E.coli*.

For each library, the PCR product was digested with *Hind*III and *Bam*HI and was cloned into the same sites in the plasmid pDG1730. The resulting plasmids were transformed into *E.coli* DH5α and plated on LB plates containing ampicillin (100 μg/mL). The transformants were collected together and the plasmids were isolated. The library was integrated into the *amyE* locus into *B. subtilis* strain 1S101 (Ohio State University, *Bacillus* Genetic Stock Center, Columbus Ohio) (Figure 2.3).

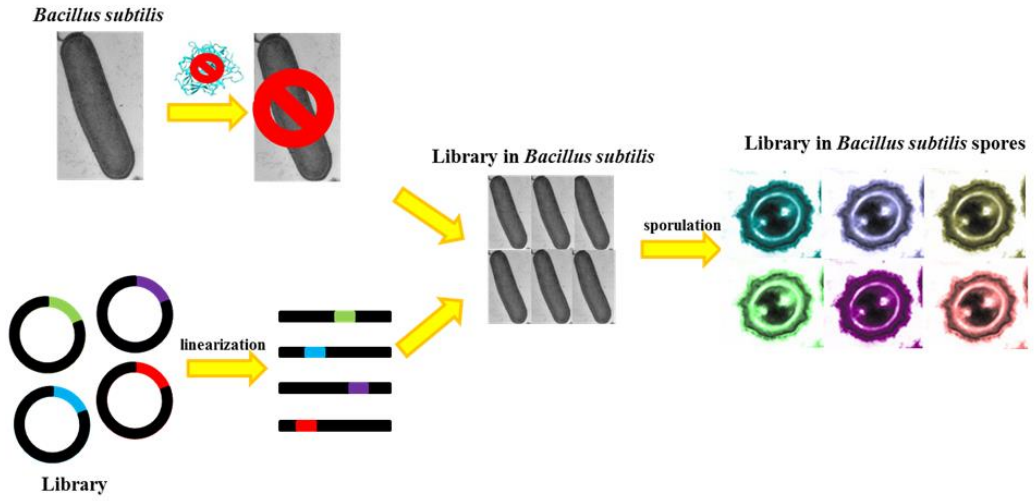

Figure 2.3 CotA library was transformed into *Bacillus subtilis* and displayed on cell surface.

This transformation was achieved by double cross-over recombination. This strain is a *cotA* knockout strain (Figure 2.4).

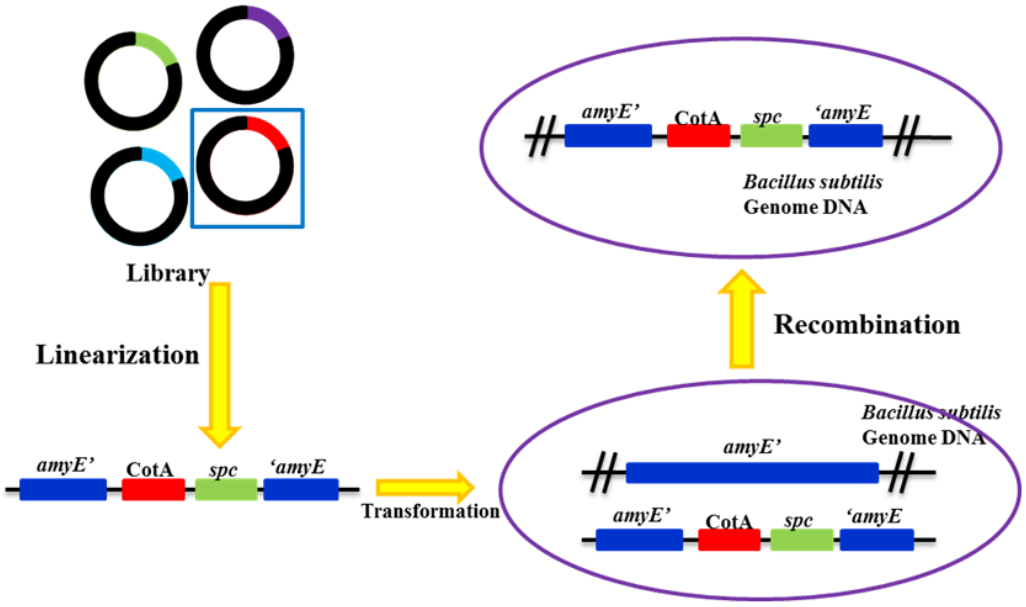

Figure 2.4 CotA was integrated into the genome of *Bacillus subtilis* by double-cross recombination.

2.2 Methods

2.2.1 Spore Screening for Acid-stability

Expression of the library in 96-deep-well plates was previously described [71]. After expression, the plates were centrifuged and the media discarded. The spores were resuspended in 200 μL spore control solution [sterile water containing $CuCl_2$ (0.25 mM)] and incubated at room temperature for 30 min. Next, two assay plates were constructed for screening. One plate had 40 μL spore control solution in each well as control plate, and the other had 40 μL spore control solution with 100 μL citrate phosphate buffer (100 mM, pH 4) containing $CuCl_2$ (0.25 mM) as assay plate. Both plates were at room temperature for two hours. After incubation, 100 μL citrate phosphate buffer (100 mM, pH 4) containing $CuCl_2$ (0.25 mM) was added into each well of the control plate. ABTS (1.0 mM, pH 4) was added into each well for both plates to initiate the reaction, and allowed to react for 20 minutes. The plates were centrifuged and the supernatants were transferred to another microtiter plate. The endpoint was measured at 420 nm (ε = 36,000 M^{-1} cm^{-1}). Next, the ratio of $Abs_{pH\ 4\ at\ 420\ nm}$: $Abs_{control\ at\ 420\ nm}$ was determined. Positive clones were selected that showed at least 1.5 the mean value of wild-type ratio of $Abs_{pH\ 4\ at\ 420\ nm}$: $Abs_{control\ at\ 420\ nm}$. A rescreen was carried out to eliminate false positives. The assay was similar to above, but multiple colonies from a single clone were picked into a column of a 96-deep well plate. A wild-type control column was also included.

2.2.2 Acid Inactivation

Large-scale sporulation was initiated by media exhaustion, and the spores were purified using published procedures [72]. The half-life of acid inactivation ($t_{1/2}$) of spores was determined. Purified spores were incubated in aqueous $CuCl_2$ (0.25 mM) for 1 hour at 37 ^{o}C. Then, the spores were centrifuged and resuspended in citrate-phosphate buffer (100 mM, pH 4, 0.25 mM $CuCl_2$) and incubate in 37 ^{o}C. The resulting solution had an OD_{580} between 0.1 – 0.3. A 200 μL reaction was initiated by adding ABTS (10 mM) into the spore solution. The measurements were performed every 3 to 10 minutes at 420 nm until the activity decreased to 20 % of the initial activity. The data was recorded in triplicate.

2.2.3 Kinetics Measurements of CotA and CotA Variants

All measurements were done in triplicate with at three different batches of purified spores. The kinetic parameters of spores were determined at 37 ^{o}C by using ABTS (1 – 8000 μM) in citrate phosphate buffer (100 mM, pH 4). The spores were first suspended in aqueous $CuCl_2$ (0.25 mM) solution for 60 minutes. Then the reactions were initiated by adding 50 μL spore solution into wells of each concentration of ABTS. The final OD_{580} of spores was between 0.2 – 0.3. The initial rates were acquired from the linear portion of the reaction curve. Kinetic parameters were obtained by curve fitting (SigmaPlot 12.0, Systat Software Inc., San Jose, CA).

2.2.4 Product Yield of CotA and Its Variants

CotA recycling was investigated and the total product yield was determined over 42-hour period. The spores were resuspended in aqueous $CuCl_2$ (0.25 mM) solution for 60 minutes at 37 ℃. Next, the spores were centrifuged and the supernatant was discarded. The spores were resuspended in citrate phosphate buffer (100 mM, pH 4) at 37 ℃ with a final OD_{580} of 0.15. The spores were incubated for two hours and then the spores centrifuged and the supernatant was discarded. The reaction was initiated by resuspending the spore with 1 mL ABTS (20 mM) in citrate phosphate buffer (100 mM, pH 4) at 37 ℃. The absorbance was taken at 420 nm after 15 minutes to determine the product yield. This cycle was repeated seven times over 42-hours.

2.2.5 Cell Viability

Purified spore were incubated in aqueous $CuCl_2$ (0.25 mM) for one hour. Next, the spore solution was added to citrate phosphate buffer (100 mM, pH = 4, 0.25 mM $CuCl_2$) and incubated for 4 hours. Then, the solutions were diluted and plated on LB plates containing spectinomycin (100 μg/ml) and chloramphenicol (5 μg/mL).

2.2.6 Overproduction in *Escherichia coli* and Purificaiton of CotA and Its Variants

A 5.0 mL of the overnight culture was used to inoculate LB media (1 L) containing ampicillin (100 μg/mL). The cells were shaken at 250 rpm at 37^{o}C. The cells were then induced by adding arabinose (0.2 %) and $CuCl_2$ (0.25 mM) when OD_{600} = 0.6. After 4

hours, the cells were harvested by centrifugation at 9,000 g and 4 ^{o}C and the cell pellets were stored at -20^{o}C until purification.

CotA was purified using two chromatographic steps. The cell pellets were resuspended in 20 ml Tris-HCl (20 mM, pH 7.6) buffer containing DNaseI (10 μg/mL), $MgCl_2$ (5 mM), and protease inhibitors (CompleteTM, mini EDTA-free protease inhibitor mixture tables, Roche Molecular Biochemicals). Cells were disrupted by sonication (4 x 30 sec; output power 20 watts; Sonicator, Sonic Dismembrator Model 100, Fisher Scientific). The lysate was centrifuged at 15,000 g and 4 ^{o}C for 20 minutes. The supernatant was filtered using 0.45 μm filter (Millex-HV, Millipore) and then diluted to 50 mL with Tris-HCl buffer. The solution was loaded onto an ion exhange SP-Sepharose column (bed volume 25 mL) that was equilibrated with Tris-HCl (20 mM, pH 7.6). The sample was loaded and eluted using a two-step linear NaCl gradient (0 – 0.5 and 0.5 – 1 M) in the same buffer. Fractions displaying laccase activity were pooled, concentrated by ultrafiltration with a cutoff of 30 kDa, and equilibrated to 20 mM Tris-HCl (pH 7.6).The sample was then loaded onto MonoS 5/50 column, and eluted using a two-step linear NaCl gradient (0 – 0.5 and 0.5 – 1 M). Fractions with laccase activity were pooled, desalted, and concentrated. A single band was shown by SDS-PAGE (12.5 %) at 100 kDa after boiling for 10 min in loading dye.

2.2.7 Acid Inactivation and Kinetics Measurement of Purified CotA

0.5 μg purified enzyme was used for acid inactivation assay. Dilute the protein with aqueous $CuCl_2$ (0.25 mM) and incubate at 37 ^oC for 30 min. Then, on a 96-well microplate, each well contains 100 μl citrate phosphate buffer (100 mM, pH 4, 0.25 mM $CuCl_2$) with 0.5 μg treated protein and incubate under 37 ^oC. The reaction was initiated every 10 minutes by adding 10 μl ABTS (1 mM) into one well on the 96-well microplate. The initial rates were acquired from the linear portion of the reaction curve.

Purified enzyme was diluted in aqueous $CuCl_2$ (0.25 mM) and incubated at 37 ^oC for 30 min. The kinetic parameters were then determined at 37 ^oC by using ABTS (1 – 10 mM) in citrate phosphate buffer (100 mM, pH 4, 0.25 mM $CuCl_2$). The reactions were initiated by adding 0.5 μg enzyme. The initial rates were acquired from the linear portion of the reaction curve. Kinetic parameters were obtained by curve fitting.

2.3 Results and Discussion

Many strategies have been developed for directed evolution. They are either *in vivo* or *in vitro*. Taking advantage of the inert properties of spores, we demonstrate that proteins can be evolved under harsh condions by using a system based on spores of *B. subtilis.* In this system, the protein of interest is “preimmobilized” on the spore coat and screened as whole cell. Therefore, the connection between phenotype and genotype is intact. CotA is a laccase, which is a *B. subtilis* spore coat protein. The optimal enzymatic activity of CotA laccase was found at pH 4.0 – 5.0 for substrate ABTS oxidation. However, the

activity dramatically decreases at pH 4 (Figure 2.5). The activity is not significantly altered at pH 5.

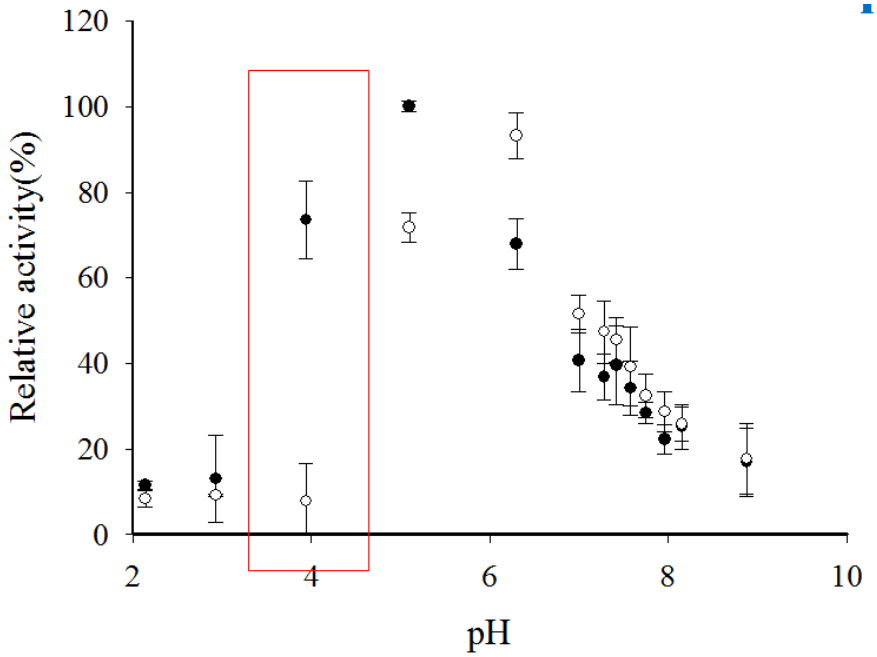

Figure 2.5 Optimal enzymatic activity was found at pH 4.0 – 5.0 for ABTS. However it also has the relatively lowest stability at pH 4.

CotA laccase was evolved for higher stability at low pH = 4 by using *B. subtilis* spores. Liraries of CotA were first created by random mutagenesis wild-type *B. subtilis* as template. They were then inserted into vector pDG1730 and transformed into *B. subilis* genome with double crossover recombination. The *B. subtilis* strain had the endogenous cotA gene knocked out. Next, the *B. subtilis* cells were sporulated in 96-deep-well plates. A screen need to be validated to reduce the probability of selecting false positives. In order to validate the screen, only wild-type CotA is arrayed in the 96-deep well plates. A low coefficienct of variance (CV) in needed. There are many factors to obtain a low CV, such as incubation time and temperture, inductution time and temperture, shaker speed,

eliminate evaporation, etc…A suitable CV is approximately 20 %. Therefore, CotA activity with ABTS was measured before and after incubating the spores in citrate phspate buffer (100 mM, pH 4) for 60 min. The average of the coefficient of variance (CV) was 15.7 % for 3 microtiter plates (Figure 2.6).

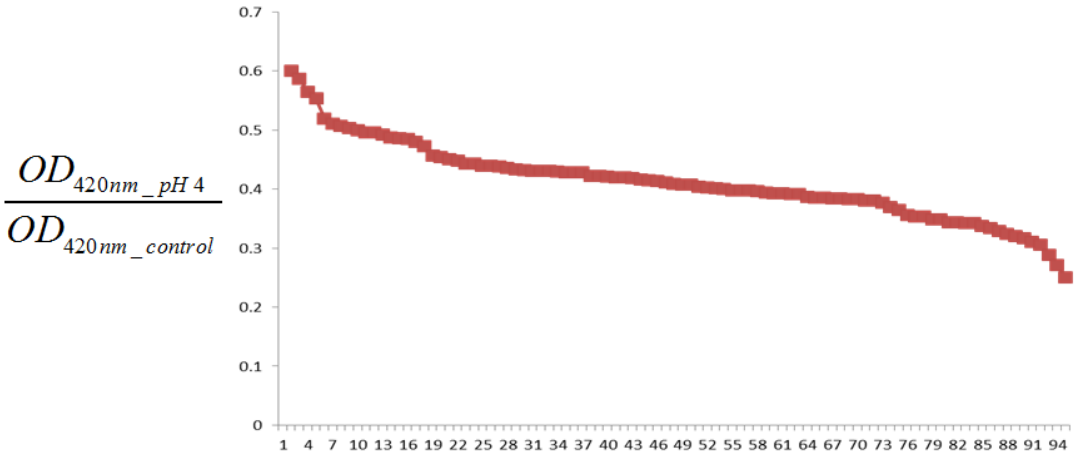

Figure 2.6 An example of one microtiter plate of coefficient of variance (CV). The clones were ranked from highest to lowest activity. CV is defined as the ratio of the standard deviation to the mean.

Positive clones were selected that showed at least 1.5 the mean value of wild-type ratio of $Abs_{pH\ 4\ at\ 420\ nm}$: $Abs_{control\ at\ 420\ nm}$. A rescreen was carried out to eliminate false positives. The assay was similar to above, but multiple colonies from a single clone were picked into a column of a 96-deep well plate. A wild-type control column was also included. Approximately 3000 mutants were screened and a mutant, Y19, was identified with a $t_{1/2}$ 5.9 times greater than wt-CotA (Table 2.1).

Table 2.1 Kinetic Parameters and Half-life of Wild-type CotA and CotA Variants

Mutation	V_{max}[a]	K_m (μM)	V_{max}/K_m	$t_{1/2}$[b]
E29V	29.4 ± 1.4	67.2 ± 9.2	0.44	60.4 ± 3.7
L343S	14.7 ± 0.5	58.2 ± 6.4	0.25	33.4 ± 2.3
E498G	41.8 ± 3.7	857.6 ± 125.9	0.05	1264.1 ± 78.0
E29V/L343S/E498G	18.5 ± 0.5	358.6 ± 29.4	0.05	302.6 ± 23.8
T480A	120.6 ± 2.5	112.3 ± 6.9	1.07	56.1 ± 1.1
T480A/E498G	45.5 ± 3.0	585.1 ± 76.4	0.08	3166 ± 431.1
Wt-CotA	33.3 ± 1.1	58.8 ± 7.2	0.57	50.9 ± 1.8

Kinetic parameter and half-life of inactivation at pH 4 for WT-CotA and CotA variants. [a] μM/min/$OD_{580\ nm}$. [b] Half-life (minutes) at pH 4.

The sequence of Y19 was determined from isolated genomic DNA and three amino acid substitutions [E29V (GAA to GTA), L343S (TTG to TCG), E498G (GAA to GGA)] were found (Appendix B). Val29 and Ser343 are on the surface, while Gly498 is close to the T1 copper center (Figure 2.7).

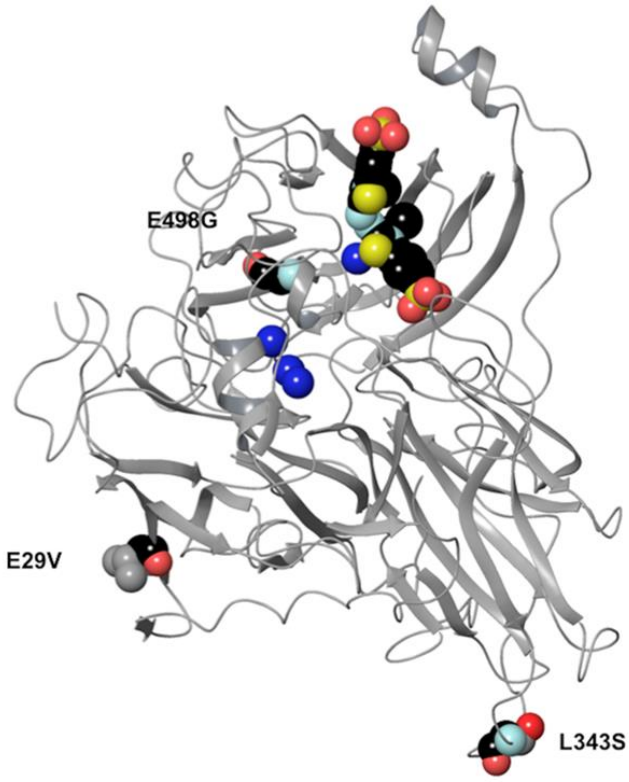

Figure 2.7 Molecular model of ABTS-Y19. Molecular model of the ABTS-Y19 complex was generated using Maestro software from Schrodinger (Schrodinger, Maestro v9.2, Portland, 2011). Copper, ABTS, and the amino acids are rendered as CPK models.

The CotA variants that carry only one mutation were also constructed to determine the contribution the amino acid substitution had on pH stability and catalytic efficiency (Figure 2.8, Table 2.1, Figure 2.9). The $t_{1/2}$ of E498G variant was 1213.2 minutes longer than wt-CotA, which was 24.8 times greater. The E498G substitution is the only amino acid required for the increased $t_{1/2}$ (*vide infra*). The The V_{max}/K_m for E498G was 8.8 % compared to wt-CotA. A lowering of V_{max}/K_m is not unusual because this property was not included in the pH stability screen (Table 2.1). The change in

V_{max}/K_m for the variant was mainly due to 14.6 fold increase in K_m, which was partially compensated with a 1.3 fold increase in V_{max}.

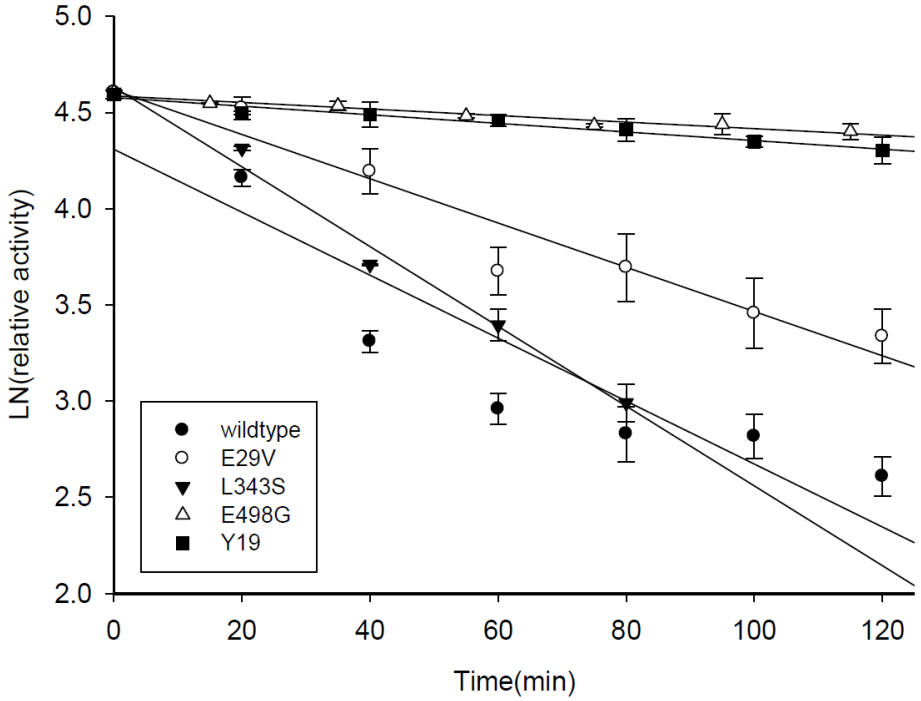

Figure 2.8 The $t_{1/2}$ at pH 4 of wt-CotA and CotA variants. The $t_{1/2}$ is determined from first order kinetic of deactivation. Wt-CotA (closed circles), E29V (open circle), L343S (closed triangles), E498G (open triangle), and Y19 (closed square) residual activity at pH 4 is plotted against time.

A

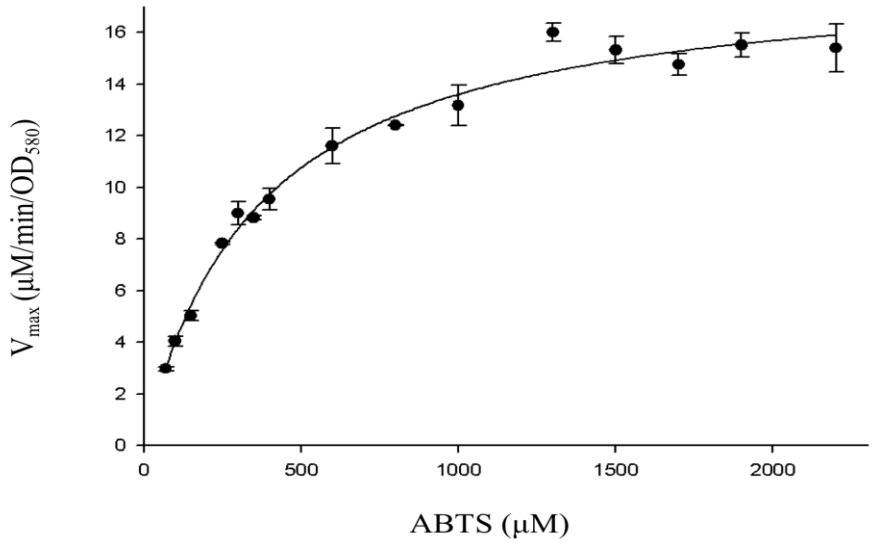

B

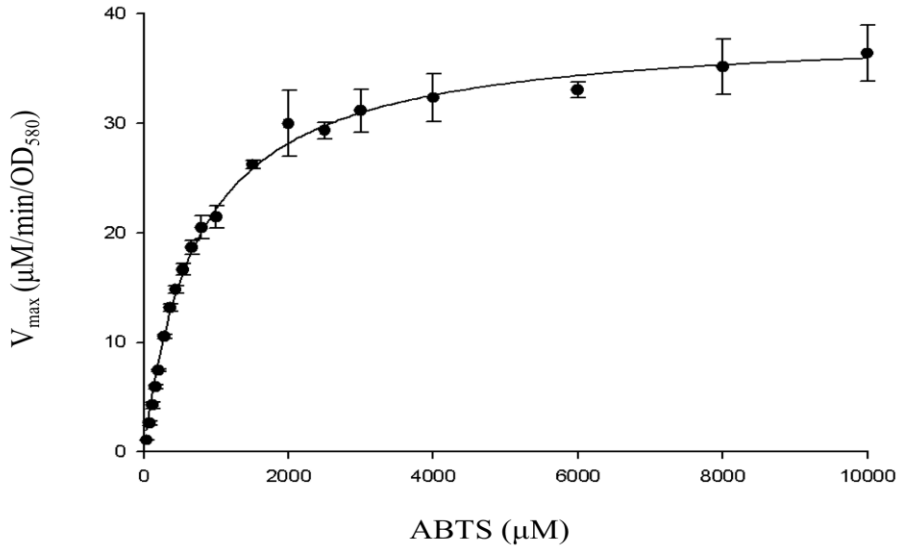

Figure 2.9 Kinetic parameters of wt-CotA and CotA variants on *Bacillus subtilis* spore coat. (A) Kinetic parameters of Y19 (E29V/L343S/E498G). K_m = 358.6 ± 29.4 μM; V_{max} = 18.5 ± 0.5 mM/min/$OD_{580nm.}$ (B) Kinetic parameters of E498G.

C

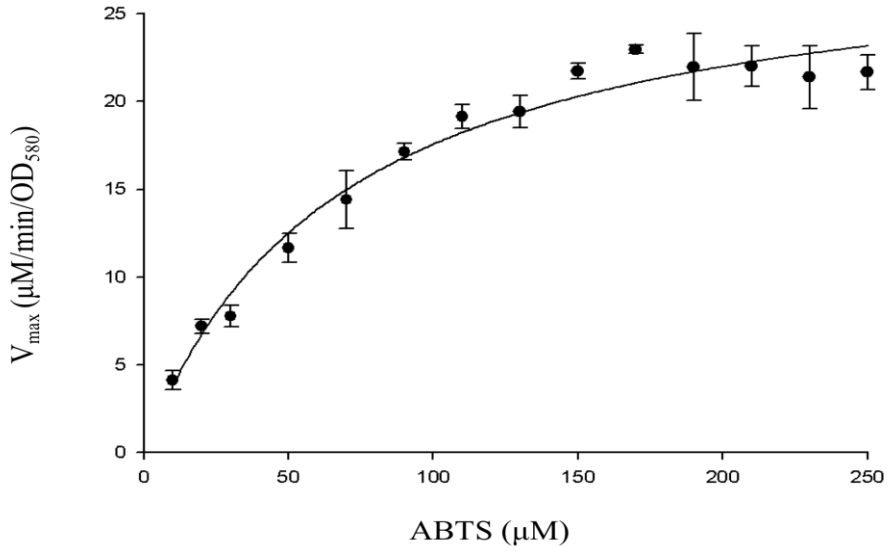

D

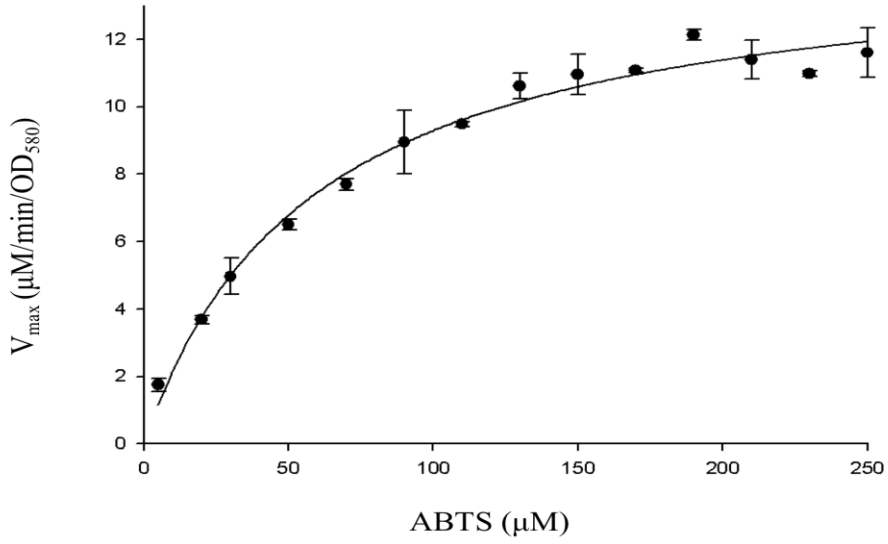

Figure 2.9 (continued) Kinetic parameters of wt-CotA and CotA variants on *Bacillus subtilis* spore coat. (C) Kinetic parameters of E29V. K_m = 67.2 ± 9.2 μM; V_{max} = 29.4 ± 1.4 mM/min/$OD_{580nm.}$ (D) Kinetic parameters of L343S. K_m = 58.2 ± 6.4 μM; V_{max} = 14.7 ± 0.5 mM/min/$OD_{580nm.}$

E

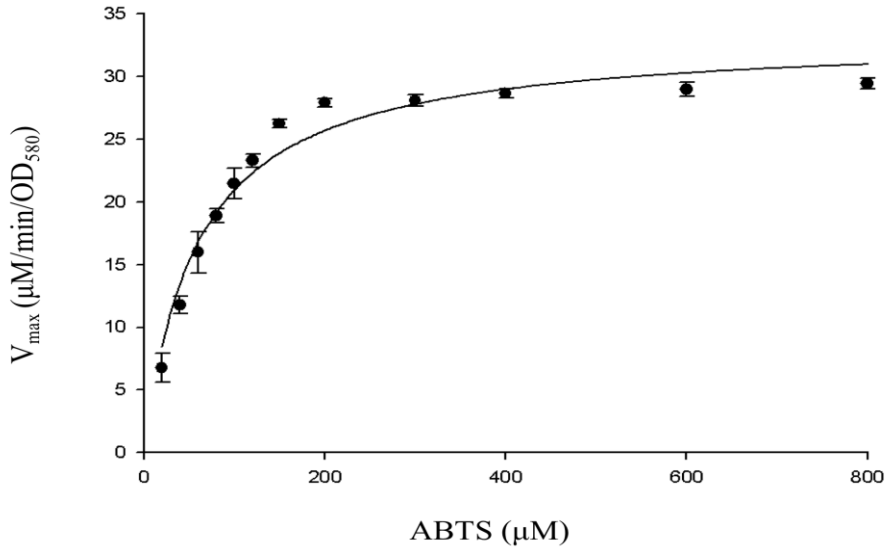

Figure 2.9 (continued) Kinetic parameters of wt-CotA and CotA variants on *Bacillus subtilis* spore coat. (E) Kinetic parameters of wt-CotA. K_m = 58.8 ± 7.2 μM; V_{max} = 33.3 ± 1.1 mM/min/$OD_{580nm.}$

In a previous investigation, Glu^{498} was mutated to aspartate, threonine and leucine, and it was suggested that these amino acid substitutions near His^{497} resulted in minor changes in substrate binding and electron transfer to the T1 site [73,74]. Substrate oxidation at the T1 site has been proposed to be the rate-limiting step in the reaction [75,76]. The mutagenesis investigations also proposed that Glu^{498} was necessary for proton assisted reductive cleavage of the O-O bond at the trinuclear copper center. The E498G variant does not have a side chain that can facilitate the cleavage. However, the amino acid substitution is also expected to alter substrate binding and electron transfer. Glycine is known to have greater conformational flexibility because the side chain is hydrogen. The mutation may have altered the position ABTS for efficient electron

transfer and the V_{max} was increased. On the other hand, this was at a cost to substrate binding which resulted in a higher K_m. In addition, the glycine substitution is adjacent to the His497, which coordinates to Cu^{2+} in the T1 site. Hence, the Cu^{2+} coordination geometry may also be affected such that metal binding has increased, and the protonation of the histidine ligands is hindered. Protonation of the histidine would result in release of Cu^{2+} from the T1 site and loss of enzymatic activity. The enzyme is imbedded in the spore coat and the structure of the mutant has not been solved. Hence, it is difficult to extract conclusions based on the structure of ABTS bound to CotA. The structure of the soluble CotA may not be identical to the enzyme that is embedded and restrained in the spore coat.

Wt-CotA was evolved for increased activity in high concentrations of organic solvents previously [44]. An assay was performed at 60 % dimethyl sulfoxide (DMSO) and a variant was identified to be 2.4-fold more active after screening 3000 clones after one round of evolution. The clone was found to have a threonine to alanine amino substitution at position 480 (T480A-CotA). T480A-CotA was also more active with different concentrations of DMSO ranging from 0 to 70 %. The mutant was also found to be more active compared with the wild-type CotA in different concentrations of methanol, ethanol, and acetonitrile [44]. The amino acid substitution in T480A-CotA was introduced into the E498G-CotA to create T480A/E498G-CotA. The $t_{1/2}$ for the T480A/E498G-CotA at pH 4 was found to be 3165.6 ± 431.1 minutes, which was 62.1-fold greater than wt-CotA (Table 2.1). When compared to wt-CotA, the V_{max} for T480A/E498G-CotA was

slightly increased by 1.4-fold; whereas, the K_m increased 10-fold. The V_{max} in the double mutant was due to the T480A amino acid substitution and the E498G mutation was mainly responsible for the increase in K_m (Table 2.1). The crystal structure has not been determined for T480A-CotA, E498G-CotA and T480A/E498G-CotA. As a result, it is difficult to conclude the effect that the T480A mutation has towards improved pH stability of T480A/E498G-CotA.

The activity of wt-CotA, T480A-CotA, E498G-CotA and T480A/E498G-CotA was determined in different organic solvent (DMSO, methanol, ethanol and acetonitrile). The variants did not show greater activity than the wt-CotA (Figure 2.10). In short, the T480A/E498G-CotA and E498G-CotA have comparable similar kinetic properties, but now T480A/E498G-CotA has greater $t_{1/2}$ compared to the wt-CotA.

A

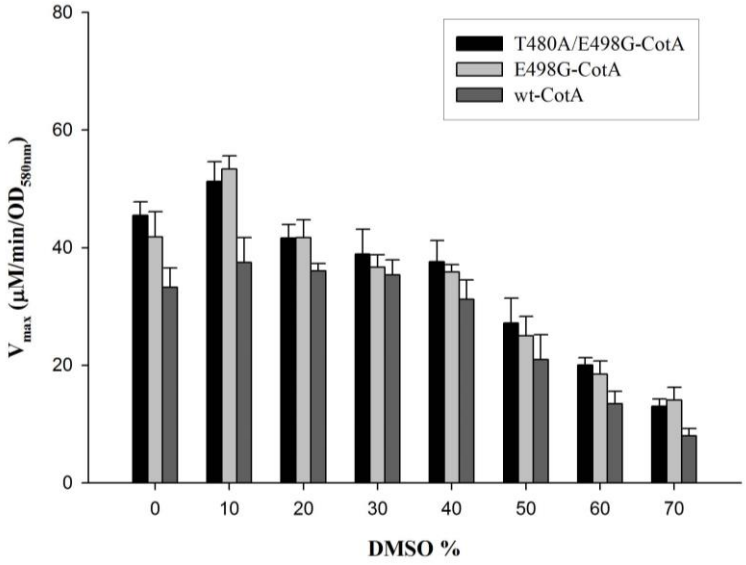

B

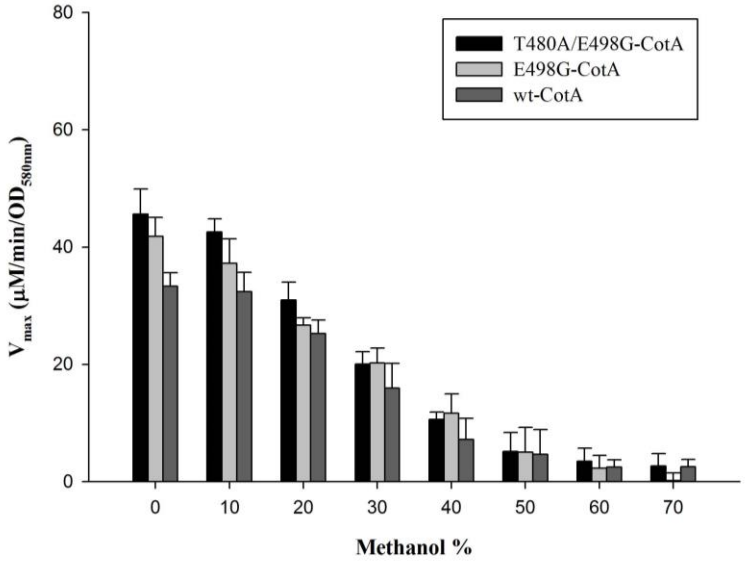

Figure 2.10 V_{max} (μM/min/OD_{580nm}) of wt-CotA (light shaded bars), T480A/E498G-CotA (dark shaded bars) and E498G-CotA (white bars) in 0 – 70 % organic solvents: (A) DMSO, (B) methanol, (C) ethanol, and (D) acetonitrile.

C

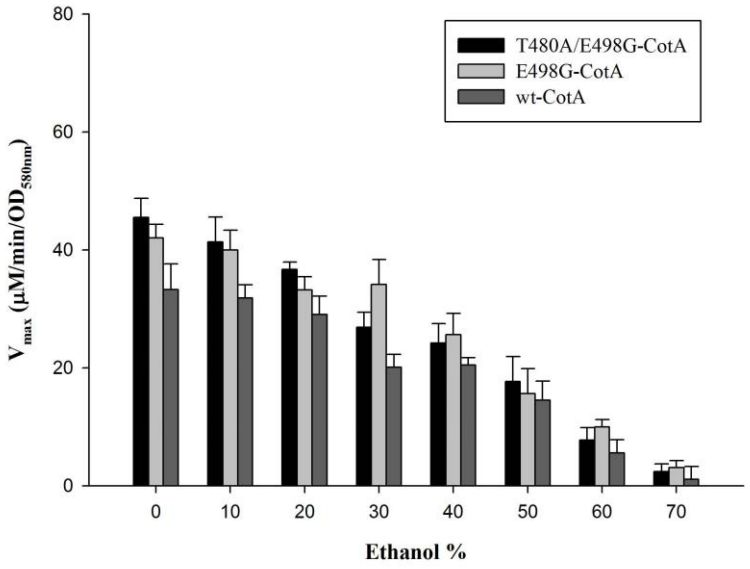

D

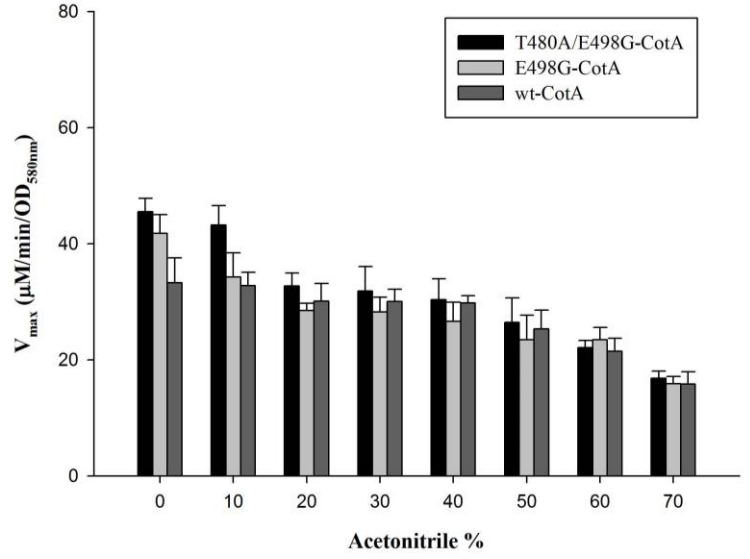

Figure 2.10 (continued) V_{max} (μM/min/OD_{580nm}) of wt-CotA (light shaded bars), T480A/E498G-CotA (dark shaded bars) and E498G-CotA (white bars) in 0 – 70 % organic solvents: (A) DMSO, (B) methanol, (C) ethanol, and (D) acetonitrile.

An important feature of a biocatalyst is that it can be reused for several cycles. E498G and T480A/E498G have a larger K_m compared to the wt-CotA, which resulted in a lower V_{max}/K_m (Table 2.1). However, the variants had a higher product yield compared to the wt-CotA, which was due to the longer $t_{1/2}$ (Table 2.1). The spores were recycled 7 times over 42 h (Table 2.2, Figure 2.11). Wt-CotA, E498G-CotA and T480A/E498G-CotA had a total yield of 24.8, 92.9, and 131.3 mmole, respectively. E498G-CotA and T480A/E498G-CotA yielded 3.7- and 5.3-fold more product than the wt-CotA. This also demonstrates that the biocatalysts can be recycled. T480A/E498G was the most stable biocatalyst and retained 42 % of its activity after the 42 h period.

Table 2.2 Product Yields of Wild-type CotA and CotA Variants

Time (hour)	Wt-CotA	E498G	T480A/E498G
0	11.1 ± 0.1	20.2 ± 0.3	19.8 ± 0.2
2	3.3 ± 0.5	19.6 ± 0.2	19.4 ± 0.2
4	2.8 ± 0.6	15.4 ± 0.9	18.9 ± 0.9
8	1.9 ± 0.7	12.4 ± 1.6	18.0 ± 1.6
18	1.6 ± 0.2	9.1 ± 0.2	15.9 ± 0.2
25	1.8 ± 0.4	7.6 ± 1.2	14.4 ± 1.2
30	1.3 ± 0.2	5.3 ± 0.9	13.4 ± 0.9
42	1.0 ± 0.3	3.3 ± 0.3	11.5 ± 0.3
Total	24.8	92.9	131.3

Product yield (mmole) of $ABTS^+$ over 42 h with wt-CotA, E498G, and T480A/E498G.

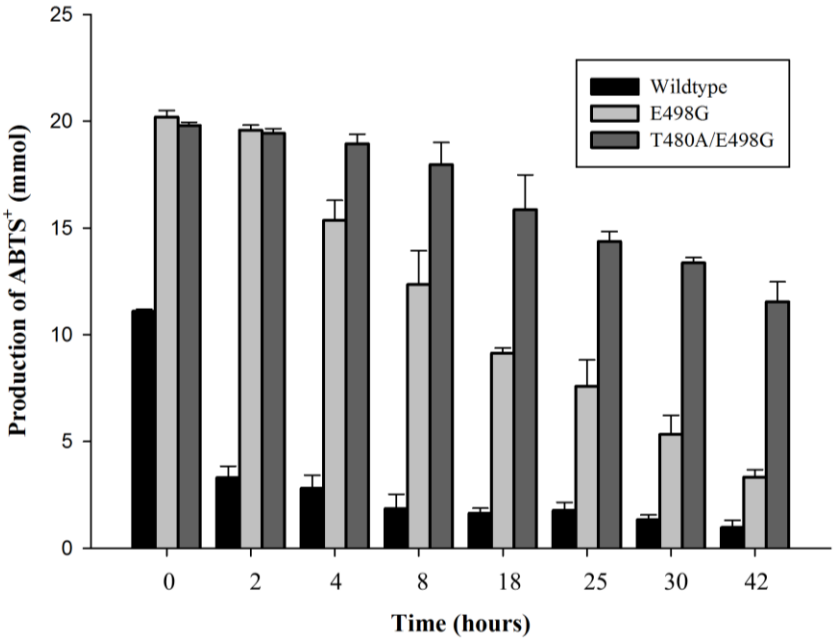

Figure 2.11 Product yields of $ABTS^+$ of wt-CotA and its variants over 42 h. The spores were recycled and measured for 7 cycles over 42 h.

The surface amino acid substitutions, E29V and L343S variants, do not significantly contribute to the pH stability to Y19 (Table 2.1). E29V mutant has a slight decrease in V_{max}/K_m (0.77-fold) and a modest increase in $t_{1/2}$ (1.2-fold) compared to wt-CotA. Next, the L343S mutant had a decreased V_{max}/K_m and a decrease in $t_{1/2}$ compared to wt-CotA of 0.44- and 0.66-fold, respectively. It appears that the E29V and L343V amino acid substitutions have a deleterious effect.

The spore coat proteins were extracted and the amount of wt-CotA and the mutants were comparable as assessed by SDS-PAGE gels (Figure 2.12). The band intensity in lanes 4 – 8 were quantified using ImageJ (https://imagej.nih.gov/ij/). The

values for lane 4 – 8 were 7045, 6798, 7716, 7171, and 7012, respectively. The average of the intensities was 7151 ± 344. The amount of protein present in the spore coat are similar between the samples.

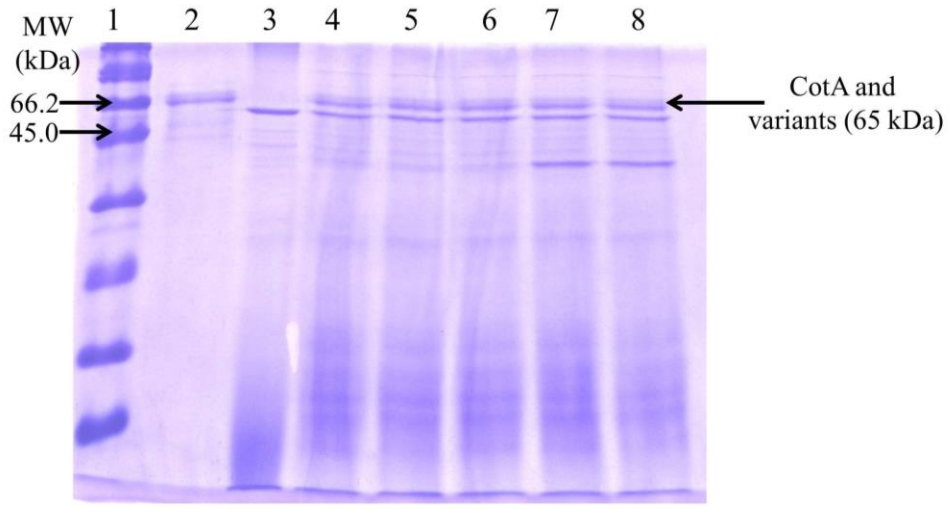

Figure 2.12 Extraction of spore coat proteins. Lane 1: Marker; Lane 2: CotA standard purified from *E. coli*; Lane 3: CotA knockout; Lane 4: Wildtype CotA; Lane 5: E29V-CotA; Lane 6: L343S-CotA Lane 7: E498G-CotA; Lane 8: T480A/E498G-CotA. Spores (A_{580} = 100) were resuspended in 50 µl of sodium dodecyl sulfate (SDS) loading dye (SDS (4 %), 2-mercaptoethanol (10 %), dithiothreitol (1 mM), Tris-HCl (0.125 M, pH 6.8), glycerol (10 %) bromophenol blue (0.05 %). The samples were heated at 100 ^{o}C for 10 minutes. Next, the samples were centrifuged, and 25 µl of the supernatant were resolved with 15 % SDS-PAGE gels. Gels were stained with Coomassie brilliant blue R-250 and destained.

Cell viability was determined in citrate phosphate buffer (100 mM, pH 4). The result showed the viability was intact in this screen condion (Figure 2.13).

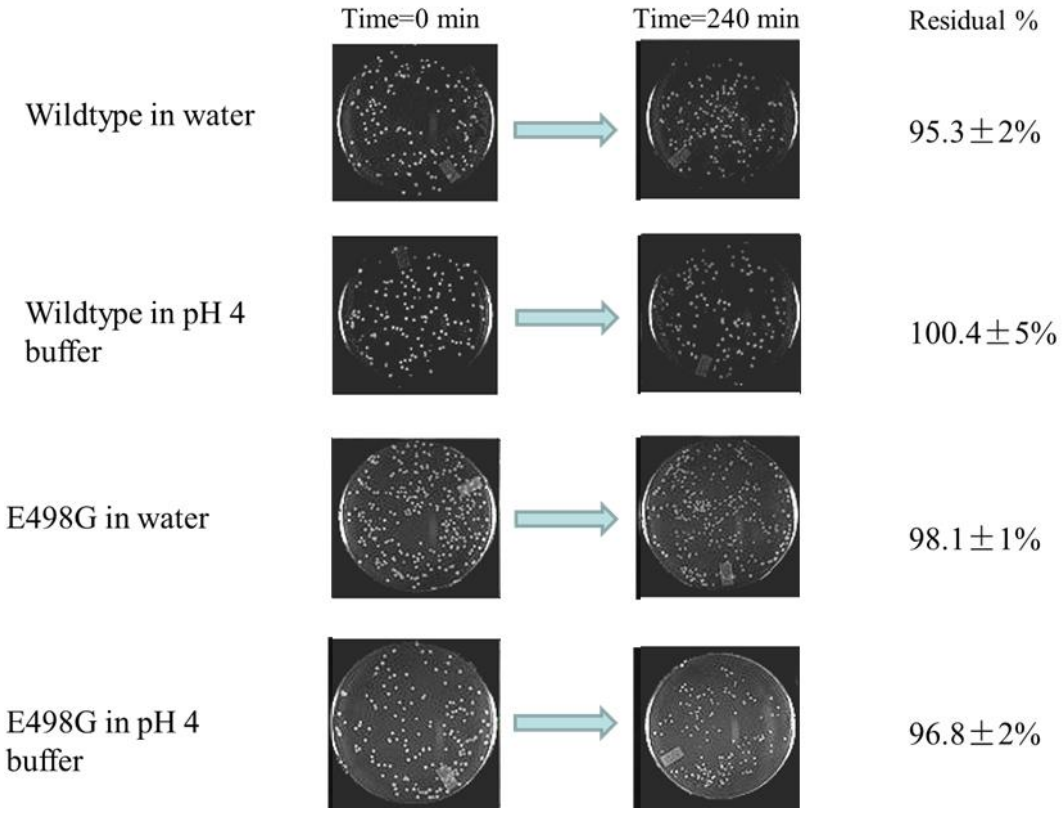

Figure 2.13 Viability assay of spores in citrate phosphate buffer (100 mM, pH 4).

Enzymes embedded in the spore coat may have different activity compared to the protein that is free in solution. Hence, wt-CotA and E498G-CotA was overproduced and purified from *E. coli*. However, T480A/E498G-CotA was expressed as inclusion bodies (Figure 2.14) and it could not be recovered. This is not unusual. In previous publication, wt-CotA was expressed in *E. coli* for molecular and biochemical characterization and only 10 % of the CotA was soluble and the rest were inclusion bodies [77]. Efforts were made to solublize and refold the protein were not successful. In our case, we see similar results. Wt-CotA and E498G-CotA have both a soluble and inclusion body fraction and

the these enzymes were purified. T480A/E498G-CotA expressed as an inclusion body and could not obtain enough soluble protein to purify and characterize.

A

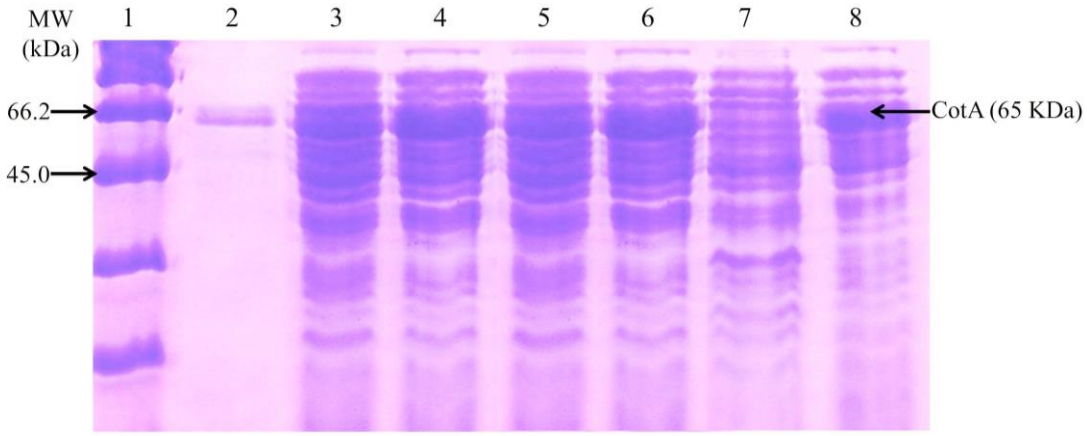

Figure 2.14 SDS-PAGE analysis of CotA overproduction in *E. coli*. (A) Lane 1: Marker; Lane 2: CotA standard purified from *E. coli*; Lane 3: supernatant of a crude extract of an arabinose-induced *E. coli* culture of wt-CotA; Lane 4: insoluble fraction of a crude extract of an arabinose-induced *E. coli* culture of wt-CotA; Lane 5: supernatant of a crude extract of an arabinose-induced *E. coli* culture of E498G-CotA; Lane 6: insoluble fraction of a crude extract of an arabinose-induced *E. coli* culture of E498G-CotA; Lane 7: supernatant of a crude extract of an arabinose-induced *E. coli* culture of T480A/E498G-CotA; Lane 8: insoluble fraction of a crude extract of an arabinose-induced *E. coli* culture of T480A/E498G-CotA.

B 1 2 3 4 5 6 7

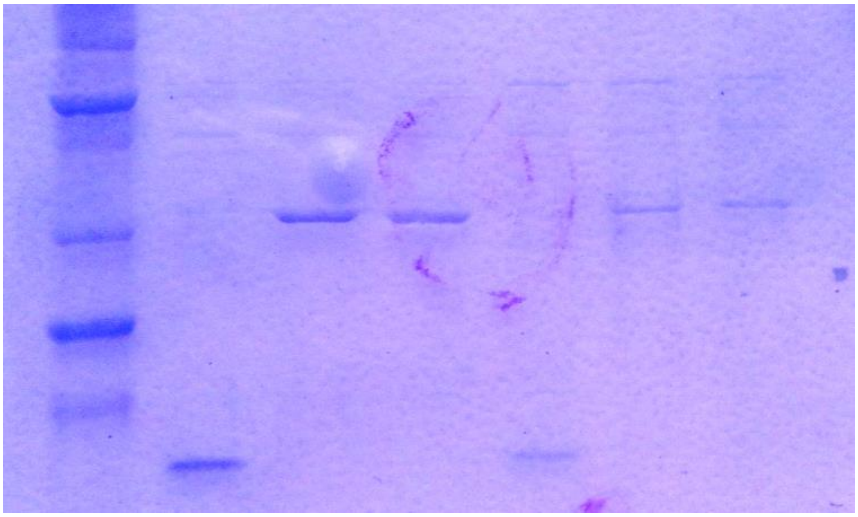

Figure 2.14 (continued) SDS-PAGE analysis of CotA overproduction in *E. coli*. (B) Lane 1: Marker; Lane 2: purified wt-CotA from *E.coli* without boiling; Lane 3: purified wt-CotA from *E.coli* boiled for 5 min; Lane 4: purified wt-CotA from *E.coli* boiled for 10 min; Lane 5: purified E498G-CotA from *E.coli* without boiling; Lane 6: purified E498G-CotA from *E.coli* boiled for 5 min; Lane 7: purified E498G-CotA from *E.coli* boiled for 10 min.

The $t_{1/2}$ (Figure 2.15) and catalytic efficiency follow the same trends for spore or *E. coli* expressed wt-CotA and E498G-CotA, although the kinetic parameters (Table 2.3) are different (Figure 2.16). The catalytic efficiency of purified or spore expressed wt-CotA is greater than E498G-CotA. It is clear that the purified enzyme and spore displayed enzyme have different catalytic efficiencies. There are many complex interactions with the spore coat proteins.

Table 2.3 Kinetics Parameters of Purified Wild-type CotA and E498G-CotA

	K_m (μM)	V_{max} (μM/s)	K_{cat} (s^{-1})	K_{cat}/K_m
Wildtype	156.3±23.7	0.512±0.03	23.2±1.3	0.15
E498G	432.7±34.5	0.103±0.002	3.7±0.1	0.01

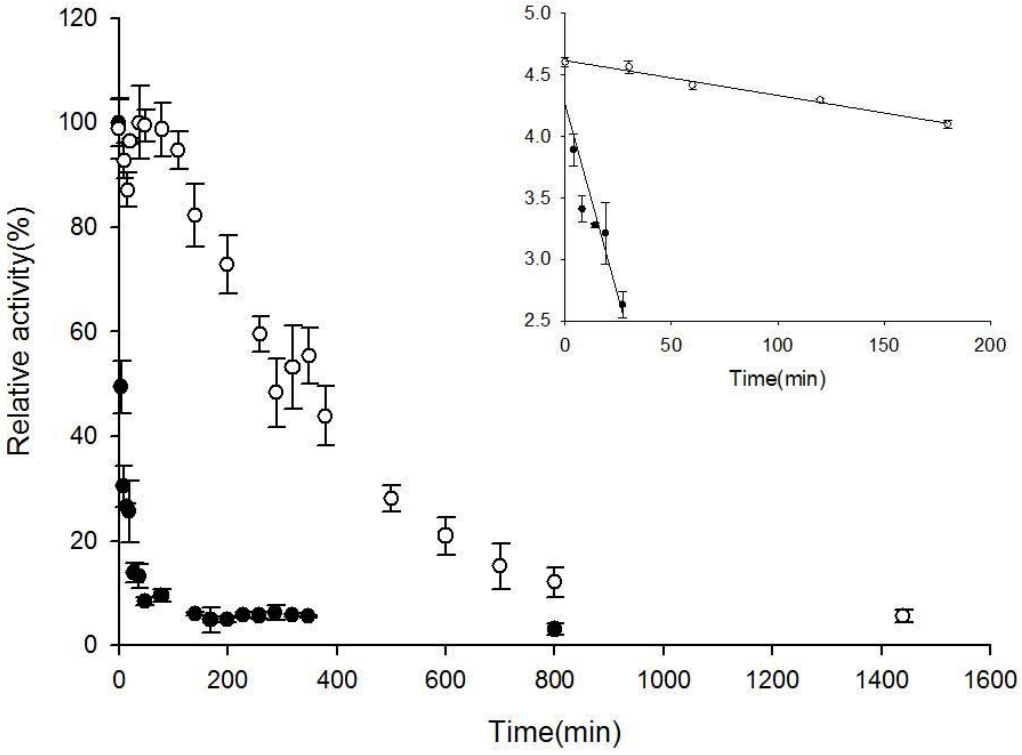

Figure 2.15 The $t_{1/2}$ at pH 4 of wt-CotA and E498G-CotA. The $t_{1/2}$ is determined from first order kinetic of deactivation. Wt-CotA (closed circles) and E498G-CotA (open circle) residual activity at pH 4 is plotted against time. The $t_{1/2}$ of wt-CotA was determined as 11 min. For E498G, there is a "stable period" around 60 min when the activity of the protein does not change relatively according to time. A half-life of inactivation of 274 min was determined; if the initial 60-min "stable period" is considered, a $t_{1/2}$ of 334 min can be estimated for E498G.

A

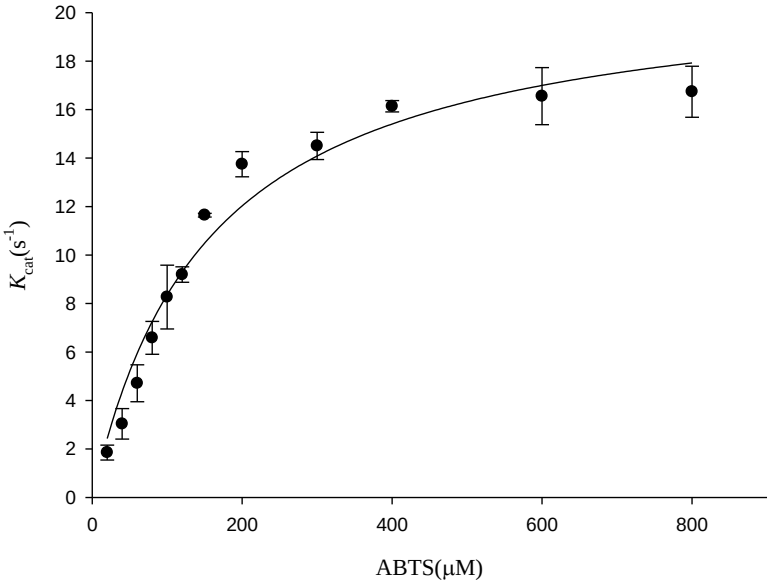

B

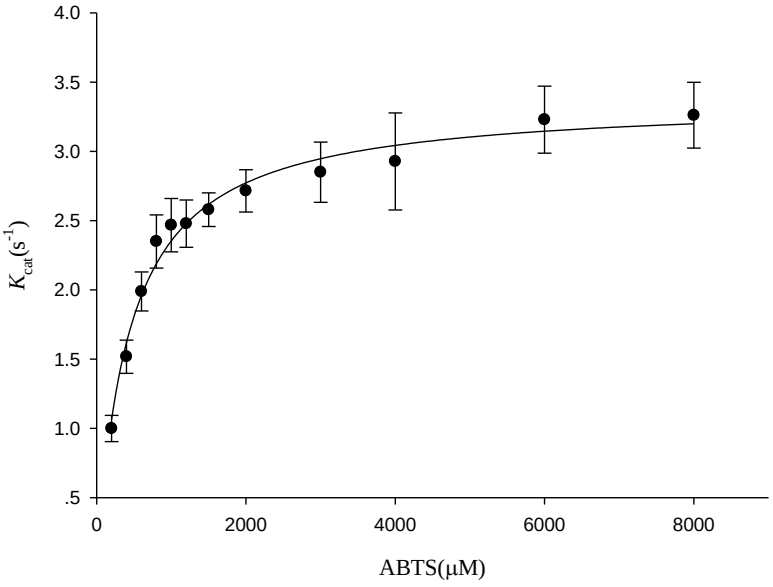

Figure 2.16 Kinetic parameters of purified wt-CotA and E498G-CotA from *E.coli*. A. Kinetics of wt-cotA. K_M = 156.3 ± 23.7 μM; K_{cat} = 23.2 ± 1.3 s^{-1}. B. Kinetics of E498G-CotA. K_M= 432.7 ± 34.5 μM; K_{cat}= 3.7 ± 0.1 s^{-1}.

2.4 Conclusion

In this study, a library of CotA laccase was constructed and transformed into *Bacillus subtilis*. An assay at acidic pH was then developed and a mutant was found with improved $t_{1/2}$ in acidic pH than wildtype. Also, the viability of spores was proven to be intact in this condition. The spores were able to be recycled and the total amount of product formed after approximately 2 days was greater for the variants when compared to wt-CotA. Spore display was demonstrated to be able to evolve proteins for pH resistance.

CHAPTER 3

OXIDATION OF PHENOLIC COMPOUNDS WITH COTA LACCASE AND ITS MUTANT ON BACILLUS SUBTILIS SPORE COAT IN ORGANIC MEDIA

Enzymes are green and efficient catalysts because they operate at room temperature and aqueous solutions. Furthermore, they have high substrate specificity that can produce chiral products with high enantiomeric excess. Therefore, the application of enzymes in industry is continuously increasing. However, these desired characteristics may not be suited for industrial applications [78-80]. For example, enzymes may have low catalytic efficiency with non-natural substrates. Next, hydrophobic substrates are not soluble in aqueous solutions and an organic co-solvent must be added for the reaction to occur. In general, enzymes are not stable in organic solvents and they lose activity [81-83]. Protein structure is due to the balance of forming the hydrophobic core, Van der Waals forces, electrostatic interactions, and hydrogen bonding. Organic solvent disrupts the hydrophobic core and the protein will unfold. Furthermore, organic solvents can strip water from the protein surface, which is necessary for structure and function. Finally, the enzymatic activity will decrease in organic solvent due to thermodynamic reasons. In aqueous solution, the substrate is surrounded by water and oftentimes the active site is hydrophobic. It is energetically favorable for the substrate to be desolvated and partition into the hydrophobic active site. Hydrophobic substrates are thermodynamically stabilized in the organic solvent compared to water.

Enzyme immobilization has several advantages [84,85]. First, protein stability

can be increased. Next, they are more resistant to environment changes, which can enhance the lifetime in organic solvents. Furthermore, substrates are freely accessible to biocatalyst. Finally, the enzyme can be easily removed from reaction mixture for reuse [86]. Protein display on the surface of the microorganisms is one strategy to immobilize enzymes [87].

Traditional cell surface display systems, such as *Escherichia coli* and yeast, appear ideal; however, there are several issues [39]. Lysis may occur during the reaction and contents of the cells will enter into the solution. As a result, this will add additional contamination and separating the enzyme from the reaction solution may be required. Spores overcome these issues. Spores remain viable under extreme chemical and physical conditions [88,89]. As a result, enzymes displayed on its surface can tolerate extreme properties. They will not lyse and can be easily removed from the reaction solution. In addition, protein folding problems associated with the target protein crossing cell membranes is eliminated. Furthermore, there is no need to overexpress, purify, and attach the protein to an inert surface. This is due to the natural sporulation process [90]. In addition, the whole cell biocatalyst can be recycled and reused, which reduces the overall cost associated with product yield.

Natural phenolic compounds have beneficial biological effects. They can act as antioxidants [91], antimutagens [92] and anticarcinogens [93]. For example, (+)-catechin (Figure 3.1A) and (-)-epicatechin (Figure 3.1B), are two phenolic isomers that can be found in green tea, and they are responsible for the potential health benefits [94].

However, they affects the flavor and mouth-feel and these compounds can be removed by polymerization [95]. As a result, the sensory quality is enhanced [96]. Polycatechins can be utilized to prevent neurodegenerative and cardiovascular diseases [97,98]. Enzymes, such as laccase, have been used to polymerize phenolic compounds for a variety of applications [99,100] (Figure 3.2A). One limitation is that these polymers are insoluble and require organic co-solvents.

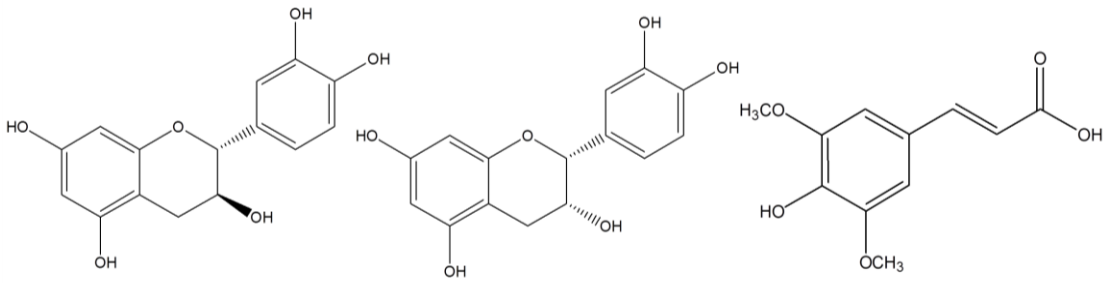

A B C

Figure 3.1 Structure of phenolic substrates. (A) (+)-catechin; (B) (-)-epicatechin; and (C) sinapic acid.

Next, rapeseed meal (RSM) is widely utilized to feed all classes of livestock. Sinapic acid (Figure 3.1C) and the choline ester of sinapic acid (sinapine) are the major phenolic compounds found in RSM [101,102]. These compounds or their derivatives lower the nutritional value of RSM. In addition, they render RSM to be bitter and astringent [103,104] . Biocatalysts can be used to eliminate these antinutrients [105]. The oxidation of sinapic acid by laccase is shown in Figure 3.2B.

A

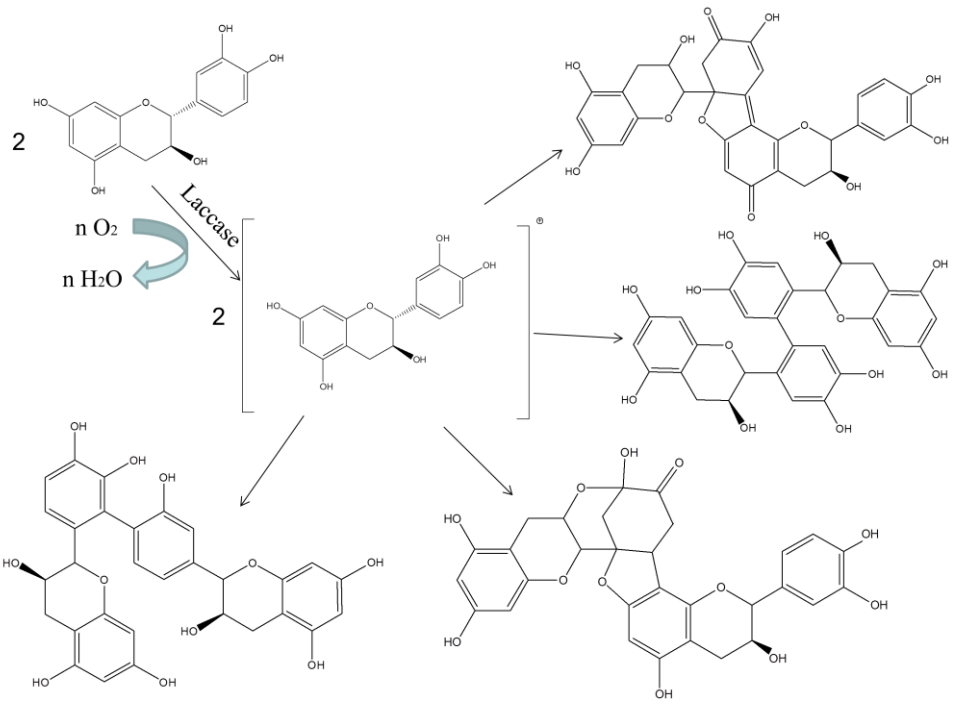

B

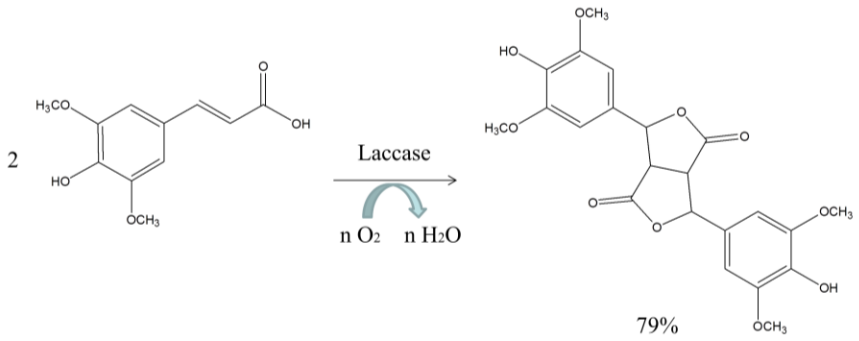

Figure 3.2 Oxidation of phenols by laccase. (A) Two molecules of (+)-catechin are oxidized to polycatechin by laccase. (B) Sinapic acids are oxidized by laccase into dimers.

In a previous investigation, a laccase (CotA), which is found on the spore coat of *Bacillus subtilis*, was engineered by directed evolution for improved activity in organic

solvents. A CotA variant was identified with a Thr480Ala (T480A-CotA) amino acid substitution [44] after only one round of evolution. The screen was performed at 60 % DMSO and it was 2.38-fold more active than the wild-type CotA (wt-CotA) with substrate 2,2′-azino-bis(3-ethylbenzothiazoline-6-sulfonic acid) (ABTS). T480A-CotA was more active from a range of 0 – 70 % DMSO. In addition, the variant was more active in ethanol, methanol and acetonitrile. In this study, the catalysis of T480A-CotA and wt-CotA in the spore coat was determined with natural phenolic compounds, such as (+)-catechin, (-)-epicatechin and sinapic acid in aqueous-organic media.

3.1 Materials

Wt-CotA and T480A-CotA was expressed and purified on *B. subtilis* spores by following published procedures [44]. One unit is defined as a δA of 0.001 per min at 37 ◦C in a 300 µl reaction volume on a 96-well microplate at absorbance 433 nm (SpectraMax_M2) using (+)-catechin (433 nm), or absorbance 440 nm using (-)-epicatechin, or absorbance at 512nm using sinapic acid. Dimethyl sulfoxide (DMSO), acetonitrile, methanol, ethanol, acetonitrile, (+)-catechin, (−)-epicatechin, sinapic acid were procured from Sigma-Aldrich (St. Louis, MO).

3.2 Methods

3.2.1 Wt-CotA and T480A-CotA Activity Versus pH

Substrate stocks were prepared for (+)-catechin (200 mM), (−)-epicatechin (200 mM) and sinapic acid (200 mM) in methanol. Each stock solution was prepared fresh before use. The purified spore pellets of wt-CotA or T480A-CotA were resuspended in aqueous $CuCl_2$ (0.25 mM) for 60 minutes. Next, spore suspension was diluted in citric phosphate buffer (100 mM, 0.25 mM $CuCl_2$).

The total volume of the reaction was 300 μl. Substrate (30 μl; 20 mM) was added to citrate phosphate buffer (250 μl; 100 mM) and methanol (10% v/v) solution containing $CuCl_2$ (0.25 mM). The reaction was initiated with the spore resuspension (20 μl, OD_{580} = 0.1 – 0.3). The pH was varied from 2 - 8 for the reactions. The absorbance 433 nm for (+)-catechin (433 nm), (−)-epicatechin (440 nm), or sinapic acid (512 nm) was measured every 5 min for 60 min at 37 ◦C. Each reaction was done in triplicate. Control experiments were done with spores that had the *cotA* gene knockout (strain1S101, Bacillus Genetic Stock Center, The Ohio State University, Columbus, OH, USA).

3.2.2 Determination of Kinetic Parameters of Wt-CotA and T480A-CotA

The total volume of the reaction was 300 μl. Substrate (30 μl; 0.05 – 6.0 mM) was added to citrate phosphate buffer (250 μl; 100 mM; pH 7) and methanol (20% v/v) solution containing $CuCl_2$ (0.25 mM). The reaction was initiated with the spore resuspension (20

μl; OD_{580nm} = 0.1 – 0.3). K_m and V_{max} was determined for wt-CotA and T480A-CotA. The absorbance 433 nm for (+)-catechin (433 nm), (−)-epicatechin (440 nm), or sinapic acid (512 nm) was measured every 5 min for 60 min at 37 ◦C. Each reaction was done in triplicate. Control experiments were done with spores that had the *cotA* gene knockout (strain1S101, Bacillus Genetic Stock Center, The Ohio State University, Columbus, OH, USA).

3.2.3 Wt-CotA and T480A-CotA Activity in Organic Solvents

The activity of wt-CotA and T480A-CotA was determined in DMSO, methanol, ethanol, and acetonitrile. The concentration of organic solvents used in the reaction media ranged from 0 – 70 % (v/v). The substrates used were (+)-catechin, (-)-epicatechin and sinapic acid and concentrations were 10 mM for each substrate. An OD_{580nm} 0.1 – 0.3 was used for wt-CotA and T480A-CotA. Control experiments were done with spores that had the *cotA* gene knockout (strain1S101, Bacillus Genetic Stock Center, The Ohio State University, Columbus, OH, USA). The *V*max measurement is similar to section 3.2.2.

3.2.4 Wt-CotA and T480A-CotA Recylcing in Organic Solvents

CotA was recycled and the total product yield was determined over a 23-hour period. The spores were resuspended in aqueous $CuCl_2$ (0.25 mM) solution for 60 minutes at 37 ℃. Next, the spores were centrifuged and the supernatant was discarded. The spores were resuspended in citrate phosphate buffer (100 mM, pH 7) with organic solvents (60, 20, 40,

and 30 % (v/v) for DMSO, acetonitrile, methanol, and ethanol) at 37 ℃ with a final OD_{580} of 0.2. The spores were incubated for four hours and then the spores centrifuged and the supernatant was discarded. The reaction was initiated by resuspending the spore with 300 μL (+)-catechin (10 mM) in citrate phosphate buffer (100 mM, pH 7) with organic solvents (60, 20, 40, and 30 % (v/v) for DMSO, acetonitrile, methanol, and ethanol) at 37 ℃. The absorbance was taken at 433 nm after 60 minutes to determine the product yield ($\delta A_{433nm\_product}$). This cycle was repeated seven times over 23-hours. Control experiments were done with spores that had the *cotA* gene knockout (strain1S101, Bacillus Genetic Stock Center, The Ohio State University, Columbus, OH, USA).

3.3 Results and Discussion

3.3.1 Wt-CotA and T480A-CotA Activity Versus pH

The activity was measured for wt-CotA and T480A-CotA with (+)-catechin, (-)-epicatechin or sinapic acid under different pH (range from 2 to 8) (Figure 3.3). The activity trends were similar for wt-CotA and T480A-CotA towards (+)-catechin, (-)-epicatechin and sinapic acid. For example, wt-CotA and T480A-CotA have low activity at acidic pH and the activity rise to a maximum at approximately pH 7 for all the substrates. In addition, T480A-CotA always has greater activity than the wt-CotA. The amino acid substitution does not change the pH optimum for both enzymes; however, the T480A displays a higher V_{max} [44]. A dramatic increase of laccase activity from pH 6 to 7

for the oxidation of (+)-catechin, (-)-epicatechin and sinapic acid was observed (Figure 3.3A-C). At pH 7, wt-CotA activity increases 2.9, 1.8 and 2.6-fold for substrate (+)-catechin, (-)-epicatechin and sinapic acid in comparison to that at pH 6. For T480A-CotA, the activity at pH 7 increases 3.9, 2.5 and 2.3-fold for substrate (+)-catechin, (-)-epicatechin and sinapic acid comparing to that at pH 6. Also, the laccase activity dropped from pH 7 to 8. Therefore, the optimum pH values of wt-CotA and T480A-CotA for substrates (+)-catechin, (-)-epicatechin and sinapic acid were around pH 7. Also, T480A-CotA shows 1.8, 4.4, 1.7-fold higher activity than wt-CotA in pH 7 for substrates (+)-catechin, (-)-epicatechin and sinapic acid, respectively. Therefore, T480A-CotA is more active than wt-CotA at their optimum pH for these substrates.

A

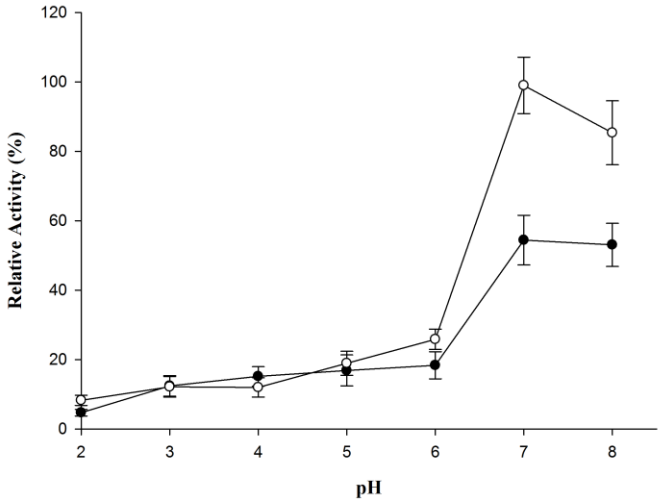

B

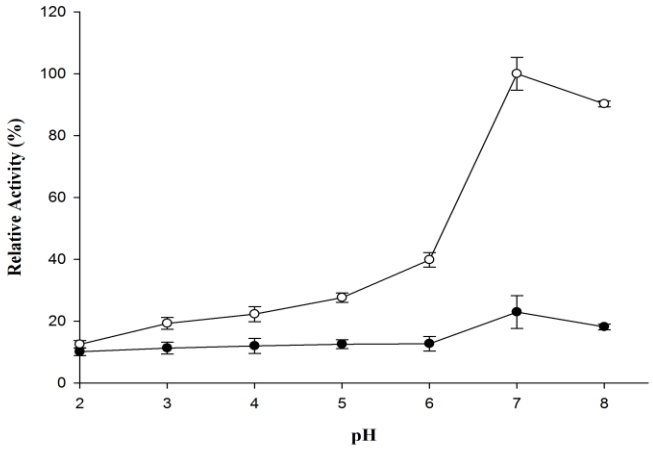

Figure 3.3 Effect of pH on laccase-catalyzed oxidation of (+)-catechin (A), (-)-epicatechin (B), and sinapic acid (C) is determined for wt-CotA (closed circles) and T480A-CotA (open circles).

C

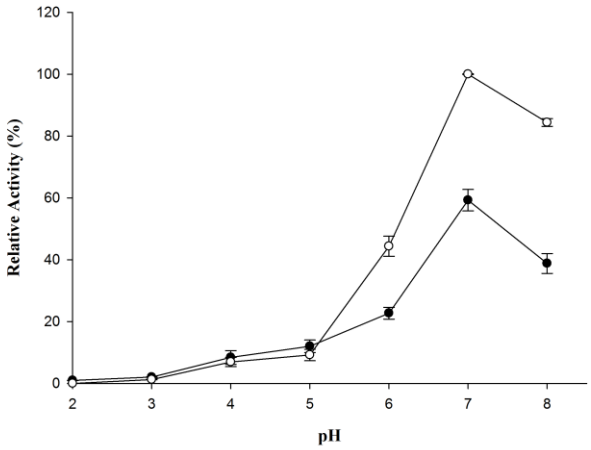

Figure 3.3 (continued) Effect of pH on laccase-catalyzed oxidation of (+)-catechin (A), (-)-epicatechin (B), and sinapic acid (C) is determined for wt-CotA (closed circles) and T480A-CotA (open circles).

3.3.2 Determination of Kinetic Parameters

V_{max} and K_m was determined for wt-CotA and T480A-Cot with (+)-catechin, (-)-epicatechin and sinapic acid (Figure 3.4, Table 3.1). T480A-CotA has a K_m smaller for (+)-catechin, (-)-epicatechin than the wt-CotA. Wt-CotA has a K_m 1.46-fold and 1.84-fold greater than T480A-CotA for (+)-catechin and (-)-epicatechin, respectively. On the other hand, T480A-CotA has a K_m larger for sinapic acid. In all cases, T480A-CotA has a greater V_{max} [44]. The V_{max}/K_m for T480A-CotA was 4.1-fold, 5.6-fold, and 1.4 greater than that of wt-CotA for (+)-catechin, (-)-epicatechin, and sinapic acid, respectively.

A

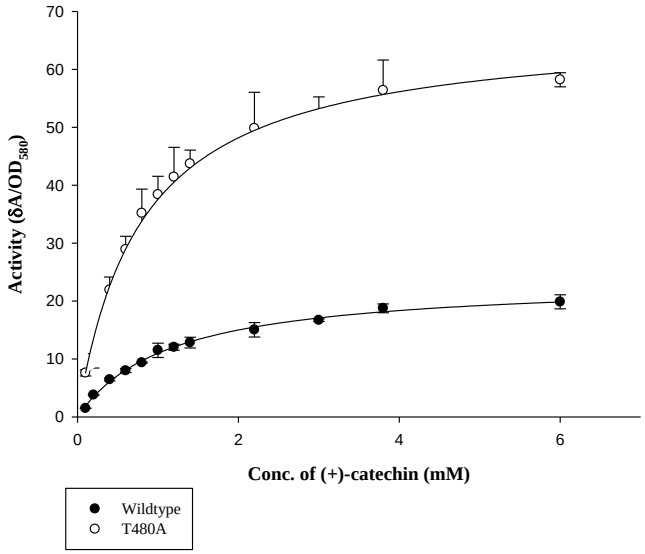

B

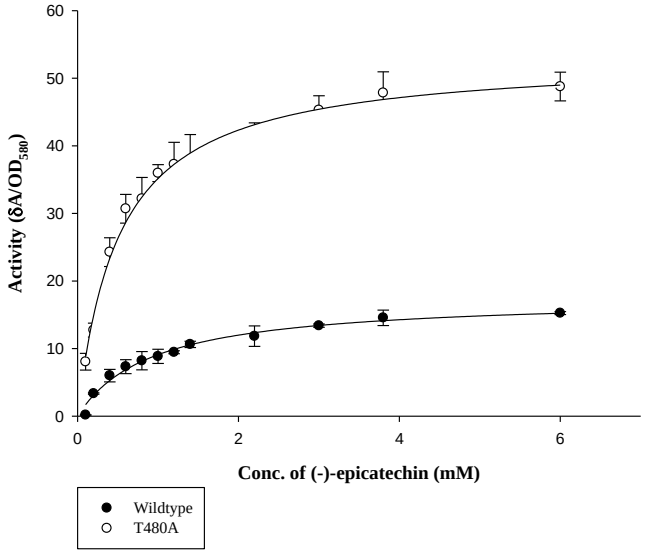

Figure 3.4 Kinetic parameters of wt-CotA and T480A-CotA on *Bacillus subtilis* spore coat for substrates (+)-catechin, (-)-epicatechin and sinapic acid. (A) Kinetics of wt-CotA and T480A-CotA for substrate (+)-catechin. K_m = 1.15 ± 0.06 mM, V_{max} = 23.7 ± 0.49 $\delta A/OD_{580\ nm}$ for wt-CotA; K_m = 0.79 ± 0.05 mM, V_{max} = 67.2 ± 1.54 $\delta A/OD_{580\ nm}$ for T480A-CotA. (B) Kinetics of wt-CotA and T480A-CotA for substrate (-)-epicatechin. K_m = 0.94 ± 0.1 mM, V_{max} = 17.6 ± 0.69 $\delta A/OD_{580nm}$ for wt-CotA; K_m = 0.51 ± 0.03 mM, V_{max} = 53.2 ± 0.99 $\delta A/OD_{580nm}$ for T480A-CotA.

C

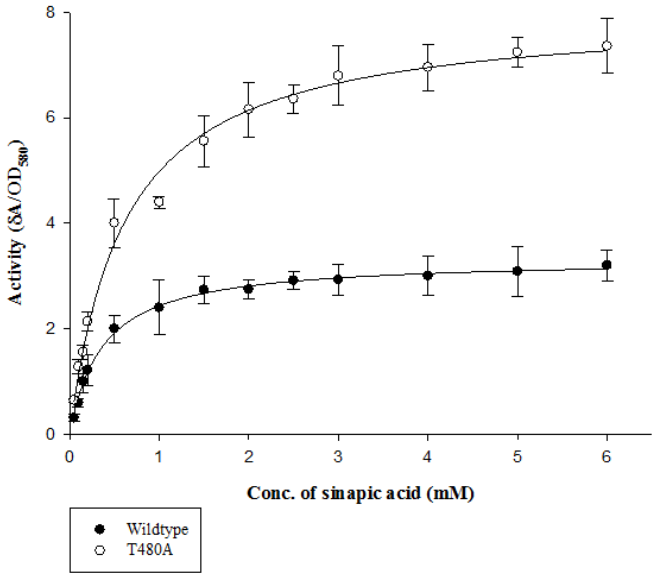

Figure 3.4 (continued) Kinetic parameters of wt-CotA and T480A-CotA on *Bacillus subtilis* spore coat for substrates (+)-catechin, (-)-epicatechin and sinapic acid. (C) Kinetics of wt-CotA and T480A-CotA for substrate sinapic acid. K_m = 0.36 ± 0.02 mM, V_{max} = 3.33 ± 0.04 $\delta A/OD_{580nm}$ for wt-CotA; K_m = 0.61 ± 0.05 mM, V_{max} = 8.00 ± 0.18 $\delta A/OD_{580nm}$ for T480A-CotA.

Table 3.1 Kinetics Parameters of Wt-CotA and T480A-CotA with Different Substrates

Substrate	Mutation	K_m [a]	V_{max} [b]	V_{max} / K_m
(+)-catechin	Wildtype	1.15 ±0.06	23.7 ±0.49	20.6
	T480A	0.79 ±0.05	67.2 ±1.54	85
(-)-epicatechin	Wildtype	0.94 ±0.1	17.6 ±0.69	18.7
	T480A	0.51 ±0.03	53.2 ±0.99	104.3
Sinapic acid	Wildtype	0.36 ±0.02	3.33 ±0.04	9.3
	T480A	0.61 ±0.05	8.00 ±0.18	13.1

[a] = mM, [b] = $\delta A/OD_{580}$

3.3.3 Activity of Wt-CotA and T480A-CotA in Organic Solvent

The activity of wt-CotA and T480A-CotA was measured at different concentrations of DMSO, acetonitrile, methanol and ethanol (Figure 3.4A-C, Table 3.2). In general, the V_{max} for T480A-CotA was greater than the wt-CotA in all organic solvents. Wt-CotA and T480A-CotA showed slight activity over the background in buffer alone. It is clear that organic co-solvents are necessary to solubilize the substrate for enzymatic activity. For the substrates (+)-catechin and (-)-epicatechin, T480A-CotA has an optimum concentration of 60, 20, 40, and 30 % (v/v) for DMSO, acetonitrile, methanol, and ethanol (Figure 3.5A-B). For substrate (+)-catechin, T480A-CotA is 1.4 – 3.0, 1.1 – 3.0, 1.7 – 3.4, and 1.2 – 2.4-fold more active than wt-CotA in DMSO, acetonitrile, methanol, and ethanol, respectively. For substrate (-)-epicatechin, T480A-CotA is 1.0 – 4.1, 1.0 – 5.6, 1.1 – 7.9 and 1.3-6.2-fold more active in DMSO, acetonitrile, methanol, and ethanol, respectively. For substrate sinapic acid, T480A-CotA has an optimum concentration of 30, 30, 30, and 20 % (v/v) for DMSO, acetonitrile, methanol, and ethanol (Figure 3.5C). T480A-CotA is 2.4 – 4.8, 1.4 – 2.3, 1.5 – 6.4 and 1.5 – 5.2-fold more active in DMSO, acetonitrile, methanol, and ethanol, respectively.

A

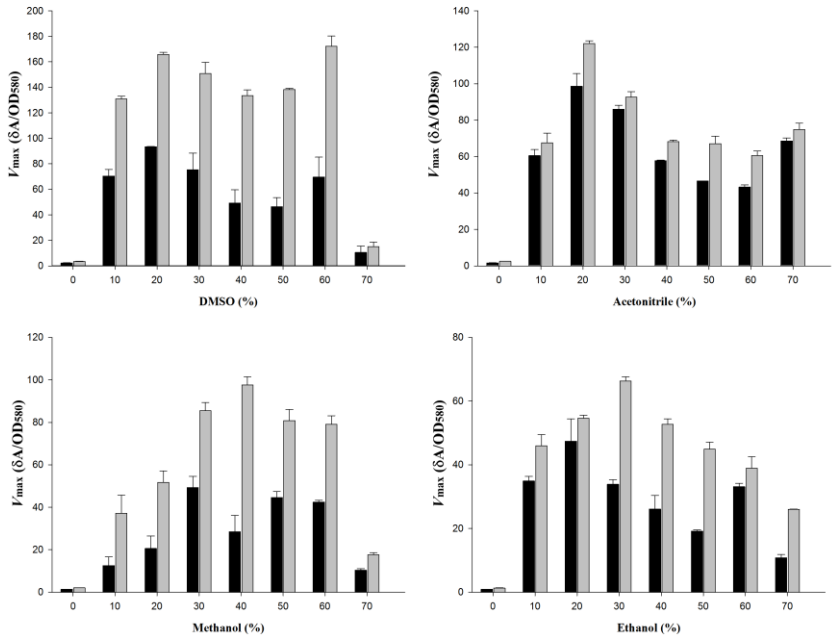

B

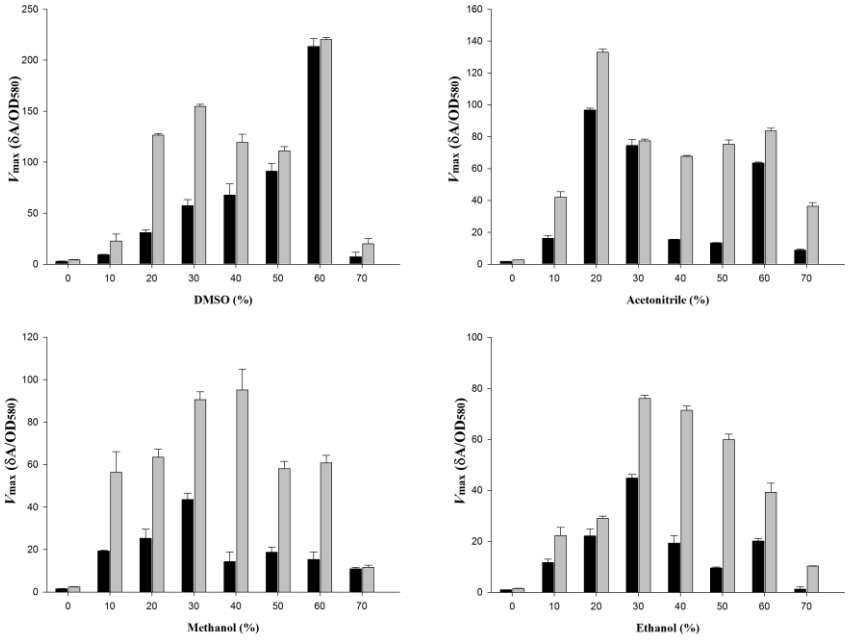

Figure 3.5 V_{max} (δA/OD_{580}) of wt-CotA (black bars) and T480A-CotA (grey bars) in 0 – 70 % organic solvents for substrate (+)-catechin (A), (-)-epicatechin (B), and sinapic acid (C).

C

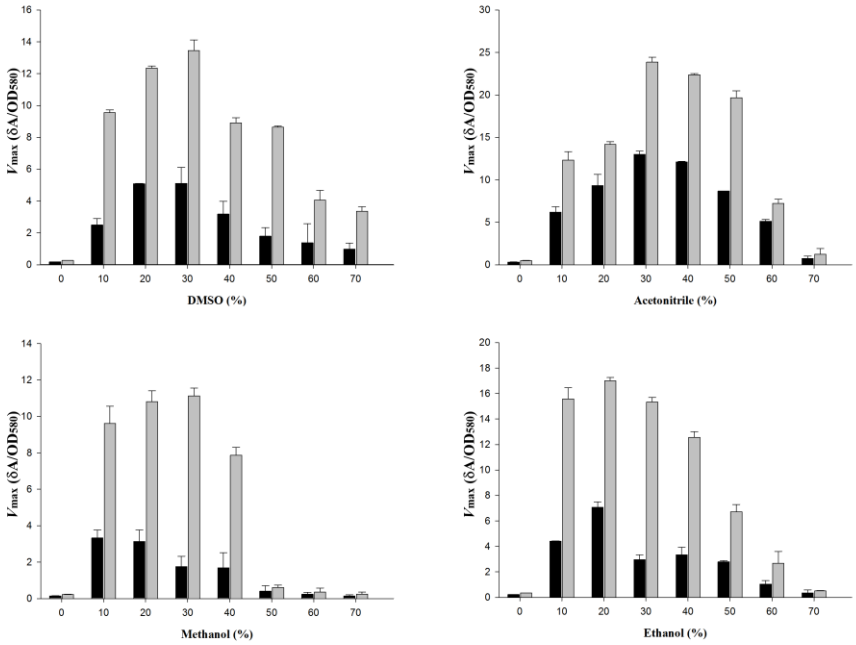

Figure 3.5 (continued) V_{max} ($\delta A/OD_{580}$) of wt-CotA (black bars) and T480A-CotA (grey bars) in 0 – 70 % organic solvents for substrate (+)-catechin (A), (-)-epicatechin (B), and sinapic acid (C).

Table 3.2 V_{max} ($\delta A/OD_{580}$) of Wt-CotA and T480A-CotA in 0 – 70 % Organic Solvents for Substrate (+)-Catechin (A), (-)-Epicatechin (B) and Sinapic Acid (C)

A

Conc. of solvents	V_{max} ($\delta A/OD_{580}$)							
	DMSO		Acetonitrile		Methanol		Ethanol	
	wt	T480A	wt	T480A	wt	T480A	wt	T480A
0 %	2.3 ±0.1	3.5 ±0.2	1.6 ±0.1	2.5 ±0.1	1.32 ±0.2	2.01 ±0.1	0.9 ±0.0	1.33 ±0.1
10 %	70.4 ±5.3	130.9 ±2.3	60.5 ±3.3	67.6 ±5.3	12.4 ±4.0	36.6 ±8.4	34.9 ±1.4	46.0 ±3.4
20 %	93.5 ±0.2	165.7 ±1.7	98.7 ±6.9	122 ±1.6	20.3 ±5.8	50.9 ±5.4	47.4 ±7	54.6 ±1.0
30 %	75.3 ±13.1	150.9 ±8.7	86.0 ±2.1	92.7 ±2.9	48.6 ±5.2	84.2 ±3.8	33.8 ±1.5	66.3 ±1.4
40 %	49.1 ±10.5	133.6 ±4.3	57.7 ±0.3	68.2 ±0.9	28.1 ±7.5	96.1 ±3.9	26.1 ±4.3	52.7 ±1.7
50 %	46.3 ±7.1	138.3 ±0.8	46.6 ±0.1	67.0 ±4.2	44.0 ±2.7	79.6 ±5.2	19.2 ±0.4	44.9 ±2.2
60 %	69.7 ±15.6	172.2 ±8.0	43.3 ±1.2	60.6 ±2.6	41.8 ±0.9	77.9 ±4.0	33.2 ±1.0	38.9 ±3.7
70 %	10.5 ±5.0	15.1 ±3.5	68.6 ±1.5	74.8 ±3.5	10.2 ±0.7	17.4 ±1.0	10.8 ±1.0	26.0 ±0.1

Table 3.2 (continued) V_{max} ($\delta A/OD_{580}$) of Wt-CotA and T480A-CotA in 0 – 70 % Organic Solvents for Substrate (+)-Catechin (A), (-)-Epicatechin (B) and Sinapic Acid (C)

B

Conc. of solvents	V_{max} ($\delta A/OD_{580}$)							
	DMSO		Acetonitrile		Methanol		Ethanol	
	wt	T480A	wt	T480A	wt	T480A	Wt	T480A
0 %	2.9±0.1	4.4±0.2	1.7±0.1	2.7±0.1	1.6±0.1	2.4±0.1	1.0±0.0	1.5±0.1
10 %	9.2±0.5	22.6±6.9	16.2±1.7	42.0±3.4	19.3±0.4	56.4±9.6	11.7±1.4	22.3±3.2
20 %	31.0±2.7	126.6±1.6	96.8±1.1	133±1.9	25.4±4.2	63.6±3.8	22.2±2.8	29.0±1.0
30 %	57.4±5.9	154.7±2.3	74.5±3.6	77.4±1.0	43.6±3.0	90.7±3.6	44.9±1.4	76.1±1.3
40 %	67.8±11.1	119.6±7.8	15.6±0.1	67.8±0.6	14.4±4.4	95.1±9.9	19.4±2.9	71.5±1.6
50 %	91.2±7.8	111.0±4.3	13.4±0.1	75.3±2.8	18.7±2.6	58.2±3.4	9.6±0.4	59.9±2.1
60 %	213.6±7.5	220.4±2.0	63.5±0.6	83.7±1.7	15.4±3.6	60.9±3.5	20.1±1.0	39.3±3.5
70 %	7.4±4.3	20.1±5.0	8.7±0.8	36.4±2.3	10.9±0.6	11.6±0.9	1.3±1.0	10.3±0.1

C

Conc. of solvents	V_{max} ($\delta A/OD_{580}$)							
	DMSO		Acetonitrile		Methanol		Ethanol	
	wt	T480A	wt	T480A	wt	T480A	Wt	T480A
0 %	0.2±0.0	0.3±0.0	0.3±0.0	0.5±0.0	0.1±0.0	0.2±0.0	0.2±0.0	0.3±0.0
10 %	2.5±0.4	9.6±0.2	6.2±0.6	12.3±1.0	3.3±0.4	9.6±1.0	4.4±0.0	15.6±0.9
20 %	5.1±0.0	12.3±0.1	9.3±1.3	14.2±0.3	3.1±0.6	10.8±0.6	7.1±0.4	17.0±0.2
30 %	5.1±1.0	13.5±0.7	13.0±0.4	23.9±0.6	1.8±0.6	11.1±0.4	3.0±0.4	15.3±0.4
40 %	3.2±0.8	8.9±0.3	12.1±0.0	22.4±0.2	1.7±0.8	7.9±0.4	3.4±0.6	12.6±0.4
50 %	1.8±0.5	8.7±0.0	8.7±0.0	19.7±0.8	0.4±0.3	0.6±0.1	2.8±0.1	6.7±0.6
60 %	1.4±1.2	4.1±0.6	5.1±0.2	7.2±0.5	0.2±0.1	0.4±0.2	1.0±0.3	2.7±0.9
70 %	1.0±0.4	3.4±0.3	0.7±0.3	1.2±0.7	0.1±0.1	0.2±0.1	0.3±0.3	0.5±0.0

3.3.4 Wt-CotA and T480A-CotA Recycling in Organic Solvents

Enzyme recycling improves overall product by reusing the catalysts for several batches. This reduces the cost associate with product yield. Typically, the enzyme is expressed purified and attached to an inert particle. This is avoided in spore display because the enzyme is attached to the inert surface of the spore coat. CotA recycling was investigated

and the total product yield was determined for (+)-catechin over 23-hour period (Figure 3.6, Table 3.3). These percentages (v/v) were chosen at the maximum rates for the organic solvents, which were 60, 20, 40, and 30 % (v/v) for DMSO, acetonitrile, methanol and ethanol, respectively. The trend of total product is similar for wt-CotA and T480A-CotA. The total product yield diminishes after recycling. The product yield retains 60, 30, and 10 % from t = 0 to 23 hours in DMSO, acetonitrile, and ethanol, respectively (Figure 3.5). In methanol, wt-CotA and T480A-CotA also has lowered product over time, which is 10 and 30 %, respectively. The total product yields from T480A-CotA were 11.2, 7.1, 3.9 and 4.2 $\delta A_{433nm\_product}$ in DMSO, acetonitrile, methanol and ethanol, respectively. The optimum solvent was DMSO for the mutant. Next, the total product yields from wt-CotA were 3.6, 4.7, 1.4, and 2.4 $\delta A_{433nm\_product}$ in DMSO, acetonitrile, methanol, and ethanol, respectively. Wt-CotA catalyzes the most products in acetonitrile. In general, the biocatalysts have a greater yield in polar aprotic solvents. In addition, T480A-CotA out performs the wt-CotA in all organic solvents.

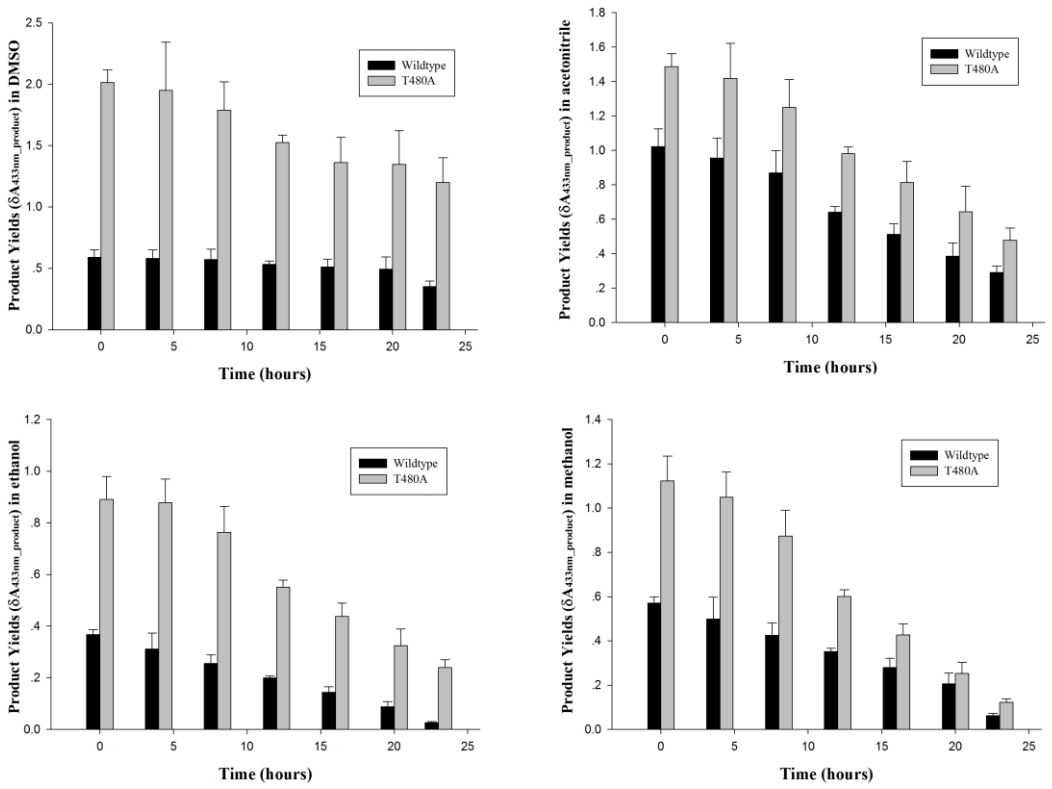

Figure 3.6 The (+)-catechin products yields for wt-CotA (black bars), and T480A-CotA (white bars) were determined for 7 cycles over a 23 h period.

Table 3.3 The (+)-catechin Products Yields for Wt-CotA and T480A-CotA Were Determined for 7 cycles Over A 23 h Period.

Time (hours)	Product yields ($\delta_{A433nm\_product}$)							
	DMSO		Acetonitrile		Methanol		Ethanol	
	wt	T480A	wt	T480A	wt	T480A	wt	T480A
0	0.59	2.01	1.02	1.49	0.37	0.89	0.57	1.12
4	0.58	1.95	0.96	1.42	0.31	0.88	0.5	1.05
8	0.57	1.79	0.87	1.25	0.26	0.76	0.43	0.87
12	0.53	1.53	0.64	0.98	0.20	0.55	0.35	0.6
16	0.51	1.36	0.51	0.81	0.14	0.44	0.28	0.43
20	0.49	1.35	0.39	0.64	0.09	0.32	0.21	0.25
23	0.35	1.20	0.29	0.48	0.03	0.24	0.06	0.12

3.4 Conclusion

The kinetic parameters and the relative activity were determined with wt-CotA and T480A-CotA on *B. subtilis* spore coat for substrate (+)-catechin, (-)-epicatechin and sinapic acid in organic solvents. In general, the catalytic efficiency (V_{max}/K_m ($\delta A/OD_{580}$)/mM) of T480A-CotA is higher than wt-CotA for all the substrates. Then, the V_{max} for T480A-CotA was greater than the wt-CotA in all organic solvents used in this study. The V_{max} for T480A-CotA was up to 3.4-fold, 7.9-fold and 6.4-fold greater than wt-CotA for substrate (+)-catechin, (-)-epicatechin and sinapic acid, respectively. In addition, the catalyst can be easily removed from the reaction solution and reused. This allows for simpler recovery of the product from the enzyme. This investigation indicates that enzymes expressed on the spore coat can be utilized for industrial applications.

APPENDIX A

ENZYME DISPLAY FOR ALKANE OXIDATION

Cytochrome P450 monooxygenases (CYPs) belong to a superfamily of enzymes that contains heme as a cofactor. They are also known as hemoproteins. CYP enzymes have been widely found in animals, plants, and microorganisms. The most common reaction catalyzed by cytochromes P450 is a monooxygenase reaction. For example, one atom of oxygen is inserted into the aliphatic position of an organic substrate (RH) while the other oxygen atom is reduced to water (Equation A.1). Furthermore, P450s also catalyze a variety of reactions (Figure A.1).

$$RH + O_2 + NADPH + H^+ \longrightarrow ROH + H_2O + NADP^+ \qquad \textbf{Equation A.1}$$

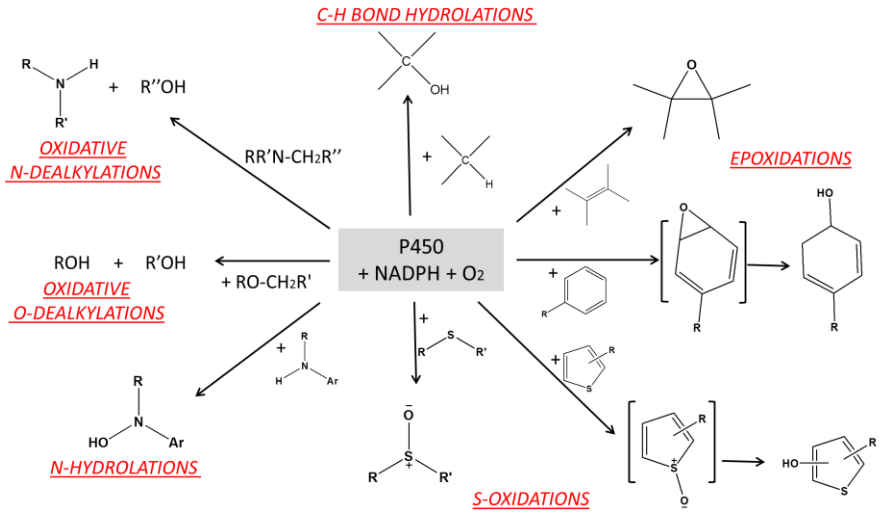

Figure A.1 Additional P450 reactions.

In humans, CYPs are primarily membrane-associated proteins located either in the inner membrane of mitochondria or in the endoplasmic reticulum of cells. They metabolize thousands of endogenous and exogenous chemical [106,107]. CYPs are the major enzymes involved in drug metabolism, accounting for about 75% of the total metabolism [108]. Most drugs undergo deactivation by CYPs, either directly or by facilitated excretion from the body [108]. In biotechnology, their unique catalytic properties are attractive because they could catalyze difficult chemical reactions, as they even act on non-activated carbon–hydrogen bonds. Recent progress towards realizing the potential of using P450s towards difficult oxidations have included [109,110]:

(1) eliminating the need for natural co-factors by replacing them with inexpensive peroxide containing molecules, (2) exploring the compatibility of p450s with organic solvents, and (3) the use of small, non-chiral auxiliaries to predictably direct P450 oxidation. P450 systems can be used in a variety of applications (Figure A.2)

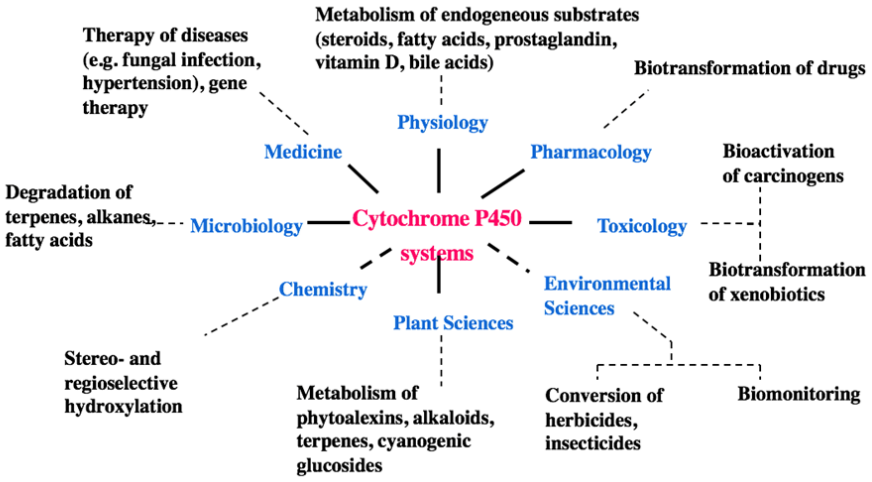

Figure A.2 Function and potential applications of Cytochrome P450 systems.

Spore display will be used to synthesize carboxylic acids from alkanes (Figure A.3; see Chapter 1 for background of spore display). The first step is oxidizing the alkane to an alcohol by a cytochrome P450. Then, the alcohol will be converted to the aldehyde by an alcohol dehydrogenase. Finally, the aldehyde will be transformed to the acid by an aldehyde dehydrogenase. The final target is to enzymatically synthesize adipic acid (1, 6-hexandioic acid). Adipic acid is widely used in industry. About 60% of the 2.5 billion kg of adipic acid produced annually is used as monomer for the production of nylon (textiles, carpets, and tire chords), polyurethanes, and plasticizers [111,112]. In medicine, adipic acid has been incorporated into controlled-release formulation matrix tablets to obtain pH-independent release for both weakly basic and weakly acidic drugs [113]. The synthesis of adipic acid is energy intensive, uses toxic, heavy metals, and nitric acid. The goal is to enzymatically synthesize hexanoic acid from hexane. A P450 will oxidize hexane to hexanol. Next, alcohol dehydrogenase will oxidize the alcohol to aldehyde. Finally, aldehyde dehydrogenase will oxidize the aldehyde to the acid.

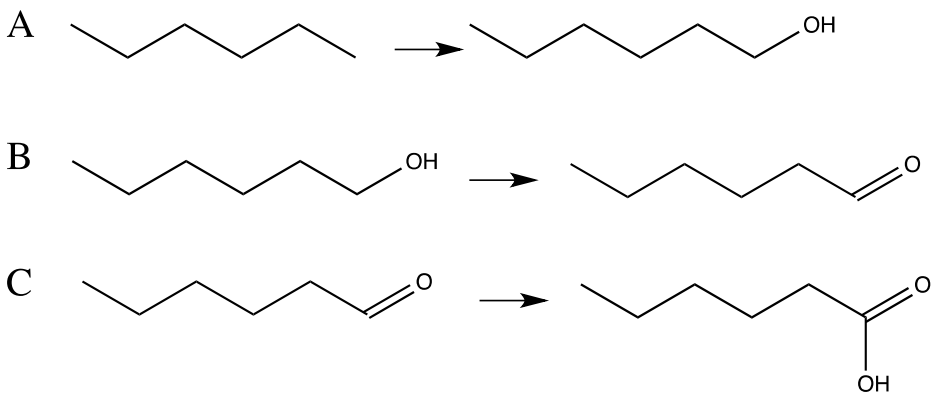

Figure A.3 Enzymatic synthesis of carboxylic acids from alkanes. (A) Cytochrome P450 catalysis of alkane to alcohol. (B) Alcohol dehydrogenase catalysis of alcohol to aldehyde. (C) Aldehyde dehydrogenase catalysis of aldehyde to carboxylic acid.

The Cytochrome P450 that will be used is CYP102A3. It is found in the *Bacillus subtilis* and has 76% similarity to the cytochrome P450 BM-3 from *B. megaterium* (CYP102A1). The structure has not been solved for CYP102A3, but it is known for CYP 102A1 (Figure A.4). Cytochrome P450 CYP102A3 is a fusion protein that consists of a heme and a FAD/FMN-reductase domain.

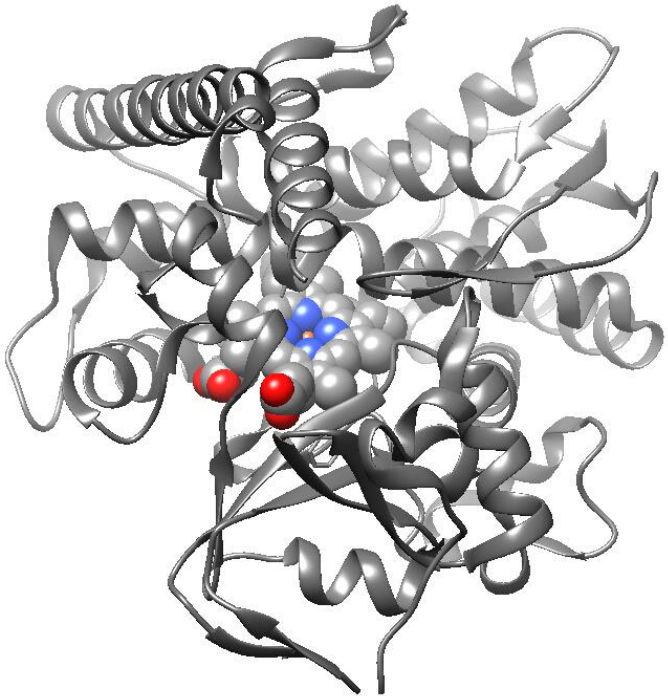

Figure A.4 Structure of CYP102A1 heme domain (PDB 2IJ2). The heme is shown as CPK spheres.

These enzymes typically oxidize fatty acids at the ω–1, ω–2, and ω–3 and not the terminal position. Wild-type CYP102A3 is most active with myristic acid (1-tetradecanoic acids). However, CYP102A3 S189Q/A330V mutant was found to oxidize octane at the terminal position and the specificity was 42%. In this study, we integrated CYP102A3 S189Q/A330V (P450) gene, fused with a green fluorescence

protein (GFP) as signaling label into the genome of *B. subtilis*. The first step is to display CYP102A3 on the spore coat.

Materials

All chemicals were of analytical reagent grade or higher quality and were purchased from Sigma-Aldrich (St. Louis, MO). Enzymes were purchased from Invitrogen (Carlsbad, CA) and New England Biolabs (Ipswich, MA). Primers were procured from Invitrogen (Carlsbad, CA). Plasmid pDG364_CotB_ HuPTH1r_GFP was previously constructed in our lab. CYP102A3 S189Q/A330V mutant was constructed and modified for *Bacillus subtilis* expression and inserted into plasmid pJ241 to construct pJ241_P450 by DNA2.0 (Newark, California, U.S.).

Methods

Gibson Assembly

Gibson Assembly was developed by Dr. Daniel Gibson and his colleagues at the J. Craig Venter Institute and licensed to NEB by Synthetic Genomics, Inc. This method efficiently joins multiple overlapping DNA fragments in a single-tube isothermal reaction. Oligonucleotides, DNA with varied overlaps (15–80 bp) and fragments hundreds of kilobases long have been successfully assembled by using Gibson Assembly. The overview of Gibson Assembly is shown below (Figure A.5):

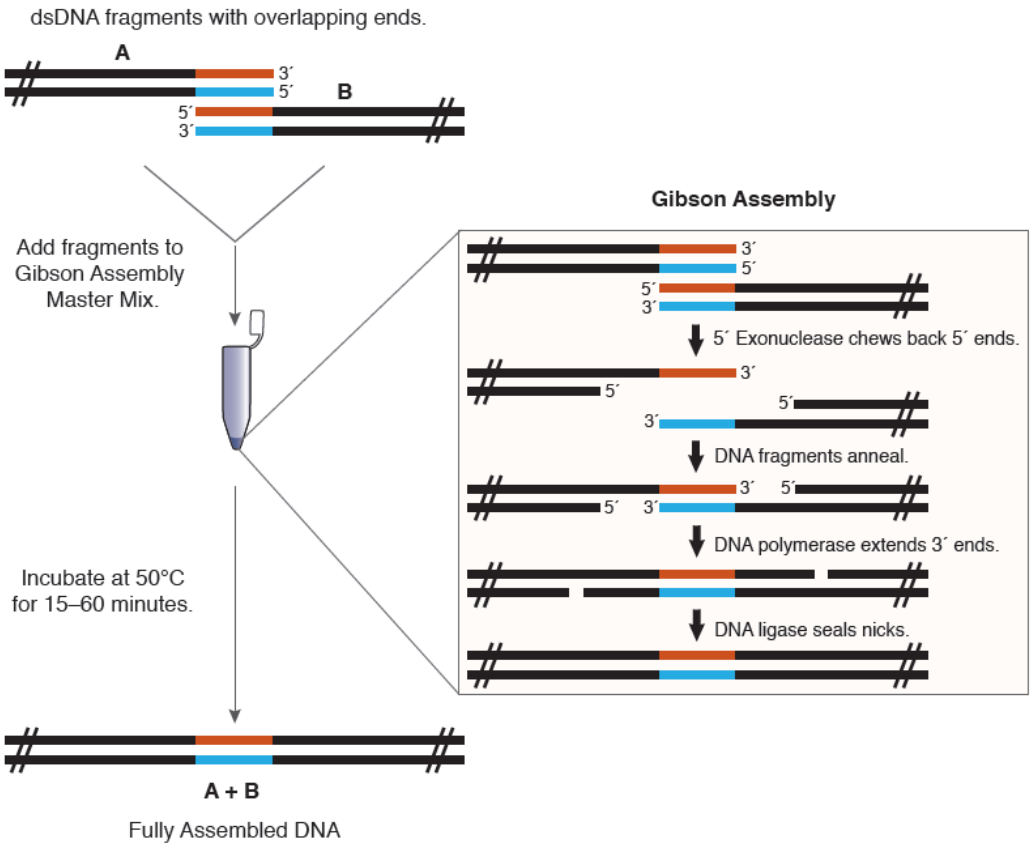

Figure A.5 Overview of the Gibson Assembly Cloning Method.

In Gibson Assembly, DNA fragments that need to be assembled are first amplified by PCR. Overalp was added by using overlapping primers. Next, these DNA fragments are mixed with a cocktail of three enzymes, along with other buffer components. The three required enzyme activities are: exonuclease, DNA polymerase, and DNA ligase. The exonuclease chews back DNA from the 5' end. The resulting single-stranded regions on adjacent DNA fragments can anneal. The DNA polymerase extends 3’ ends to fill in any gaps along the gene. The DNA ligase covalently joins the DNA of adjacent segments, thereby removing any nicks in the DNA.

DNA Construction

Plasmid pDG364_CotB_P450_GFP was constructed from pDG364_CotB_HuPTH1r_GFP. First, pDG364_CotB_ HuPTH1r_GFP were digested with PmeI and *Bam*H1 to create the vector. P450 gene was amplified from pJ241_P450. GFP was amplified from pDG364_CotB_ HuPTH1r_GFP. The overlapping primers for amplification are shown in Table A.1. Then, DNA fragments P450 and GFP were inserted into the vector by using Gibson Assembly (Figure A.6). The constructed plasmid was transformed into *E.coli* DH5α and plated on LB plates containing ampicillin (50 μg/mL). Four colonies were randomly picked and the plasmids were isolated for DNA sequencing. The correct plasmid was integrated into the *amy*E locus into *B. subtilis* strain PY79 (Ohio State University, *Bacillus* Genetic Stock Center, Columbus Ohio).

The insert includes CotB as carrier protein then is followed by a linker (-GlyPheLysLeu Gly_4Ser-) that connects CYP102A3 S189Q/A330V. The P450 has a linker (-LeuGlu-) to GFP.

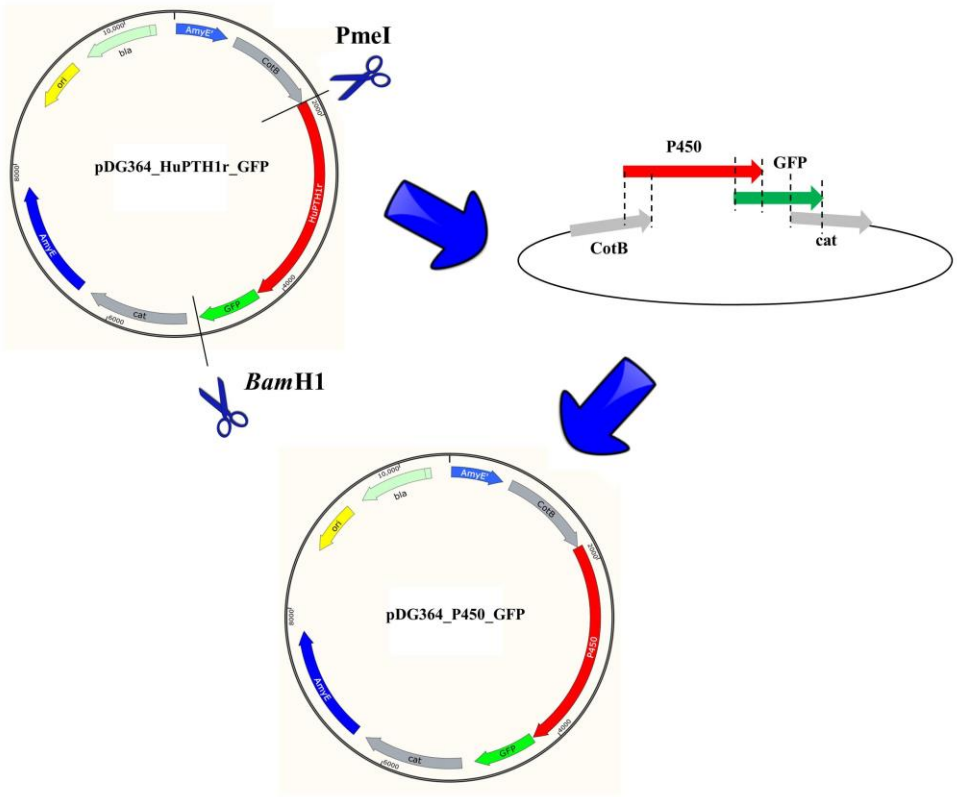

Figure A.6 Overview of the Gibson Assembly cloning method.

Table A.1 Overlapping Primers Used in DNA Construction for Plasmid pDG364_CotB_P450_GFP.

Name	Primer Sequence
P450-forward	5'-GGAAACGTAAATTTGGGTTTAAACTCGGAGGAGGAGGATC-3'
P450-reverse	5'-AGTTCTTCTCCTTTACTCATCTCGAGCATACCAGTCCAAA-3'
GFP-forward	5'-TATGCTCGAGATGAGTAAAGGAGAAGAACTTTTCACTGGA-3'
GFP-reverse	5'-GCGACCGGCGCTCAGGATCCTTATTTGTATAGTTCATCCA-3'

Results

Four colonies were randomly collected after the transformation of Gilbson Assembly assembled plasmid into *E.coli* DH5a. The plasmids were insolated and double digested with PmeI and *Bam*H1. The gel picture showed that one plasmid (at lane 4) has a ~4000bp DNA fragment after double digestion, indicating the success of Gilbson

Assembly (Figure A.7). The sequence of this DNA fragment was investigated by using six primers (Figure A.8, Figure A.9). Next, the chromosome DNA was isolated from transformed *B. subtilis* and P450 region was amplified with P450-forward and P450-reverse. The sequence of the resulting PCR product was investigated. The sequencing data indicates the successful construction of pDG364_CotB_P450_GFP and successful integration into *B.subtilis*.

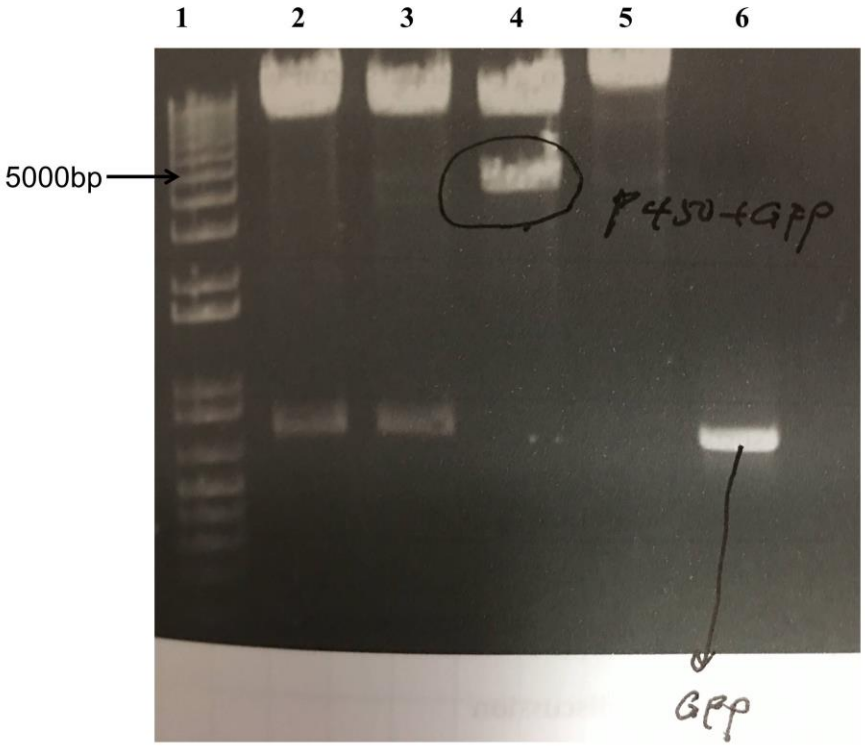

Figure A.7 Agarose gel of isolated plasmids after PmeI and *Bam*H1 double restrction digestion. Lane 1: Marker; Lane 2 - 5: isolated pladmids after double digestion; Lane 6: GFP PCR product.


Sequence: CotB_P450_GFP.pdf.dna (Linear / 4718 bp)
Enzymes: < Unsaved Enzyme Set > (4 of 646 total)
Features: 7 visible, 7 total
Primers: 4 visible, 4 total
Unique Cutters Bold
Start (0)
CotB
MssI
p450-forward
linker
P450
PmeI

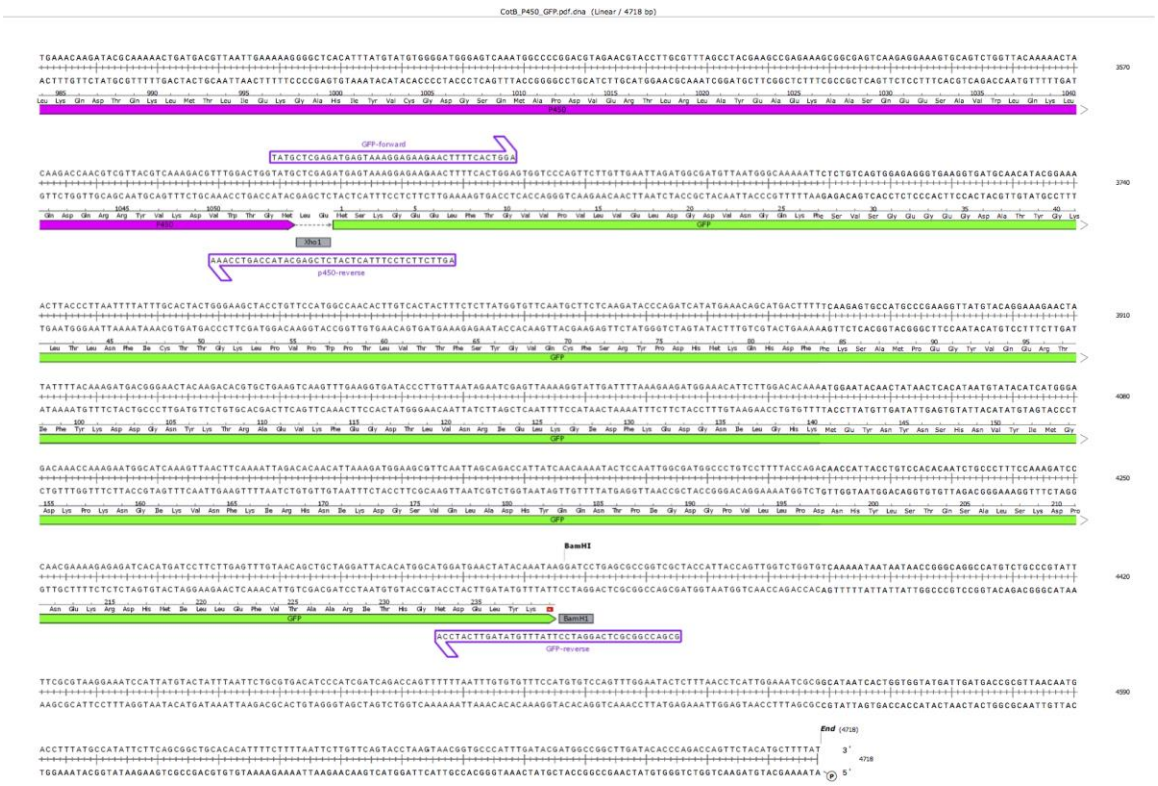

Figure A.8 Sequence of CotB_P450_GFP was acquired by SnapGene (GSL Biotech LLC, Chicago, IL). CotB is labeled as blue. P450 is labeled as pink. GFP is labeled as green.

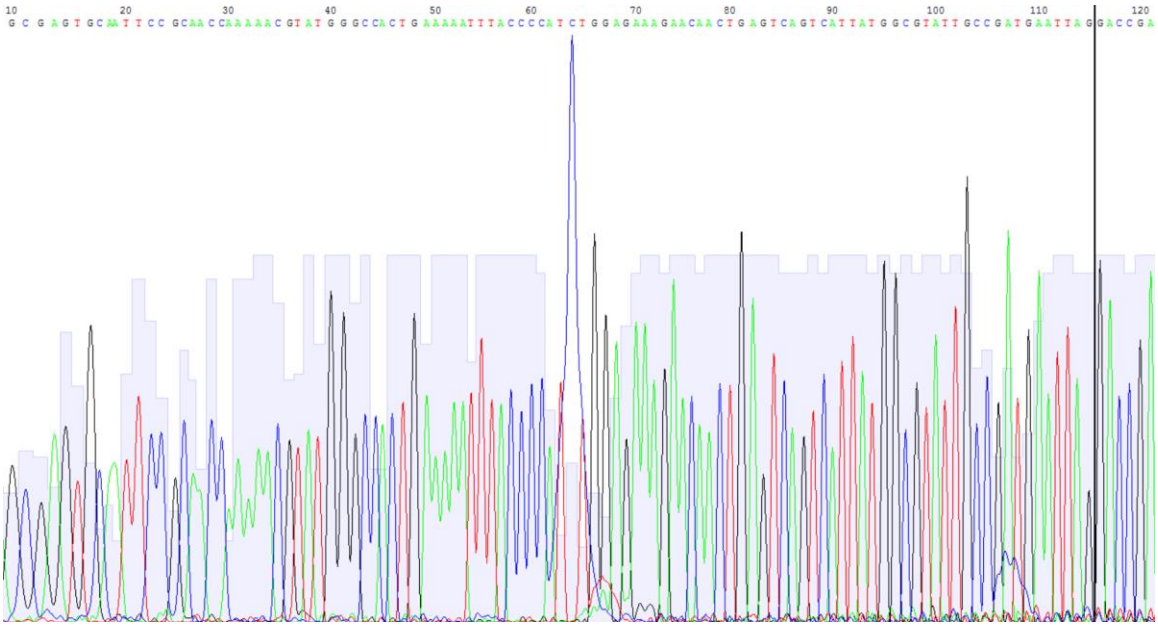

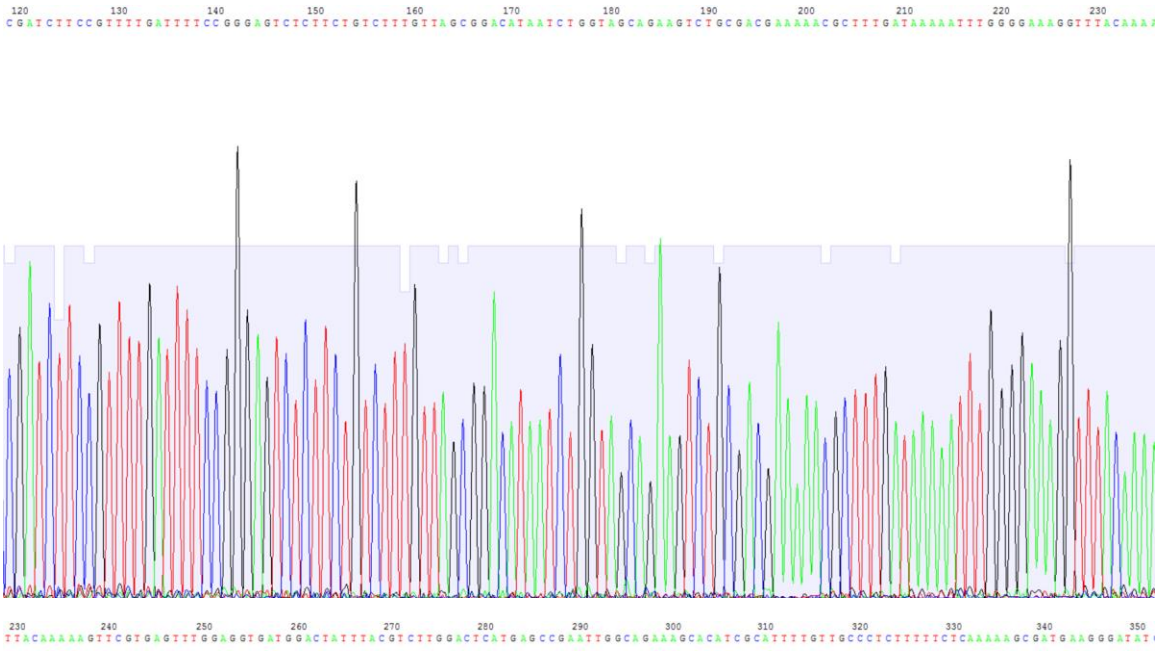


350 360 370 380 390 400 410 420 430 440 450 460
460 470 480 490 500 510 520 530 540 550 560 570


570 580 590 600 610 620 630 640 650 660 670
20 30 40 50 60 70 80 90 100 110 120 130
42%


140 150 160 170 180 190 200 210 220 230 240 250
42%
250 260 270 280 290 300 310 320 330 340 350 360 370
44%

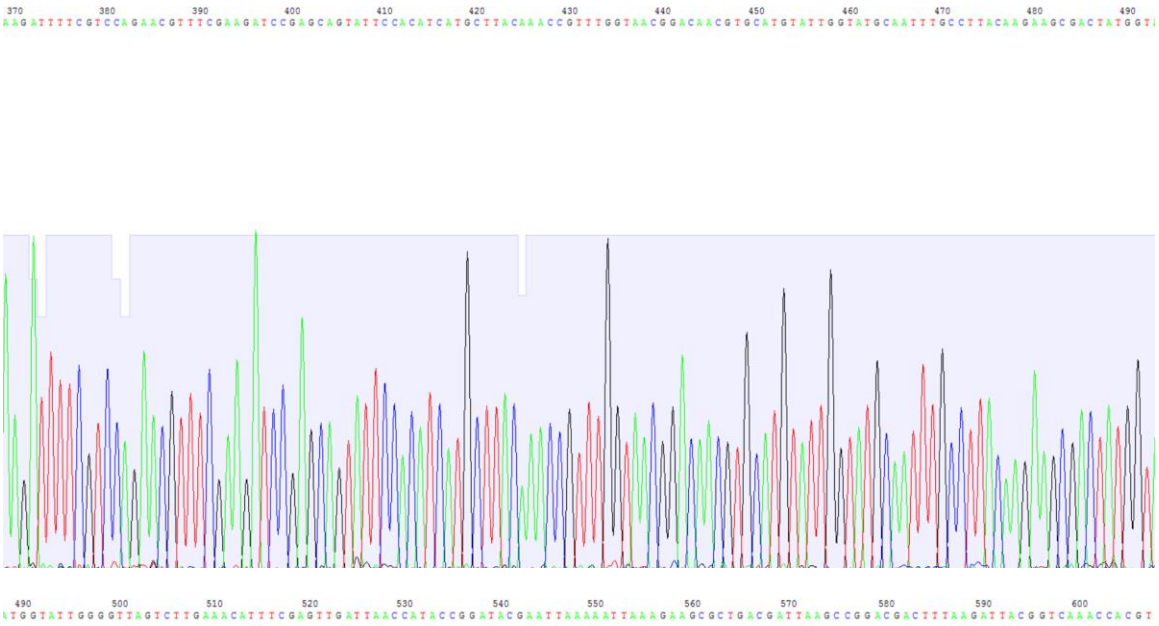


580 590 600 610 620 630 640 650 660 670 680 690
CGTTTGAAGGTATTGTCTTAGAGAATCGCGAATTACAAACCGCGGCGTCAACCCGCAGCACCCGTCACATTGAGTTGGAAATCCCGGCTGGAAAAACTTACAAAGAGGGAGATCATAT
360 370 380 390 400 410 420 430 440 450 460 470
TGGAAAAACTTACAAAGAGGGAGATCATATTGGAATTTTACCGAAAAACTCACGTGAGCTGGTACAACGTGTTCTAAGTCGTTTTGGTCTGCAGAGTAATCACGTCATTAAGGTCAGCGGT

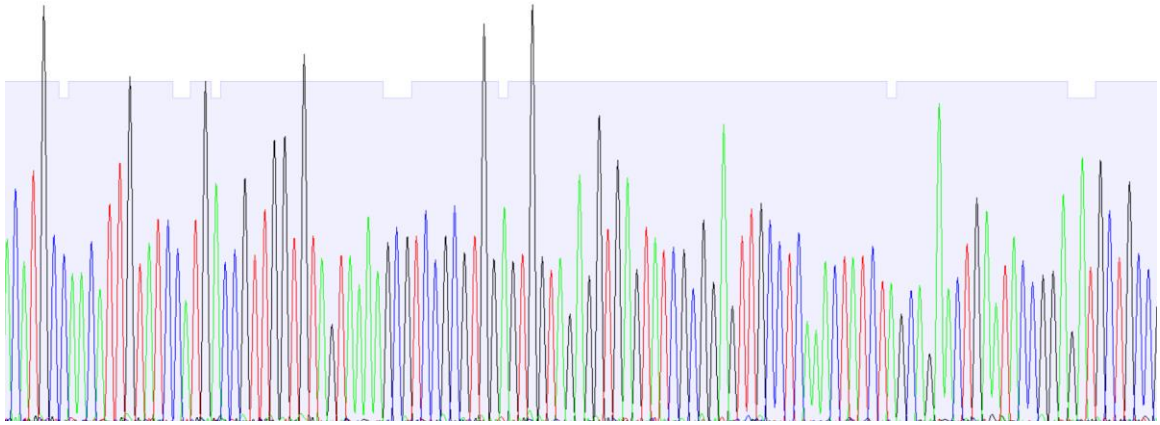


280 290 300 310 320 330 340 350 360 370 380 390
GATGCTGCCGCATGTTTTATTCGTACTCCGCAGAGTGGATTTCAAATGCCGAACGATCCCGAAACTCCCATGATCATGGTCGGACCGGGAACCGGAATTGCACCGTTTCGTGGATTCATCCA

390 400 410 420 430 440 450 460 470 480 490 500
TGGATTCATCCAGGCTCGCAGCGTATTGAAGAAAGAGGGATCTACGTTAGGTGAGGCTTTACTGTATTTTGGATGTCGTAGACCGGATCATGACGACCTATATCGCGAGGAATTAGATCAAG

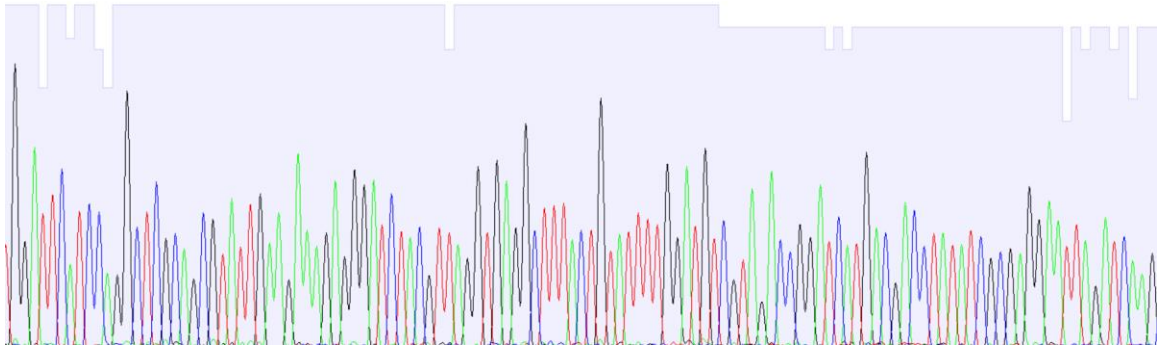

Figure A.9 Full sequence result of CotB_P450_GFP for P450. The sequence is analyzed by ApE-A plasmid Editor (by M. Wayne Davis).

APPENDIX B

SEQUENCE DATA OF COTA VARIANTS

Raw data of sequencing of Y19-CotA and other variants.

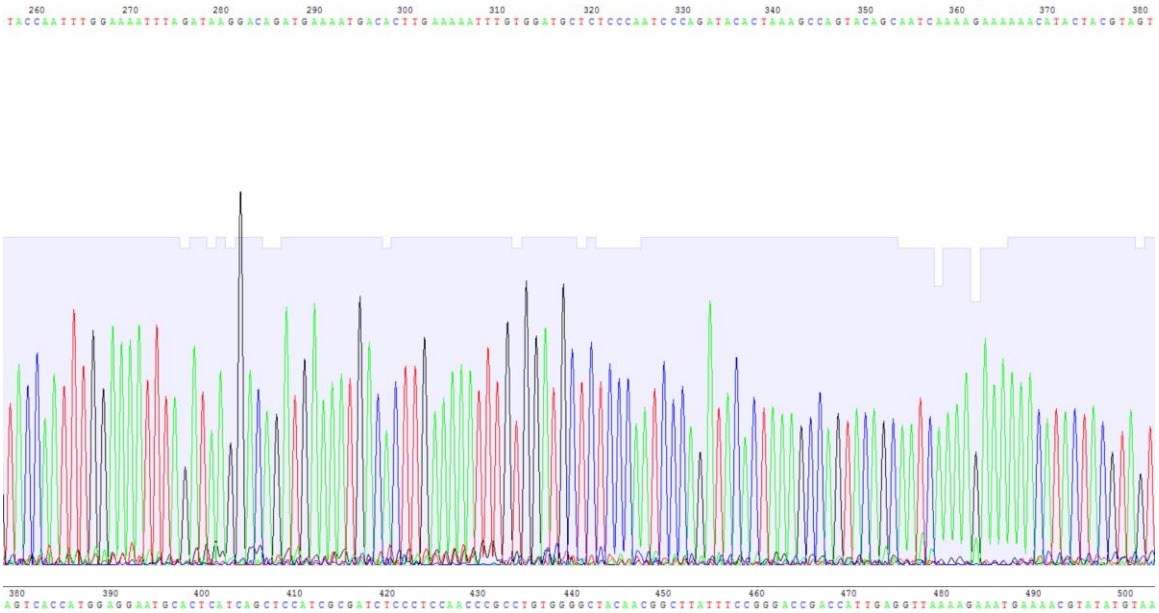
260 270 280 290 300 310 320 330 340 350 360 370 380
TACCAATTTGGAAAATTTAGATAAGGACAGATGAAAATGACACTTGAAAAATTTGTGGATGCTCTCCCAATCCCAGATACACTAAAGCCAGTACAGCAATCAAAAGAAAAAACATACTACGTAGT
380 390 400 410 420 430 440 450 460 470 480 490 500
AGTCACCATGGAGGAATGCACTCATCAGCTCCATCGCGATCTCCCTCCAACCCGCCTGTGGGGCTACAACGGCTTATTTCCGGGACCGACCATTGAGGTTAAAAGAAATGAAAACGTATATGTAA

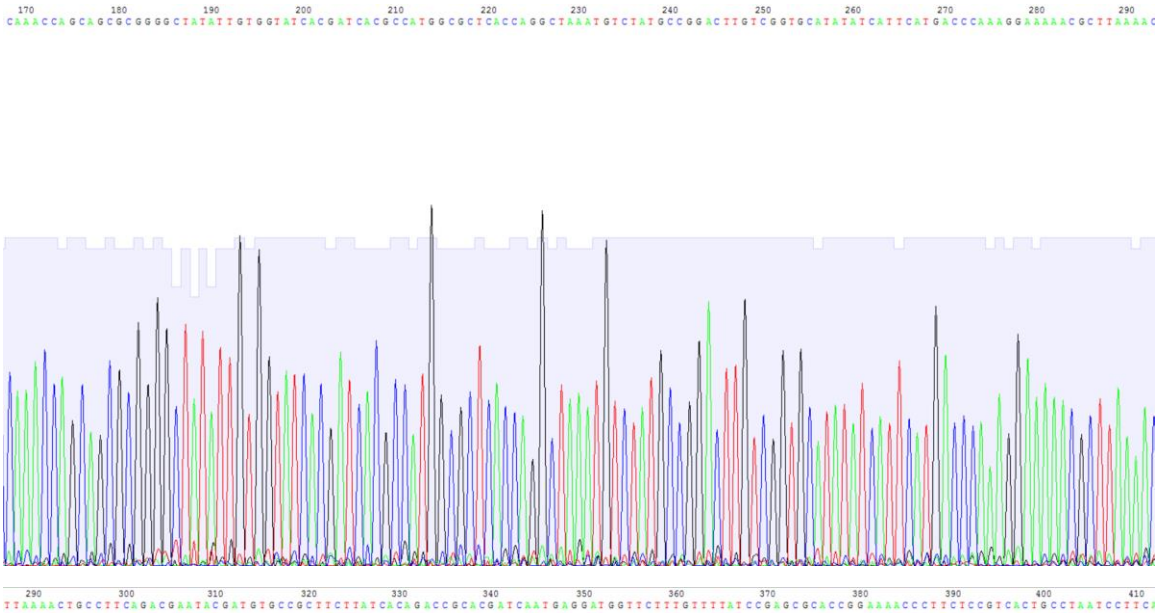

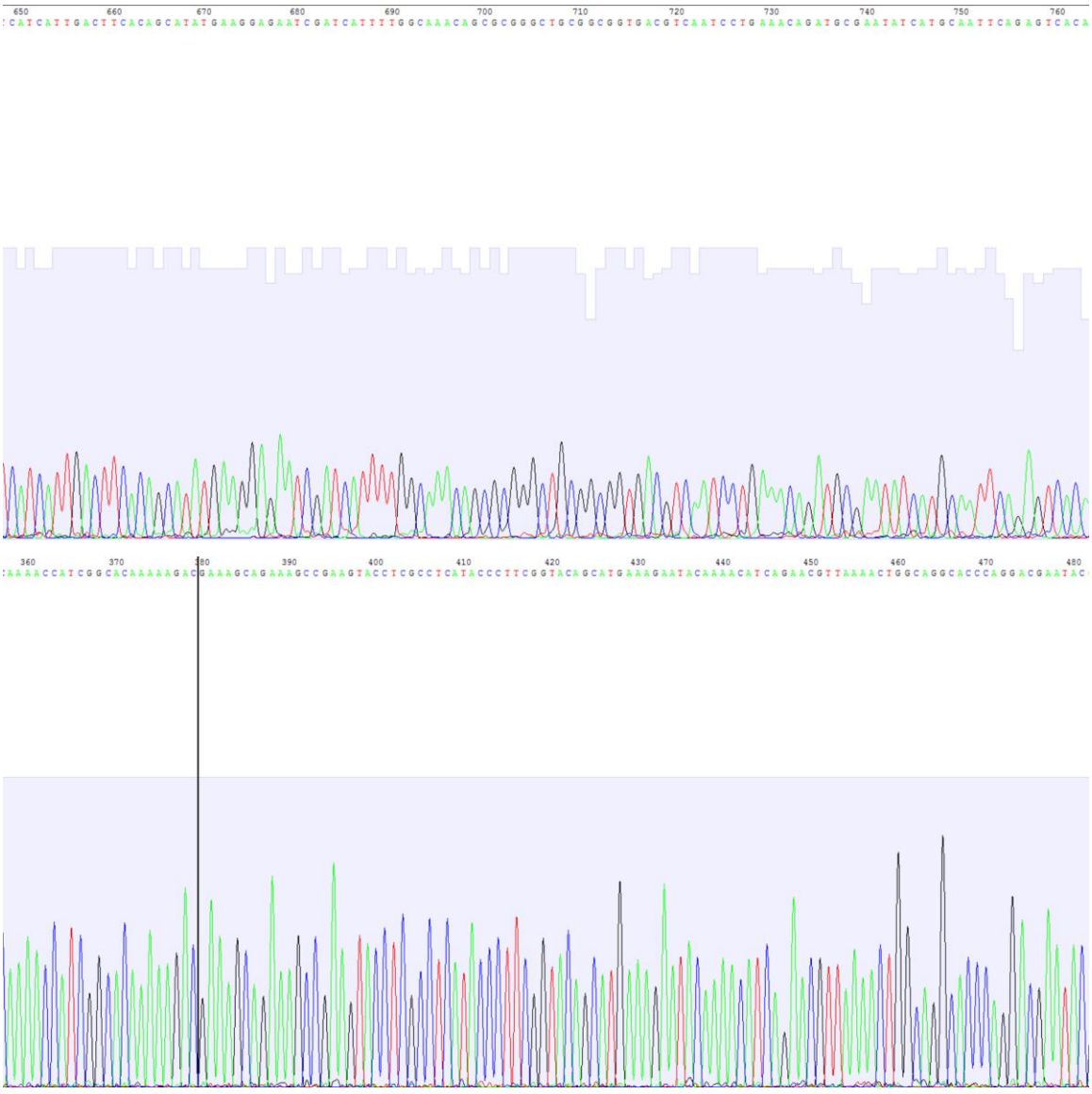

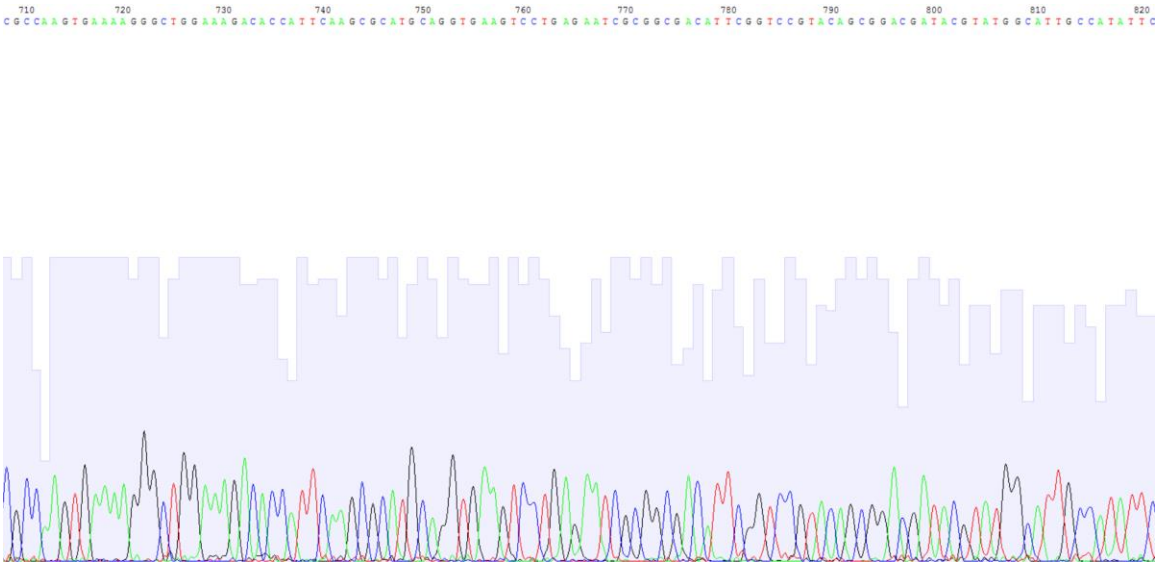

Figure B.1 Full sequence results of Y19-CotA. The sequence is analyzed by ApE-A plasmid Editor (by M. Wayne Davis).

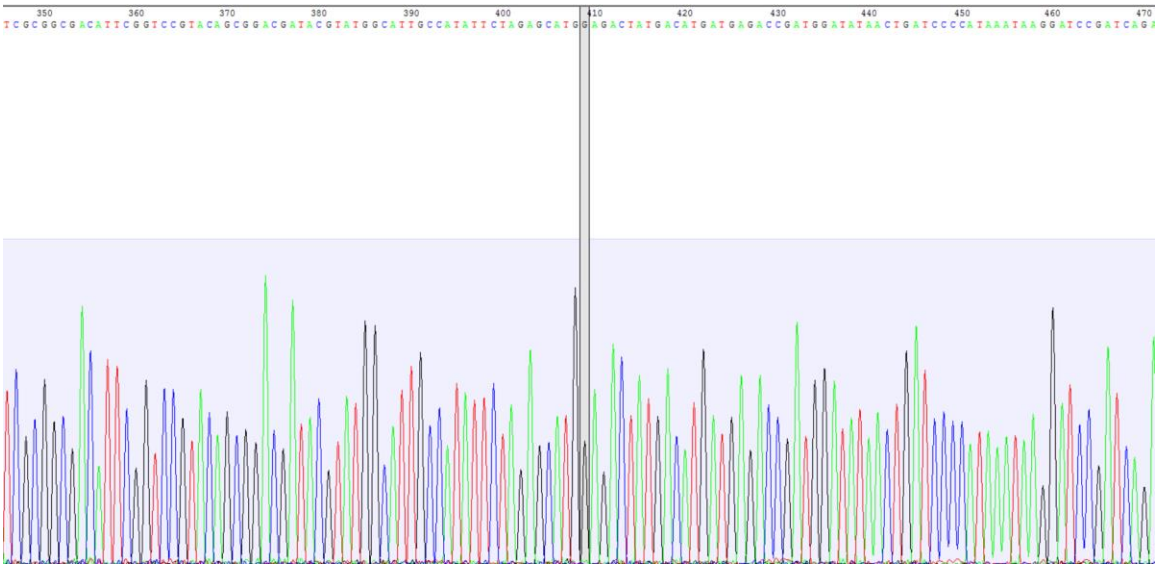

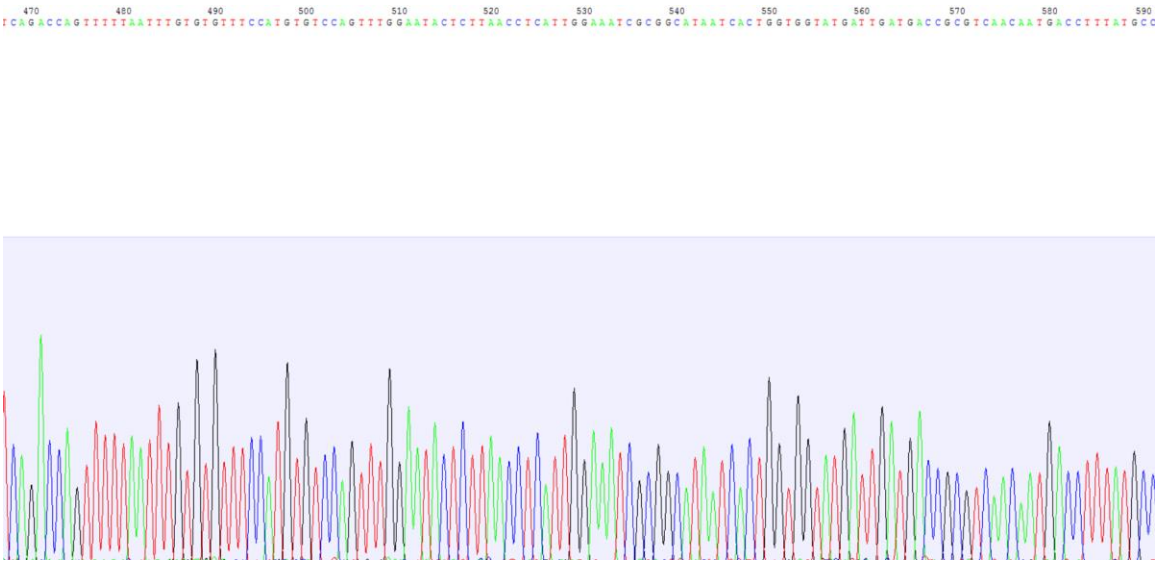

Figure B.2 Sequence results of E498G-CotA near the subtitution site. The mutated sites is highlighted in grey bar. The sequence is analyzed by ApE-A plasmid Editor (by M. Wayne Davis).

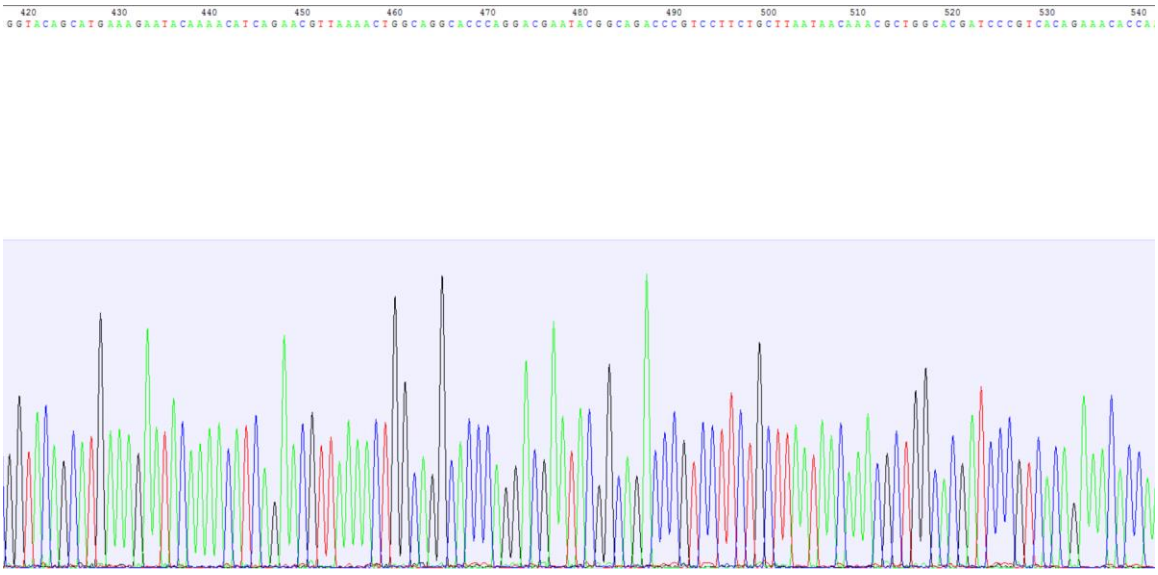

Figure B.3 Sequence results of L343S-CotA near the subtitution site. The mutated sites is highlighted in grey bar. The sequence is analyzed by ApE-A plasmid Editor (by M. Wayne Davis).

REFERENCES

1. Bains W (2016) How likely are we? Evolution of organismal complexity. Evolutionary Biology: Convergent Evolution, Evolution of Complex Traits, Concepts and Methods. pp. 255-272.

2. Sokal RR CT (1970) The biological species concept: A critical evaluation. The American Naturalist 104: 127-153.

3. Darwin C (1859) On the Origin of Species: p. 503.

4. Darwin C (1859) On the Origin of Species by Means of Natural Selection, or the Preservation of Favoured Races in the Struggle for Life. Nature (London: John Murray) 5: 502.

5. Pearson H (2006) What is a gene? Nature 441: 398-401.

6. Hurst LD (2009) Fundamental concepts in genetics: Genetics and the understanding of selection. Nature Reviews Genetics 10: 83-93.

7. Hill RL, Harris CM, Naylor JF, Sams WM (1969) The partial amino acid sequence of human myoglobin. Journal of Biological Chemistry 244: 2182-2194.

8. Schoemaker HE, Mink D, WubboLts MG (2003) Dispelling the myths - Biocatalysis in industrial synthesis. Science 299: 1694-1697.

9. Liao H, McKenzie T, Hageman R (1986) Isolation of a thermostable enzyme variant by cloning and selection in a thermophile. Proceedings of the National Academy of Sciences of the United States of America 83: 576-580.

10. Wilson CJ (2015) Rational protein design: Developing next-generation biological therapeutics and nanobiotechnological tools. Wiley Interdisciplinary Reviews: Nanomedicine and Nanobiotechnology 7: 330-341.

11. Giger L, Caner S, Obexer R, Kast P, Baker D, et al. (2013) Evolution of a designed retro-aldolase leads to complete active site remodeling. Nature Chemical Biology 9: 494-498.

12. Kumar S, Chen CS, Waxman DJ, Halpert JR (2005) Directed evolution of mammalian cytochrome P450 2B1: Mutations outside of the active site enhance the metabolism of several substrates, including the anticancer prodrugs cyclophosphamide and ifosfamide. Journal of Biological Chemistry 280: 19569-19575.

13. Davids T, Schmidt M, Böttcher D, Bornscheuer UT (2013) Strategies for the discovery and engineering of enzymes for biocatalysis. Current Opinion in Chemical Biology 17: 215-220.

14. Khersonsky O, Röthlisberger D, Wollacott AM, Murphy P, Dym O, et al. (2011) Optimization of the in-silico-designed Kemp eliminase KE70 by computational design and directed evolution. Journal of Molecular Biology 407: 391-412.

15. Allen D. Bosley MO (2005) Mathematical expressions useful in the construction, description and evaluation of protein libraries. Biomolecular Engineering 22: 57-61.

16. Leemhuis H, Kelly RM, Dijkhuizen L (2009) Directed evolution of enzymes: Library screening strategies. IUBMB Life 61: 222-228.

17. Neylon C (2004) Chemical and biochemical strategies for the randomization of protein encoding DNA sequences: Library construction methods for directed evolution. Nucleic Acids Research 32: 1448-1459.

18. Stemmer WPC (1994) Rapid evolution of a protein in vitro by DNA shuffling. Nature 370: 389-391.

19. Labrou NE (2010) Random mutagenesis methods for in vitro directed enzyme evolution. Current Protein and Peptide Science 11: 91-100.

20. Giver L, Gershenson A, Freskgard PO, Arnold FH (1998) Directed evolution of a thermostable esterase. Proceedings of the National Academy of Sciences of the United States of America 95: 12809-12813.

21. Cadwell RC, Joyce GF (1992) Randomization of genes by PCR mutagenesis. PCR methods and applications 2: 28-33.

22. Cohen J (2001) How DNA Shuffling Works. Science 293: 237.

23. Crameri A, Whitehorn EA, Tate E, Stemmer WPC (1996) Improved green fluorescent protein by molecular evolution using DNA shuffling. Nature Biotechnology 14: 315-x311.

24. Smith GP (1985) Filamentous fusion phage: Novel expression vectors that display cloned antigens on the virion surface. Science 228: 1315-1317.

25. Sergeeva A, Kolonin MG, Molldrem JJ, Pasqualini R, Arap W (2006) Display technologies: Application for the discovery of drug and gene delivery agents. Advanced Drug Delivery Reviews 58: 1622-1654.

26. Lipovsek D, Plückthun A (2004) In-vitro protein evolution by ribosome display and mRNA display. Journal of Immunological Methods 290: 51-67.

27. Lin H, Cornish VW (2002) Screening and selection methods for large-scale analysis of protein function. Angewandte Chemie - International Edition 41: 4402-4425.

28. Fitzgerald K (2000) In vitro display technologies - New tools for drug discovery. Drug Discovery Today 5: 253-258.

29. He M, Khan F (2005) Ribosome display: Next-generation display technologies for production of antibodies in vitro. Expert Review of Proteomics 2: 421-430.

30. Mattheakis LC, Bhatt RR, Dower WJ (1994) An in vitro polysome display system for identifying ligands from very large peptide libraries. Proceedings of the National Academy of Sciences of the United States of America 91: 9022-9026.

31. Bradbury ARM, Sidhu S, Dübel S, McCafferty J (2011) Beyond natural antibodies: The power of in vitro display technologies. Nature Biotechnology 29: 245-254.

32. Smith GP (1985) Filamentous fusion phage: Novel expression vectors that display cloned antigens on the virion surface. . Science 228: 1315-1317.

33. Charbit A, Boulain, JC, Ryter, A, Hofnung, M (1986) Probing the topology of a bacterial membrane protein by genetic insertion of a foreign epitope; expression at the cell surface. EMBO J 5: 3029-3037.

34. Georgiou G, Stathopoulos C, Daugherty PS, Nayak AR, Iverson BL, et al. (1997) Display of heterologous proteins on the surface of microorganisms: From the screening of combinatorial libraries to live recombinant vaccines. Nature Biotechnology 15: 29-34.

35. Tanaka T, Yamada R, Ogino C, Kondo A (2012) Recent developments in yeast cell surface display toward extended applications in biotechnology. Applied Microbiology and Biotechnology 95: 577-591.

36. Boder ET, Wittrup KD (1997) Yeast surface display for screening combinatorial polypeptide libraries. Nature Biotechnology 15: 553-557.

37. Traxlmayr MW, Obinger, C (2012) Directed evolution of proteins for increased stability and expression using yeast display. Archives of Biochemistry and Biophysics 526: 174-180.

38. Lee SY, Choi JH, Xu Z (2003) Microbial cell-surface display. Trends in Biotechnology 21: 45-52.

39. Bessette PH, Åslund F, Beckwith J, Georgiou G (1999) Efficient folding of proteins with multiple disulfide bonds in the Escherichia coli cytoplasm. Proceedings of the National Academy of Sciences of the United States of America 96: 13703-13708.

40. Løset GÅ, Roos N, Bogen B, Sandlie I (2011) Expanding the versatility of phage display II: Improved affinity selection of folded domains on protein VII and IX of the filamentous phage. PLoS ONE 6.

41. Pepper LR, Yong KC, Boder ET, Shusta EV (2008) A decade of yeast surface display technology: Where are we now? Combinatorial Chemistry and High Throughput Screening 11: 127-134.

42. Van Der Vaart JM, Te Biesebeke R, Chapman JW, Toschka HY, Klis FM, et al. (1997) Comparison of cell wall proteins of Saccharomyces cerevisiae as anchors for cell surface expression of heterologous proteins. Applied and Environmental Microbiology 63: 615-620.

43. Gai SA, Wittrup KD (2007) Yeast surface display for protein engineering and characterization. Current Opinion in Structural Biology 17: 467-473.

44. Jia H, Lee FS, Farinas ET (2014) Bacillus subtilis spore display of laccase for evolution under extreme conditions of high concentrations of organic solvent. ACS Combinatorial Science 16: 665-669.

45. Driks A (1999) Bacillus subtilis spore coat. Microbiology and Molecular Biology Reviews 63: 1-20.

46. Setlow P, Waites WM (1976) Identification of several unique, low molecular weight basic proteins in dormant spores of Clostridium bifermentans and their degradation during spore germination. Journal of Bacteriology 127: 1015-1017.

47. Zhao G, Miao Y, Guo Y, Qiu H, Sun S, et al. (2014) Development of a heat-stable and orally delivered recombinant M2e-expressing B. subtilis spore-based influenza vaccine. Human Vaccines and Immunotherapeutics 10: 3649-3658.

48. Kim J, Schumann W (2009) Display of proteins on bacillus subtilis endospores. Cellular and Molecular Life Sciences 66: 3127-3136.

49. Isticato R, Cangiano G, Tran HT, Ciabattini A, Medaglini D, et al. (2001) Surface display of recombinant proteins on Bacillus subtilis spores. Journal of Bacteriology 183: 6294-6301.

50. Seok JK, Jung HC, Pan JG (2007) Transgalactosylation in a water-solvent biphasic reaction system with β-galactosidase displayed on the surfaces of Bacillus subtilis spores. Applied and Environmental Microbiology 73: 2251-2256.

51. Gupta N, Farinas ET (2010) Directed evolution of CotA laccase for increased substrate specificity using Bacillus subtilis spores. Protein Engineering, Design and Selection 23: 679-682.

52. Zilhão R, Serrano M, Isticato R, Ricca E, Moran Jr CP, et al. (2004) Interactions among CotB, CotG, and CotH during Assembly of the Bacillus subtilis Spore Coat. Journal of Bacteriology 186: 1110-1119.

53. Sacco M, Ricca E, Losick R, Cutting S (1995) An additional GerE-controlled gene encoding an abundant spore coat protein from Bacillus subtilis. Journal of Bacteriology 177: 372-377.

54. Donovan W, Zheng L, Sandman K, Losick R (1987) Genes encoding spore coat polypeptides from Bacillus subtilis. Journal of Molecular Biology 196: 1-10.

55. Isticato R, Esposito G, Zilhão R, Nolasco S, Cangiano G, et al. (2004) Assembly of Multiple CotC Forms into the Bacillus subtilis Spore Coat. Journal of Bacteriology 186: 1129-1135.

56. Nguyen QA, Schumann W (2014) Use of IPTG-inducible promoters for anchoring recombinant proteins on the Bacillus subtilis spore surface. Protein Expression and Purification 95: 67-76.

57. Sirec T, Strazzulli A, Isticato R, De Felice M, Moracci M, et al. (2012) Adsorption of β-galactosidase of Alicyclobacillus acidocaldarius on wild type and mutants spores of Bacillus subtilis. Microbial Cell Factories 11.

58. Chen H, Zhang T, Jia J, Vastermark A, Tian R, et al. (2015) Expression and display of a novel thermostable esterase from Clostridium thermocellum on the surface of Bacillus subtilis using the CotB anchor protein. Journal of Industrial Microbiology and Biotechnology 42: 1439-1448.

59. Nguyen HD, Phan TTP, Schumann W (2011) Analysis and application of Bacillus subtilis sortases to anchor recombinant proteins on the cell wall. AMB Express 1: 22.

60. Driks A (2002) Maximum shields: the assembly and function of the bacterial spore coat. Trends in Microbiology 10: 251-254.

61. Morozova OV, Shumakovich GP, Gorbacheva MA, Shleev SV, Yaropolov AI (2007) "Blue" laccases. Biochemistry (Moscow) 72: 1136-1150.

62. Bao W, O'Malley DM, Whetten R, Sederoff RR (1993) A laccase associated with lignification in loblolly pine xylem. Science 260: 672-674.

63. Rochefort D, Leech D, Bourbonnais R (2004) Electron transfer mediator systems for bleaching of paper pulp. Green Chemistry 6: 14-24.

64. Mayer AM, Staples RC (2002) Laccase: new functions for an old enzyme. Phytochemistry 60: 551-565.

65. Claus H (2004) Laccases: structure, reactions, distribution. Micron 35: 93-96.

66. Rodr ́guez Couto S, Toca Herrera JL (2006) Industrial and biotechnological applications of laccases: A review. Biotechnology Advances 24: 500-513.

67. Hullo MF, Moszer I, Danchin A, Martin-Verstraete I (2001) CotA of Bacillus subtilis is a copper-dependent laccase. Journal of Bacteriology 183: 5426-5430.

68. Engel A, Fujiyoshi Y, Agre P (2000) The importance of aquaporin water channel protein structures. EMBO Journal 19: 800-806.

69. Nielsen JE, Borchert TV (2001) Protein engineering of bacterial α-amylases. Biochimica et Biophysica Acta - Protein Structure and Molecular Enzymology 1543: 253-274.

70. Sharma A, Kawarabayasi Y, Satyanarayana T (2012) Acidophilic bacteria and archaea: Acid stable biocatalysts and their potential applications. Extremophiles 16: 1-19.

71. Gupta N, Farinas ET (2010) Directed evolution of CotA laccase for increased substrate specificity using *Bacillus subtilis* spores. Protein Engineering, Design, & Selection 23: 679-682.

72. Nicholson WL, Setlow P (1990) Sporulation, Germination and Outgrowth. In: Harwood CR, Cutting SM, editors. Molecular Biological Methods for *Bacillus*. West Sussex: John Wiley & Sons Ltd. pp. 391-450.

73. Bento I, Silva CS, Chen Z, Martins LO, Lindley PF, et al. (2010) Mechanisms underlying dioxygen reduction in laccases. Structural and modelling studies focusing on proton transfer. BMC structural biology 10: 28.

74. Chen Z, Durão P, Silva CS, Pereira MM, Todorovic S, et al. (2010) The role of Glu498 in the dioxygen reactivity of CotA-laccase from Bacillus subtilis. Dalton Transactions 39: 2875-2882.

75. Xu F (1996) Oxidation of phenols, anilines, and benzenethiols by fungal laccases: Correlation between activity and redox potentials as well as halide inhibition. Biochemistry 35: 7608-7614.

76. Xu F, Shin W, Brown SH, Wahleithner JA, Sundaram UM, et al. (1996) A study of a series of recombinant fungal laccases and bilirubin oxidase that exhibit significant differences in redox potential, substrate specificity, and stability. Biochim Biophys Acta 1292: 303-311.

77. Martins LO, Soares CM, Pereira MM, Teixeira M, Costa T, et al. (2002) Molecular and biochemical characterization of a highly stable bacterial laccase that occurs as a structural component of the Bacillus subtilis endospore coat. Journal of Biological Chemistry 277: 18849-18859.

78. Kumar RA, Clark DS (2006) High-throughput screening of biocatalytic activity: Applications in drug discovery. Current Opinion in Chemical Biology 10: 162-168.

79. Porter JL, Rusli RA, Ollis DL (2016) Directed Evolution of Enzymes for Industrial Biocatalysis. ChemBioChem 17: 197-203.

80. Wohlgemuth R (2010) Biocatalysis-key to sustainable industrial chemistry. Current Opinion in Biotechnology 21: 713-724.

81. Klibanov A (1997) Why are enzymes less active in organic solvents than in water? Trends in Biotechnology 15: 97-101.

82. Doukyu N, Ogino H (2010) Organic solvent-tolerant enzymes. Biochemical Engineering Journal 48: 270-282.

83. Stepankova V, Bidmanova S, Koudelakova T, Prokop Z, Chaloupkova R, et al. (2013) Strategies for stabilization of enzymes in organic solvents. ACS Catalysis 3: 2823-2836.

84. Dicosimo R, McAuliffe J, Poulose AJ, Bohlmann G (2013) Industrial use of immobilized enzymes. Chemical Society Reviews 42: 6437-6474.

85. Liese A, Hilterhaus L (2013) Evaluation of immobilized enzymes for industrial applications. Chemical Society Reviews 42: 6236-6249.

86. Binay B, Alagöz D, Yildirim D, Çelik A, Tükel SS (2016) Highly stable and reusable immobilized formate dehydrogenases: Promising biocatalysts for in situ regeneration of NADH. Beilstein Journal of Organic Chemistry 12: 271-277.

87. Shao X, Ni H, Lu T, Jiang M, Li H, et al. (2012) An improved system for the surface immobilisation of proteins on Bacillus thuringiensis vegetative cells and spores through a new spore cortex-lytic enzyme anchor. New Biotechnology 29: 302-310.

88. Chen G, Driks A, Tawfiq K, Mallozzi M, Patil S (2010) Bacillus anthracis and Bacillus subtilis spore surface properties and transport. Colloids and Surfaces B: Biointerfaces 76: 512-518.

89. Moeller R, Setlow P, Reitz G, Nicholson WL (2009) Roles of small, acid-soluble spore proteins and core water content in survival of Bacillus subtilis spores exposed to environmental solar UV radiation. Applied and Environmental Microbiology 75: 5202-5208.

90. Higgins D, Dworkin J (2012) Recent progress in Bacillus subtilis sporulation. FEMS Microbiology Reviews 36: 131-148.

91. Tabassum H, Parvez, S., Rehman, H., Banerjee, B.D., Raisuddin, S. (2007) Catechin as an antioxidant in liver mitochondrial toxicity: Inhibition of tamoxifen-induced protein oxidation and lipid peroxidation. Journal of Biochemical and Molecular Toxicology 21: 110-117.

92. Sangwan NS, Shanker S, Sangwan RS, Kumar S (1998) Plant-derived products as antimutagens. Phytotherapy Research 12: 389-399.

93. Suzuki JI, Isobe M, Morishita R, Nagai R (2012) Effects of green tea catechin consumption on cardiovascular diseases. Tea Consumption and Health. pp. 87-99.

94. Wang YF, Shao SH, Xu P, Yang XQ, Qian LS (2011) Catechin-enriched green tea extract as a safe and effective agent for antimicrobial and anti-inflammatory treatment. African Journal of Pharmacy and Pharmacology 5: 1452-1461.

95. Han ZX, Rana MM, Liu GF, Gao MJ, Li DX, et al. (2016) Green tea flavour determinants and their changes over manufacturing processes. Food Chemistry 212: 739-748.

96. Papp A, Winnewisser W, Geiger E, Briem F (2001) Influence of (+)-catechin and ferulic acid on formation of beer haze and their removal through different polyvinylpolypyrollidone-types. Journal of the Institute of Brewing 107: 55-60.

97. Kampa M, Hatzoglou A, Notas G, Damianaki A, Bakogeorgou E, et al. (2000) Wine antioxidant polyphenols inhibit the proliferation of human prostate cancer cell lines. Nutrition and Cancer 37: 223-233.

98. Matito C, Mastorakou F, Centelles JJ, Torres Simón JL, Serratosa MC (2003) Antiproliferative effect of antioxidant polyphenols from grape in murine Hepa-1c1c7. European Journal of Nutrition 42: 43-49.

99. Kurisawa M, Chung JE, Uyama H, Kobayashi S (2003) Laccase-catalyzed Synthesis and Antioxidant Property of Poly(catechin). Macromolecular Bioscience 3: 758-764.

100. Madeira Junior JV, Jr., Teixeira CB, Macedo GA (2015) Biotransformation and bioconversion of phenolic compounds obtainment: An overview. Critical Reviews in Biotechnology 35: 75-81.

101. Krygier K, Sosulski F, Hogge L (1982) Free, esterified, and insoluble-bound phenolic acids. 2. Composition of phenolic acids in rapeseed flour and hulls. Journal of Agricultural and Food Chemistry 30: 334-336.

102. Liu Q, Wu L, Pu H, Li C, Hu Q (2012) Profile and distribution of soluble and insoluble phenolics in Chinese rapeseed (Brassica napus). Food Chemistry 135: 616-622.

103. Naczk M, Amarowicz R, Sullivan A, Shahidi F (1998) Current research developments on polyphenolics of rapeseed/canola: A review. Food Chemistry 62: 489-502.

104. Shahidi F, Naczk M (1992) An overview of the phenolics of canola and rapeseed: Chemical, sensory and nutritional significance. Journal of the American Oil Chemists Society 69: 917-924.

105. Zhang Y, Li X, Hao Z, Xi R, Cai Y, et al. (2016) Hydrogen peroxide-resistant CotA and YjqC of bacillus altitudinis spores are a promising biocatalyst for catalyzing reduction of sinapic acid and sinapine in rapeseed meal. PLoS ONE 11.

106. Lamba JK, Lin YS, Schuetz EG, Thummel KE (2002) Genetic contribution to variable human CYP3A-mediated metabolism. Advanced Drug Delivery Reviews 54: 1271-1294.

107. Pavek P, Dvorak Z (2008) Xenobiotic-induced transcriptional regulation of xenobiotic metabolizing enzymes of the cytochrome P450 superfamily in human extrahepatic tissues. Current Drug Metabolism 9: 129-143.

108. Guengerich FP (2008) Cytochrome P450 and chemical toxicology. Chemical Research in Toxicology 21: 70-83.

109. Chefson A, Zhao J, Auclair K (2006) Replacement of natural cofactors by selected hydrogen peroxide donors or organic peroxides results in improved activity for CYP3A4 and CYP2D6. ChemBioChem 7: 916-919.

110. Chefson A, Auclair K (2007) CYP3A4 activity in the presence of organic cosolvents, ionic liquids, or water-immiscible organic solvents. ChemBioChem 8: 1189-1197.

111. Kruyer NS, Peralta-Yahya P (2017) Metabolic engineering strategies to bio-adipic acid production. Current Opinion in Biotechnology 45: 136-143.

112. Deng Y, Ma L, Mao Y (2016) Biological production of adipic acid from renewable substrates: Current and future methods. Biochemical Engineering Journal 105: 16-26.

113. Shoham N, Sasson AL, Lin FH, Benayahu D, Haj-Ali R, et al. (2013) The mechanics of hyaluronic acid/adipic acid dihydrazide hydrogel: Towards developing a vessel for delivery of preadipocytes to native tissues. Journal of the Mechanical Behavior of Biomedical Materials 28: 320-331.